POLITECNICO DI TORINO

Master's degree in Energy and Nuclear Engineering

Master's degree Thesis

Feasibility study of a hybrid solar cooling-trigeneration system

Supervisors:
Prof. Vittorio VERDA
Dott. Ing. Luca CASTELLINO
Dott. Antonino GIUMMULÈ

Candidate:
Lorenzo TRAVERSO

October 2023

Abstract

The following text is about a techno-economic study of an absorption chiller fueled by the hot water produced from both a cogenerating system and a solar thermal system.

In the first part, after a brief introduction on the air-cooling needs, there is a general overview on the solar thermal collectors, with a focus on flat-plate solar collectors and the energy balance in a solar thermal system. This brings to the definition of the *solar cooling* and its advantages.

In the following chapter, a general overview on the combined heat and power (CHP) systems is reported. The comparison with traditional systems and the different layouts of a cogenerating system are presented. Then, the *trigeneration* is explained, reporting its advantages.

In the fourth chapter there is a description of the different chillers that are available in the market, with a deep description of the absorption chillers: the functioning, the components, and the different solutions to increase the efficiency.

In the fifth and sixth chapters, the real analysis of this work is carried out. At the beginning there is a short description of the company under analysis and its plant, the Pessione plant of Martini & Rossi. Then, a detailed description of the solar field and the CHP existing systems is carried out. The different components, the circuits, the products, some KPIs, are included in the analysis. After the strong comprehension of the actual available energy infrastructure, the cooling needs of the three bottling departments are analyzed. Coupling the production side, with the utilization side, three different options, each one with different alternatives, are presented. Option 1 considers the solar field as unique source of hot water. Option 2 considers the CHP system as unique source of hot water. Option 3 considers both the solar field and the CHP systems as source of hot water to feed an absorption chiller. After the study of the three options related to the ambient cooling, an additional analysis is carried out. This last one analysis is not about the ambient cooling, but is referred to refrigeration, the coupling of the solar field with an absorption chiller to refrigerate glycol used in the manufacturing process. To understand the feasibility of the options, an economic analysis is performed, and some economic indicators are evaluated.

Finally, the results are obtained. The absorption chiller system, coupled with the CHP or with both the CHP and the solar field is feasible from both the technical and the economic points of view, but, since there is the need to drastically reduce the methane consumption (to feed the CHP), the future of the absorption chiller technology is uncertain.

Table of content

Introduction

In the past years an increase in air conditioning needs for both domestic and industrial purposes has been witnessed and considering the actual trends, they will continue to grow, as reported by the IEA in the evolution of the global air conditioner stock.

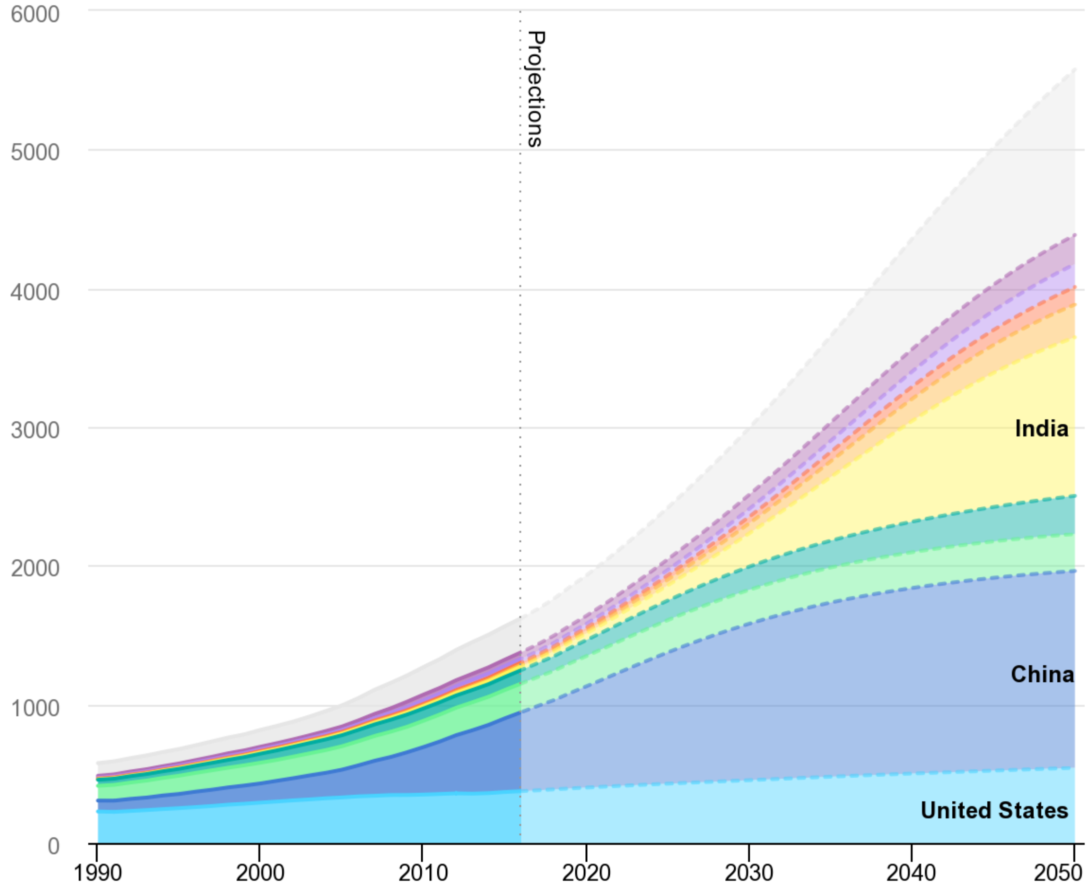

Figure 1: Global air conditioner stock, 1990 – 2050 (Last updated 15 May 2018) [1]

Since cooling needs are almost entirely satisfied by conventional vapor compression chiller, the electricity consumption has increased too. According to the International Energy Agency, the electricity consumption for the ambient cooling in the buildings account for more than the 20% of the total consumption. Usually, the energy mix to produce electricity is far from being renewable. As a result, there has been an increase of the greenhouse gases and pollutants emissions into the atmosphere. In addition, the cooling needs are one of the most important responsible of the variation in electricity demand during summer provoking high peaks and severe problems in the transmission systems.

Different solutions to these problems can be found. The usage of more efficient systems, the increase in the renewable energy production, the usage of different air-cooling systems fed by different sources.

Considering the usage of different ambient cooling technologies, one of the most promising is the absorption chiller. Since the absorption chillers are fed with heat, they don't affect the electricity system. In addition, the heat that enters the chillers is low grade heat. This makes possible the adoption of renewable heat production systems, like the solar thermal collector, or the usage of waste heat, or also the usage of the heat produced by a cogenerating system (that usually presents lower efficiencies during the summer period due to a lower heat demand).

The coupling between a solar thermal collector and an absorption chiller would allow to perform the solar cooling, while the coupling between a cogenerating system and an absorption chiller, the trigeneration.

The adoption of different technologies, the usage of more efficient systems, and the increase of the renewable share in the energy mix would allow to face the several problems linked to the air conditioning needs and the energy consumption in general.

Fortunately, nowadays several organizations and governments are stressing the above-mentioned problems, proposing solutions and introducing new policies. As an example, the Renewable Energy Directive of the European Union.

Solar energy

Solar energy is the energy exiting form the Sun. It is radiant light and heat and is converted in useful electricity and heat by a range of technologies such as photovoltaic panels and solar thermal collectors.

The Sun is a star at the center of our Solar System. It has a diameter of about 1.392.000 km (about 109 Earths) and a mass of about 2,0E+30 kg (about 330.000 times the mass of the Earth). The energy in the Sun is generated by nuclear fusion processes. In these processes, hydrogen is converted into helium. The conversion results in a mass defect and, consequently, energy is released. 26,7 MeV (4,278E-21J) per reaction. Considering the solar mass defect per second (4,3E+09 kg) the power released by the Sun is equal to 3.9E+26 W [2].

Solar energy is by far the most abundant energy source on Earth. The total amount of energy reaching the surface of the Earth each year is 3.400.000 EJ, which is more than 5.000 times bigger than the World total energy consumption.

Solar energy is a renewable source of energy, that means it is replenished at a higher rate than it is consumed. It is converted in useful energy thanks to different technologies. The most used and important, today, are the photovoltaic panels, that convert the light into electricity, and the solar thermal collectors, that absorb heat producing thermal energy.

According to International Energy Agency, in 2020, globally, the energy production from photovoltaic technologies was equal to 823.782 GWh, the 3,31% of the total electricity consumption. The electricity produced with solar thermal collectors, was only 13.718 GWh (0,06% of the total electricity consumption).

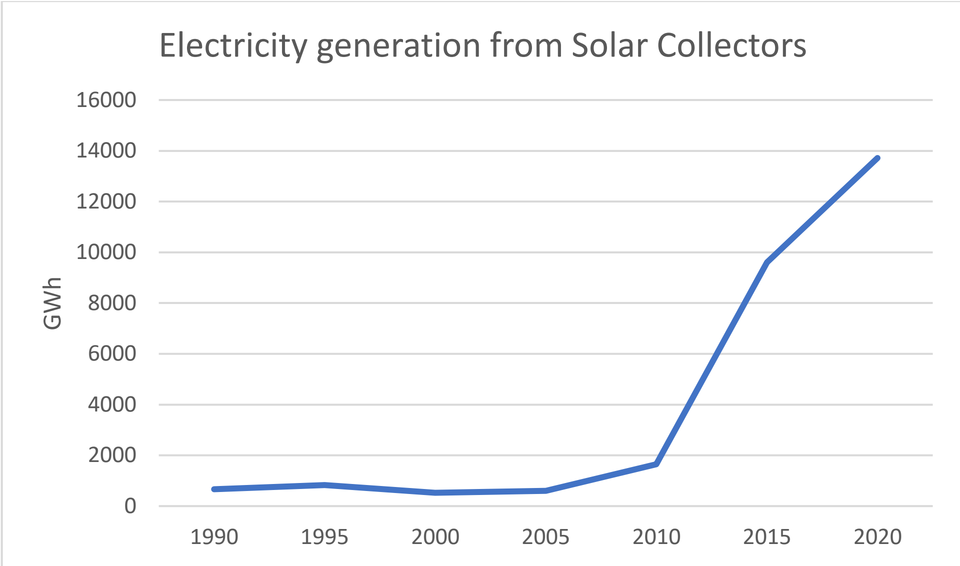

Figure 2: Evolution of the electricity generation from solar thermal collectors 1990-2020

In the previous figure it can be seen the evolution of the electricity production from solar thermal collectors.

Considering the table below, it is possible to see that starting from the 2010 the electricity production from solar thermal collectors has increased a lot. Despite this, in absolute terms it represents only the 0,20% of the total renewable electricity production.

	Total RE	Solar thermal	Percentage (RE)	RE variation	Solar thermal variation
	GWh	GWh	%	%	%
1990	2.232.378	663	0,03	-	-
1995	2.595.275	824	0,03	16,3	24,3
2000	2.781.085	526	0,02	7,2	-36,2
2005	3.185.704	597	0,02	14,5	13,5
2010	3.980.177	1.645	0,04	24,9	175,5
2015	5.151.726	9.607	0,19	29,4	484,0
2020	6.984.521	13.715	0,20	35,6	42,8

Table 1: Evolution of the electricity generation from renewable source and solar thermal collectors

Considering the thermal energy production from solar thermal collectors, in 2020, the heat produced was equal to 2.817 TJ, consisting in the 0,018% of the global heat production.

The heat production from solar thermal collectors, in the past years, has witnessed a strong relative increase too.

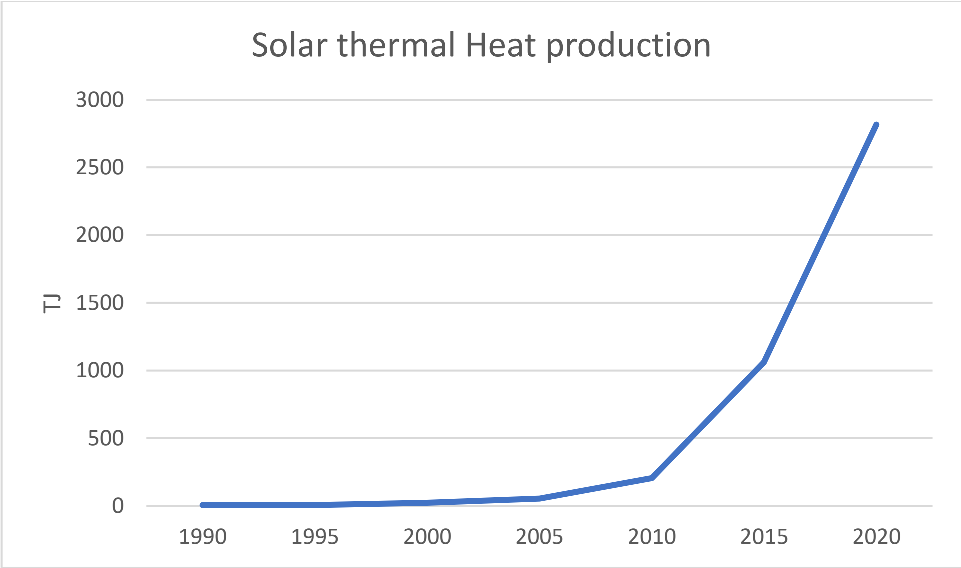

Figure 3: Evolution of the heat production from solar thermal collectors 1990-2020

Solar resource

The solar resource and the availability of solar energy are different around the globe.

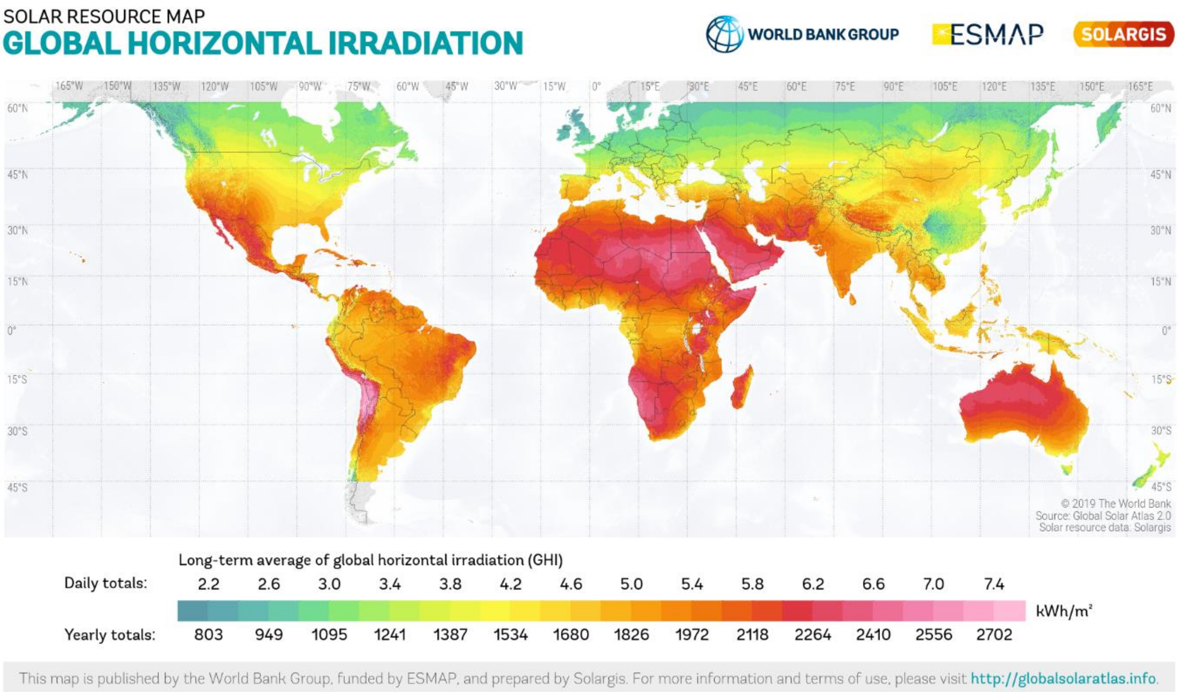

Figure 4: Solar resource map – Global Horizontal Irradiation [3]

Thanks to the image from the World Bank Group, prepared by Solargis [3] we can see the global horizontal irradiation data around the world. Strong differences can be noted between the equatorial belt and the poles (the global horizontal irradiance is mainly affected by the latitude). In the poles the irradiation is quite low, conversely between the tropics it reaches the maximum values (around 2.700 kWh/m^2*year).

The southern part of Europe presents intermediate levels of irradiation reaching values around 1.500-2.000 kWh/m^2*year. These data are available thanks to a lot of databases and open-source software.

Measurement of solar radiation

Different instruments are used to measure the solar radiation. The two most diffuse are the pyranometer and the pyrheliometer.

Figure 5: Instruments to measure solar radiation: a Pyranometer [4] (on the left) and a Pyrheliometer [5] (on the right)

The pyranometer is able to measure the global irradiance (both the direct and the diffuse) and is able to measure only the diffuse irradiance too. To measure the diffuse component, it must be added a shading ring to stop the direct solar irradiance.

To obtain the direct (beam) solar radiation it is better to use a pyrheliometer. This instrument is a bit different with respect to the pyranometer, and measures only the direct irradiance.

Another way to measure irradiance, or to estimate it is thanks to the different models that forecast the irradiance in a defined location for each day of the year, and for different climatic conditions.

One of the most used models is the ASHRAE Clear Sky model, that calculates solar radiation (beam, diffuse, and reflected) for a wide number of locations around the world for days with clear sky.

To validate the model, a comparison can be done between the measured data and the model's results.

Considering only the days in which the sky was completely clear, the following charts report the differences obtained between the measured data and those calculated. The measurements are available thanks to a pyranometer. To better understand the calculation done, see the Appendix I, where a short description of the Sun-Earth relationship is reported, with the solar angles, and the ASHRAE model.

In the charts, the x-axis represents the hour of the day, the y-axis is the irradiance, in W/m^2. The orange line represents the measured data, while the blue one those calculated according the ASHRAE Clear Sky model.

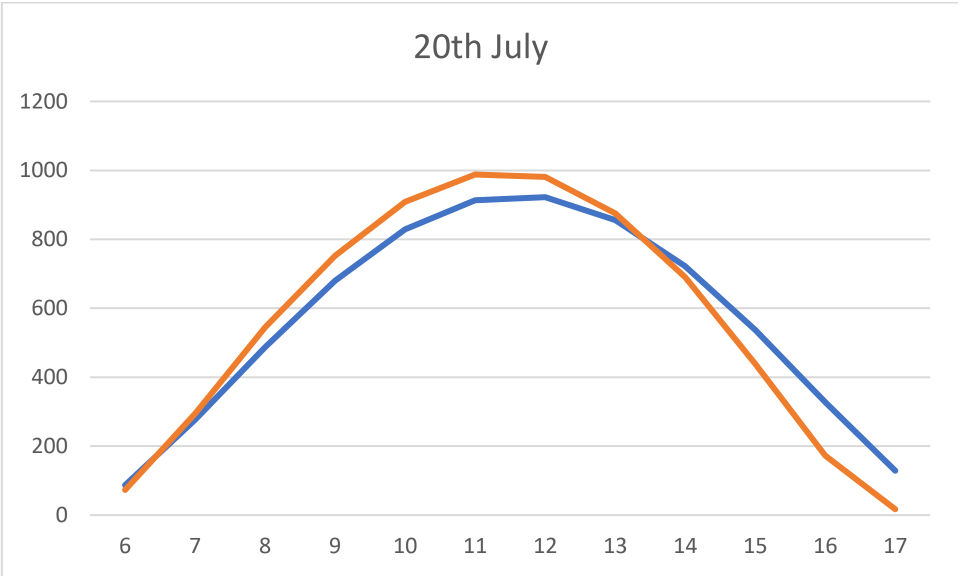

Figure 6: Comparison between the ASHRAE Clear Sky model and measured data

The graph allows to notice the typical bell shape of the solar irradiance for a clear sky day. In the morning, until the sunshine, the irradiance is low, near zero. Then it increases up to a maximum, around 12 AM and 1 PM. The maximum value depends on the day of the year. Since the location considered in this study is in the northern emisphere at a latitude of about 45°, the highest values are between April and September, while the lowest are between October and March. During the afternoon the irradiance decreases until the sunset, where it reaches negligible values.

The graph above represents an example of the comparison of the model with real data. The day selected is the 20^{th} of July. In Annex I there are reported the graphs for a sunny day of each month.

The knowledge of these data is at the base to evaluate the producibility of a solar thermal field, and consequently to know the available heat to feed an abosprtion chiller.

Solar thermal collectors

Solar thermal collectors are special kind of heat exchangers that transform solar radiation energy to internal energy of the transport medium. The solar collector is a device which absorbs the incoming solar radiation, converts it into heat, and transfers this heat to a fluid (usually air, water, or oil) flowing through the collectors [6].

Solar thermal collectors are classified by the *United States Energy Information Administration* as low, medium, or high-temperature collectors.

- Low-temperature collectors are flat plate generally used to heat swimming pools.
- Medium-temperature collectors are usually flat plates but are used for heating water or air for residential and commercial use.
- High-temperature collectors concentrate sunlight using mirrors or lenses and are generally used for electric power production.

There are many types of solar collectors. According to their shape and features, they can be divided into different categories:

- Based on radiation focusing (concentrating collectors, non-concentrating collectors)
- Based on shape (flat-plate collectors, evacuated tube collectors)
- Based on solar tracking (fixed collectors, tracking collectors)

The main difference between the concentrating and the non-concentrating solar collectors is the *concentration ratio*, that is the ratio between the solar aperture surface and the absorber surface (the maximum ideal concentration factors are 213 for the line focusing collectors, and 45.300 for the point focusing collectors).

Among the non-concentrating solar collectors, the most used are the flat plate collectors and the vacuum tubes.

Considering the concentrating solar collectors, different typologies exist. The solar tower and the dish systems, that are point focusing power plants, and the parabolic trough and the Fresnel trough, that are line focusing power plants.

For the solar collectors three different area are defined:

- Gross area: area defined by the maximum width and the maximum length.
- Aperture area: transparent area that allows the entry of solar radiation inside the collector.

- Absorber area: area of the absorption zone, which in the case of flat collectors corresponds to the collectors' plate.

Different values of efficiencies can be obtained depending to the area used as a reference.

In the next part a brief description of the flat plate, the vacuum tube and the high vacuum flat plate collectors is reported.

Flat Plate Collectors

Flat plate collectors are designed for applications requiring energy delivery at moderate temperatures, up to about 100°C above ambient temperature.

The main applications of these units are in domestic hot water, space heating, air conditioning, and industrial process heat.

A flat plate collector is made of different components:

- The cover (glass). It is transparent, usually one or more sheets of glass. It is used to reduce upper losses and needs to be transparent to let the solar radiation to pass through.
- The absorber plate, whose goal is to absorb solar radiation and to emit as low as possible. Typically, it has dark colors.
- The tubes, where the solar thermal fluid passes from the inlet to the outlet. The fluid is heated up by the absorber plate.
- The manifolds.
- The thermal insulation that is used to minimize heat losses from the back and the sides of the collector.
- The frame casing. It encloses the various components and protect them.

Figure 7: Flat plate solar thermal collector components [7]

Collector type	**CAPEX [€/kW]**
Flat Plate Collector (FPC)	250-700

Table 2: Flat Plate Collector specific cost

Energy losses in a flat plate solar collector

The solar energy reaching the solar collectors is not completely transferred to the thermal fluid. During the transmission, several losses occur.

First of all, the solar radiation hits the glass cover, that is responsible of two different losses:

- Since the cover is not perfectly transparent, a portion of the radiation is reflected (8%).
- The cover absorbs a very low amount of solar energy (2%).

These numbers are only representative of what happens. Every installation presents different values according to the shape and the characteristics. Following these data, a percentage of about 10% of the incoming solar radiation doesn't reach the collectors because of the presence of the glass.

The remaining part, reaching the collector is not completely absorbed. Other losses are present:

- Reflection (8%), similar to the cover.
- Convection losses (13%). Since in the layer between the cover and the absorber there is not vacuum, convection losses occur. This source of losses is reduced in the evacuated tubes or creating vacuum in the layer.

- Radiation (6%). This loss is due to the fact that also the absorber emits radiation. This source of losses is reduced in the evacuated tubes.
- Heat conduction (3%). This is reduced adopting a better insulation layer.

The image below sums up all the losses present in a flat plate solar collector. It can be noted that only about the 60% of the incoming solar radiation is absorbed by the absorber and is able to heat up the heat transfer fluid.

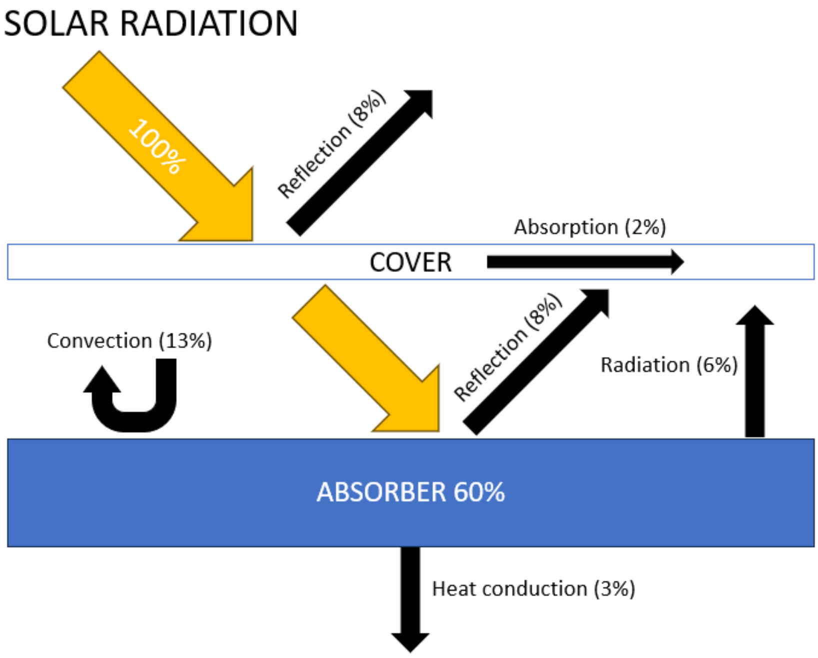

Figure 8: Energy losses in a flat plate solar collector

Other losses are present along the system between the absorber and the final useful energy. The main important are the losses due to the transmission (pipes and heat exchangers).

Evacuated Tubes

The evacuated tubes have been developed to reach higher efficiencies in comparison to flat plate collectors. These collectors are able to reach temperatures up to 180°C.

These solar collectors consist of a heat pipe inside a vacuum-sealed tube. Vacuum acts as an insulator reducing any heat loss significantly to the surrounding atmosphere either through convection or through radiation, making the collector much more efficient than the internal insulating that flat plate collectors have to offer [8].

These collectors are not as efficient as flat-plate collectors at low inlet temperatures and high incident solar radiation, because of high optical losses, but perform much better, because of low thermal losses, at temperatures above 100°C and in low solar radiation. These characteristics make them particularly suitable for high latitude locations.

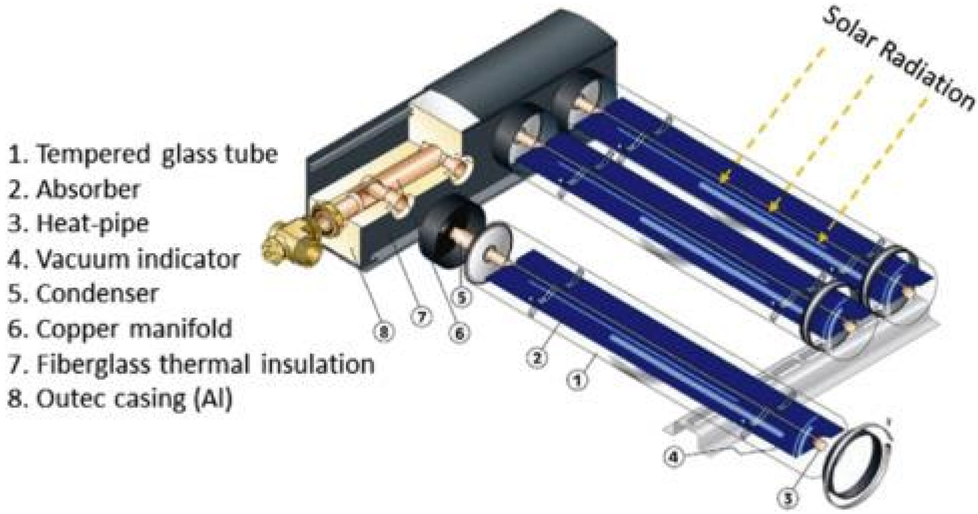

Figure 9: View of an evacuated tube collector and its main components [9]

Collector type	**CAPEX [€/kW]**
Evacuated Tube Collector (ETC)	800-1100

Table 3: Evacuated Tube Collector specific cost

High vacuum Flat Plate Collectors

Evacuated flat plate solar collectors provide all the advantages of both flat plate and evacuated tube collectors combined together. They surround a large area metal sheet absorber with high vacuum inside a flat envelope made of glass and metal. They offer the highest energy conversion efficiency of any non-concentrating solar thermal collector [10].

High Vacuum Flat Panels (HVFP) produced by TVP operate with pressurized water (typically 6 bar) in an optimal temperature range between 100 and 150°C but it is certified (Solar Keymark certificate) until 200°C. The efficiency of the panel is mainly a function of the temperature difference between the surrounding environment and the temperature of the fluid [8].

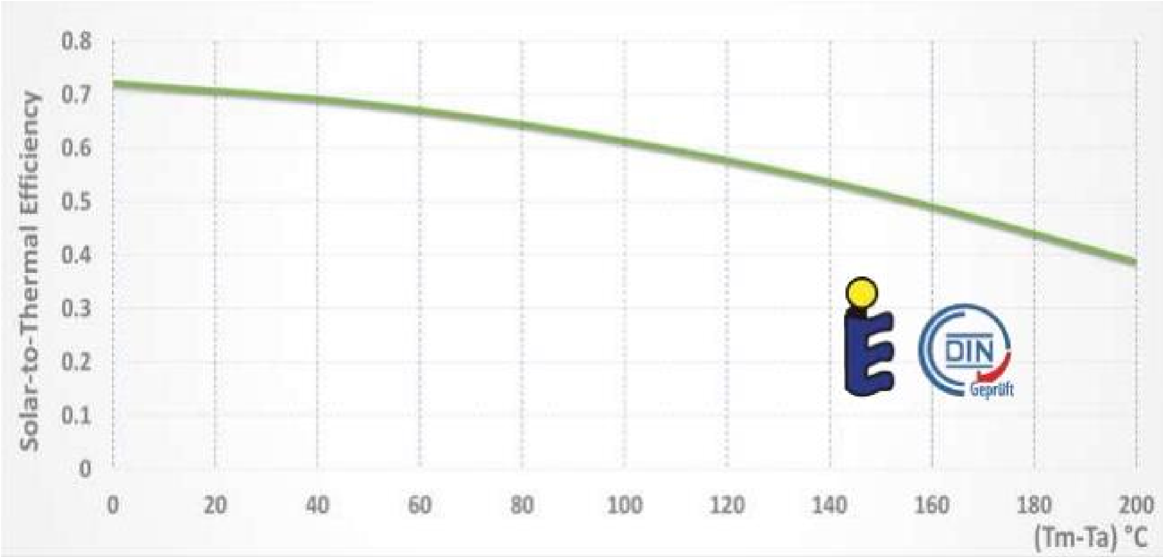

Figure 10: Solar Keymark certificate: collector's efficiency

According to its wide operational temperature range and power, this panel can be used for multiple purposes: industrial process heat, desalination, air conditioning and cooling.

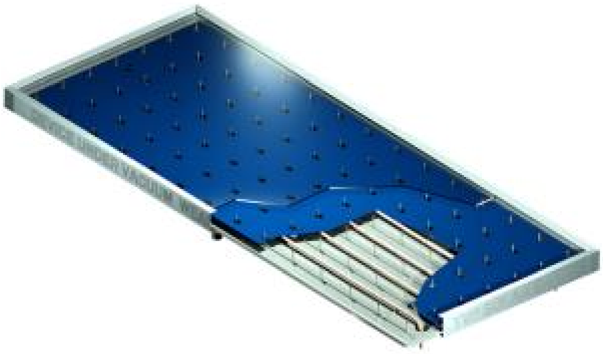

Figure 11: View of a High vacuum Flat Plate Collector [8]

Collector type	CAPEX [€/kW]
High Vacuum Flat Plate Collector (HVFPC)	1200

Table 4: High vacuum Flat Plate Collector specific cost

Energy balance

In steady state conditions, there must be an energy balance between the solar power, the useful power, and the losses. This allows to calculate easily the useful power produced by the solar collectors.

The equilibrium equation is the following:

$$Q_s = Q_{opt} + Q_{loss} + Q_u$$

Q_s: solar power

Q_{opt}: optical reflection losses

Q_{loss}: heat losses

Q_u: useful power

With the optical reflection losses defined as follow:

$$Q_{opt} = [(1-\tau) + \tau(1-\alpha)]GA_{coll}$$

τ: transparent coverage transmission factor

α: collector plate absorption factor

G: solar radiation incident on the collector plane

A_{coll}: collector surface

The heat losses are evaluated considering the temperatures involved and how the collectors are insulated:

$$Q_{loss} = UA_{coll}(T_{coll} - T_{amb})$$

U: transmittance, that includes both the front and the back of the plates (linearized).

$$T_{coll} = \frac{T_{out} - T_{in}}{2}$$

T_{coll}: average temperature of the thermal fluid in the collector

T_{out}: temperature of the fluid at the outlet of the collector

T_{in}: temperature of the fluid at the inlet of the collector

T_{amb}: ambient temperature

The useful power is calculated as the gain, in terms of temperature, between the inlet and the outlet of the heat transfer fluid.

$$Q_u = mc_p(T_{out} - T_{in})$$

m: mass flow rate of the heat transfer fluid

c_p: specific heat of the heat transfer fluid

After some manipulations, it is obtained that:

$$Q_u = mc_p(T_{out} - T_{in}) = A_{coll}[S - U(T_{coll} - T_{amb})]$$

Where S is the solar radiation absorbed by a collector per unit area:

$$S = \tau\alpha G$$

Thanks to the previous equation it is possible to evaluate the useful power starting from the irradiance and the average temperature of the working fluid.

More equations are available to evaluate the useful power starting from other parameters.

Instantaneous efficiency of a solar thermal collector

To evaluate the efficiency of a solar collector, different methods exist.

It can be calculated as the quotient between the useful thermal power and the solar radiation in the plane of collector:

$$\eta_{coll} = \frac{Q_u}{GA_{coll}}$$

In Europe it is determined by standard EN 12975, where the efficiency is a function of the mean fluid temperature:

$$\eta_{coll} = \eta_0 - \frac{a_0}{G}(T_{coll} - T_{amb}) - \frac{a_1}{G}(T_{coll} - T_{amb})^2$$

With:

$$\eta_0 = (\tau\alpha)F'$$

And

η_0: collector optical efficiency

F': solar collector efficiency factor

a_0: linear coefficient of thermal losses

a_1: quadratic coefficient of thermal losses

Another way is to evaluate the efficiency as a function of the inlet fluid temperature, the *Hottel-Whillier equation:*

$$\eta_{coll} = F_R\left(\tau\alpha - \frac{U_L(T_{in} - T_a)}{G}\right)$$

Where F_R is the heat removal factor.

Solar cooling

Summer cooling and air conditioning are very important in industry to guarantee the comfort of the workers. The energy demand related to summer air-conditioning mainly depends on two factors: the external conditions and the internal ones.

The most important external conditions are the air temperature and the air humidity, while the most important internal conditions are, first of all, the set point temperature, and then the internal loads.

Intuitively, the need for cooling is proportional to the solar intensity, thus nearly matching the time of peak cooling demand with the time of maximum sunlight [11].

The adoption of solar assisted cooling and air conditioning presents several improvements from both the environmental and the economic points of view:

- Savings in primary energy consumption and CO2 emissions.
- Load levelling
- Better performances of the solar collectors (able to exploit the summer sun-rays)
- Less noise emission and less vibration than vapor compression technologies.

In addition, there is a coupling between the solar production and the air-conditioning related energy consumptions, both on a seasonal and on a daily basis. Conversely, the need for heating is out of phase with respect to the solar production. In this way, the development of a solar cooling system would increase considerably both the efficiency and the economic return of solar collectors.

In the graph below there are reported three curves normalized to their maximum value:

- In grey, the average solar radiation. It presents a trend that increases during summer and has the minimum during the winter months.
- In blue, the heating needs. It is present only during the winter months. During summer months it is equal to zero. These data are obtained from the total gas consumption of the Pessione plant of the Martini&Rossi S.P.A.

- In orange, the cooling needs. It has the opposite behavior compared to the heating needs. It has null values during winter and the maximum during summer. These data are obtained from the meter connected to the vapor compression chiller that cools the rum bottling department of the Pessione plant of the Martini&Rossi S.P.A.

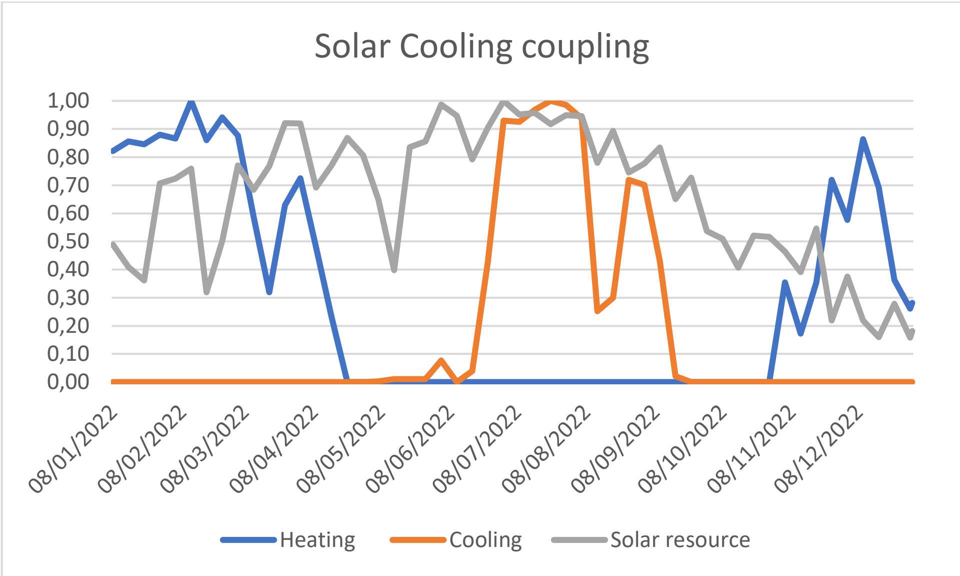

Figure 12: Solar cooling coupling: heating demand, cooling demand, and solar resource trends

The previous real data confirm the opportunity of the solar cooling and the coupling between the solar resource and the cooling demand.

Solar cooling can be applied not only to air conditioning, but also to industrial processes, especially refrigeration. The availability of high efficiency solar thermal collectors coupled with solar cooling systems working with particular solutions permits to reach temperatures below 0°C, up to -40°C, making the solar resource sufficient for refrigeration. Obviously, the coupling between the production and the demand of the system is lower in comparison to solar cooling systems used for air conditioning. This is because the cooling needs for refrigeration are typically more stable during the year (even if are affected by the external temperature too). A backup traditional system for refrigeration must be considered and dimensioned for the correct working of the industrial process.

The solar cooling applied to refrigeration seems to work better as load levelling system, to avoid high electricity consumption peaks.

Solar cooling systems

Different solar heat driven cooling technologies are available in the market, which can be used for air conditioning in combination with solar thermal collectors.

Closed cycle systems

In a closed loop cycle the operating fluid is chilled water, which is used to remove the loads from the buildings. The central cold water distribution grid may serve decentralized cooling units.

Absorption cooling system: it is a heat driven heat-pump, in fact a *thermal compression* of the refrigerant is achieved by using a liquid refrigerant/sorbent solution and a heat source, replacing the electric power to mechanical compressor. The refrigerant vapor is absorbed into a solution and pumped to the generator. Into the generator heat is supplied to let the refrigerant vaporize. Then it condensates, expands, and finally evaporate in the evaporator to cool the heat transfer fluid. At this point the cycle restarts with the absorption of the refrigerant vapor. For chilled water above 0°C typically a liquid H_2O/LiBr solution is applied with water as refrigerant.

Using a different solution, the absorption chiller is able to reach temperatures below 0°C. Thanks to this, it can be used also for refrigeration. The most used solution for this purpose is NH_3/H_2O, in which the refrigerant is ammonia, that is able to reach temperatures below 0°C. On the contrary, conventional H_2O/LiBr absorption chiller cannot produce a chilled fluid below 0°C because of the temperature of solidification of water.

Figure 13: View of an absorption chiller [12]

Adsorption cooling system: the refrigerant vapor is adsorbed onto the surface of a solid adsorbent. Solid sorption commercial systems use water as refrigerant and silica gel as adsorbent. Since the solid sorbent cannot be circulated, adsorption chillers consist of two separate chambers, both containing the adsorbent.

As for the absorption systems, the adsorption systems exploit the evaporation at low pressure of the water to take up the heat from the chilled water circuit.

Adsorption systems allow for somewhat lower driving temperatures but have a somewhat lower efficiency compared to absorption systems under the same conditions [13].

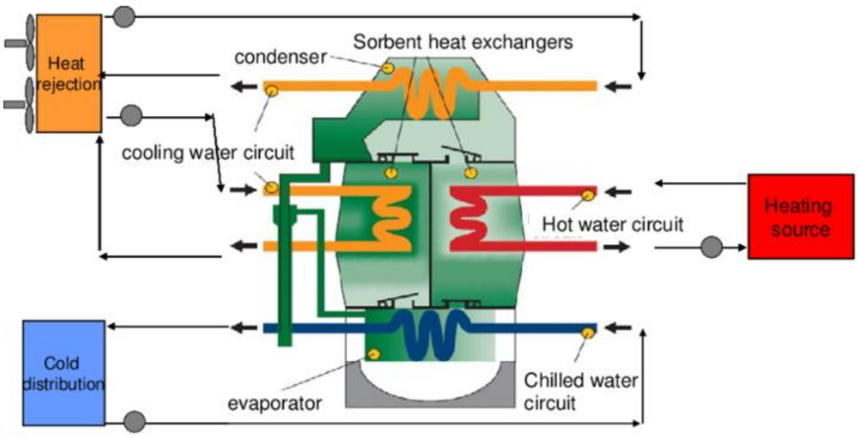

Figure 14: Schematic of an adsorption chiller [14]

Open cycle systems

Open loop cycles are also referred to as desiccant cooling systems. They can be used for a direct air treatment in HVAC systems.

Desiccant system: solar heat is used to regenerate the desiccant after it has absorbed water from incoming air stream. The desiccant cooling system takes air from the building, dehumidifies it with a solid or liquid desiccant, cools it by heat exchange and then evaporatively cools it to the desired state. The desiccant must be regenerated by heat. The desiccant can be either solid or liquid and is used to facilitate the heat exchange of sensible and latent heat of the conditioning air stream. Since the solid desiccant cannot be circulated by pumping, these systems usually employ a rotary bed carrying the sorbent material, referred to as a 'desiccant wheel', to allow continuous operation [13].

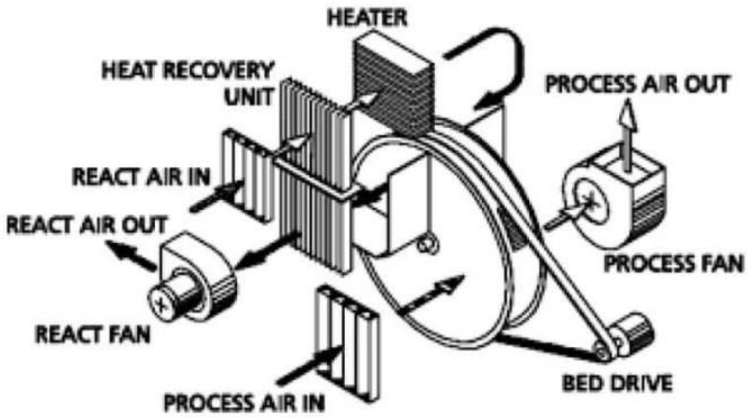

Figure 15: Schematic of a desiccant system [15]

Considering the closed cycle systems, a rule of the thumb can be followed to estimate the possible cooling capacity related to solar collectors' area. For 1 kW cooling capacity, approximately 3 m^2 collector area is needed.

The overall efficiency depends on the collector efficiency and on the coefficient of performance (COP) of the thermally driven chiller.

Cogeneration Systems - Combined heat and power (CHP)

Cogeneration systems refer to energy systems that have the ability to produce two useful commodities simultaneously. A good example of cogeneration systems are combined heat and power plants, where electricity and useful heat are both produced from one plant. Cogeneration is a highly efficient energy orientation that can achieve primary energy savings compared to conventional power and heat supply [16].

A combined heat and power system or cogeneration system is a heat engine able to produce both heat and electricity. Cogeneration supplies currently 11% of electricity and 15% of heat in Europe.

Traditional systems to produce electricity and heat, overall, present lower efficiencies in comparison to combined heat and power systems.

Thermal energy generator, like boilers, presents an efficiency around 85% (up to 95% for the most recent technologies), while electricity generators present an efficiency near 40%.

The image below, representing two traditional systems, reports the amount of energy that is needed to produce 44 kWh of thermal energy and 41 kWh of electricity.

Considering the above-mentioned efficiencies, the input energy is equal to 52 kWh for the thermal energy, and 102 kWh for the electrical energy. Globally, to produce these energies, an input of 154 kWh must be supplied.

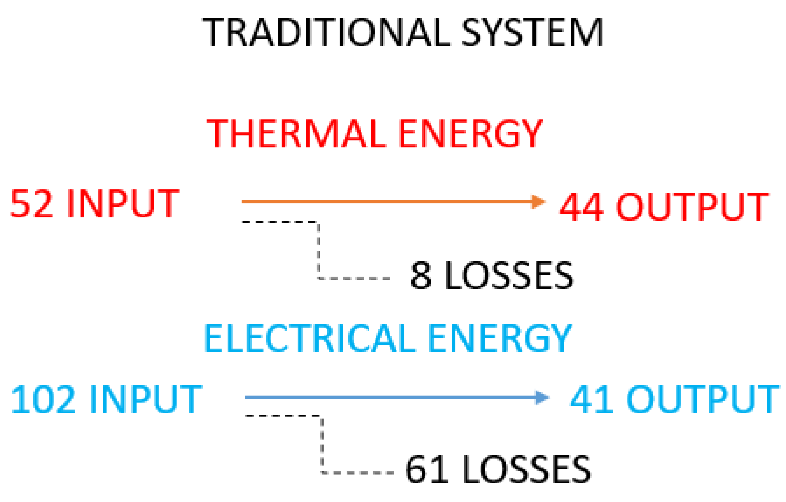

Figure 16: Thermal and electrical energy production – Traditional system

Similarly, these calculations can be done for a combined heat and power system.

The cogeneration systems present several different efficiencies.

Electrical efficiency:

$$\eta_{EL} = \frac{E_{EL}}{E_{Fuel}}$$

Thermal efficiency:

$$\eta_{TH} = \frac{E_{TH}}{E_{Fuel}}$$

Global efficiency:

$$\eta_{TOT} = \frac{E_{EL} + E_{TH}}{E_{Fuel}}$$

Typical values of efficiency for these systems are:

- Electrical efficiency: 41%
- Thermal efficiency: 44%

Considering these data, to produce the same amount as the traditional systems case, the total input energy decreases to 100 kWh.

The combined heat and power systems allow to achieve higher efficiencies in the energy production, reducing the amount of fuels needed to produce both the electricity and the thermal energy.

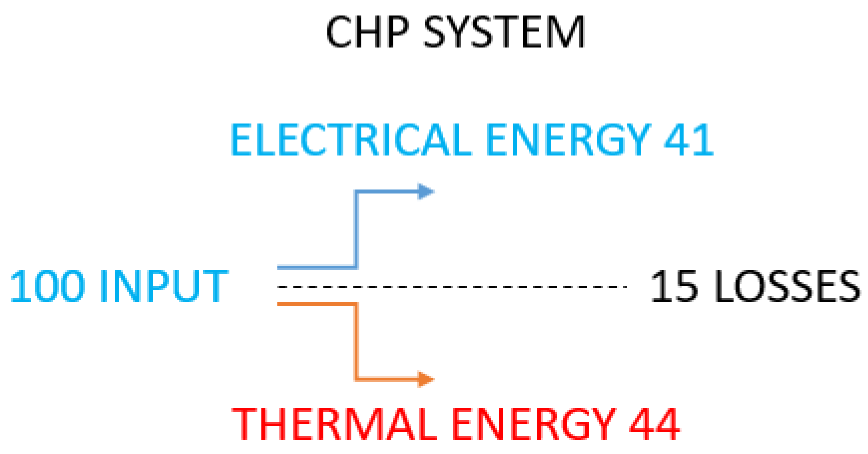

Figure 17: Thermal and electrical energy production – CHP system

The CHP systems can be classified according to how the power and heating equipment are organized:

- Topping cycle
- Bottoming cycle

In a topping cycle the primary heat is used for electricity, while waste heat is used for secondary heating or power applications. Thermal energy is a by product used for process heat or other. This is the most popular method of cogeneration.

In a bottoming cycle the primary heat is used directly for process requirements, while waste heat is used to produce electricity. The primary fuel produces high temperature thermal energy. Rejected heat is used to generate power. This cycle is suitable for manufacturing processes.

The power equipment is usually a gas turbine, a steam turbine, a gas turbine-combined cycle, or a reciprocating engine. The heating equipment can be a waste heat recovery, a boiler/heater, or a heat pump.

The fuel used in the cogeneration systems can be both fossil and renewable. It can be natural gas, diesel, coal, but also biogas, biomass.

Gas turbine topping cycle cogenerating system

A gas turbine, also called a combustion turbine, is a type of continuous flow internal combustion engine.

The main parts common to all gas turbine engines are:

- A rotating gas compressor
- A combustor
- A compressor driving turbine [17]

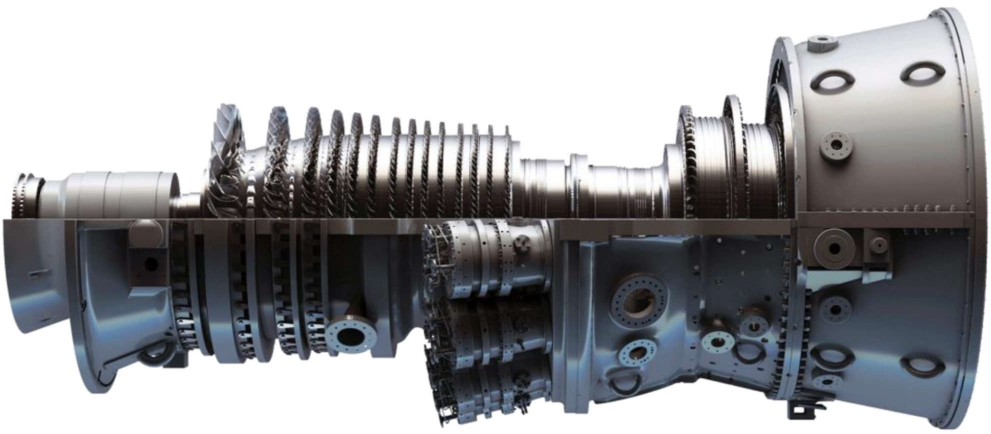

Figure 18: Heavy duty gas turbine [18]

All the components are placed along a unique axis. The coupling with the alternator is on the cold side, near the inlet of the compressor.

An ideal gas turbine works following the Brayton cycle: an isentropic compression, an isobaric combustion, an isentropic expansion, and a heat rejection.

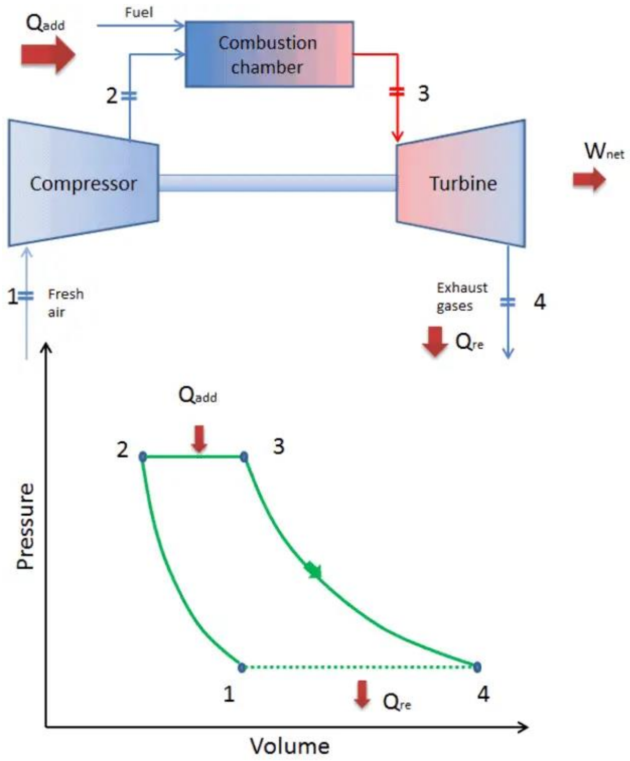

Figure 19: Brayton cycle [19]

The flue gases exiting from the gas turbine are at very high temperature. This allows to recover the heat in two different ways. In a CHP system the heat is recovered thanks to a heat recovery system that heats up water. This water can be heated up to produce steam or to produce hot water both for heating, for sanitary use, and for process purposes.

The heat exiting from the turbine of a gas engine can also be used to heat up water to produce steam that feeds a steam turbine to produce additional electrical power.

A gas turbine presents several advantages, like the short start-up time. In addition, the efficiency of a simple gas turbine is quite high. The possibility to couple the gas turbine with a heat recovery system or a steam turbine allows to achieve even higher efficiencies (higher than 80% for CHP systems and higher than 60% for combined gas and steam turbines).

Below, a sketch of a gas turbine topping cycle CHP. The prime mover is the gas turbine generator, that is placed in a room where is present an air intake. From left to right, in black, the main component of the gas turbine: the alternator, that produces electricity (arrow in green), coupled by the same shaft to the compressor and the turbine. Between the compressor and the turbine, the combustor, with the inlet for the fuel (blue arrow).

After the turbine, the exhausts flow through a bypass valve that decides to send them directly to the atmosphere or to the waste heat recovery equipment (represented in grey). If the gases are sent to the atmosphere, no heat recovery is performed. On the contrary, the heat of the exhausts is recovered, and it is available for other purposes (red arrow). The lower temperature exhausts then exit from a second stack placed after the heat recovery system.

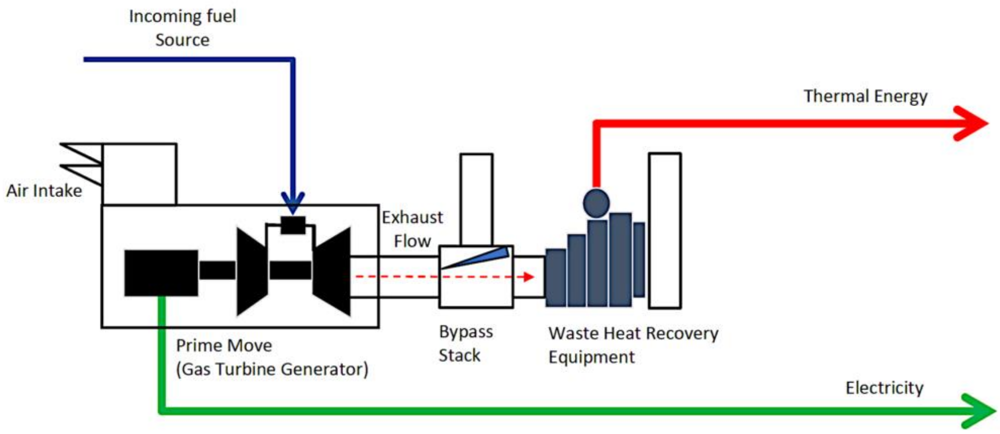

Figure 20: Sketch of a gas turbine topping cycle CHP [20]

If the gas turbine is coupled with a steam turbine, the cycle is quite similar, but differs in the heat recovery system. In fact, the heat recovery system is also a steam generator, that is fed by a closed water cycle.

A water pump pushes the water inside the heat recovery system, where it is heated up by the heat of the exhaust gases. From the heat recovery there are two outlets. The first is for the exhausts, while the second is for the steam, that goes directly to a steam turbine. After the steam turbine there is a condenser that condensates completely the steam. The steam turbine is coupled to an alternator to produce additional electricity.

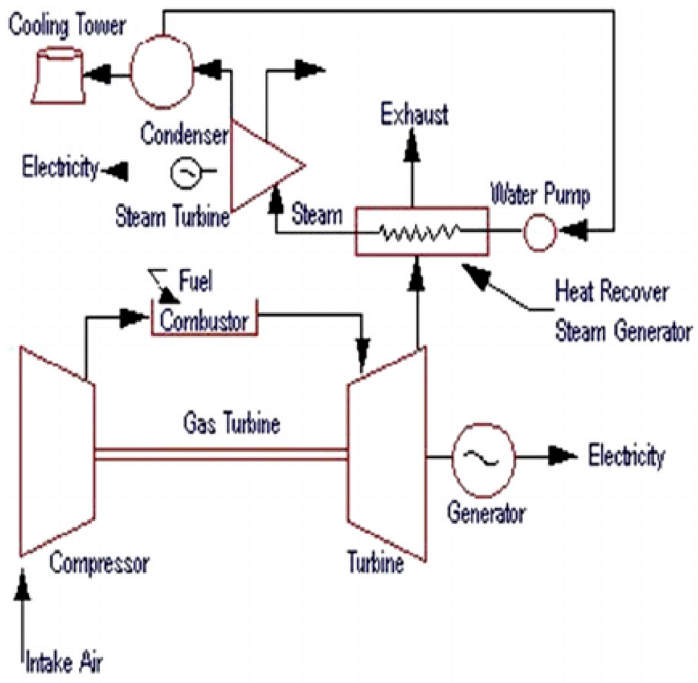

Figure 21: Sketch of a combined gas and steam turbine system [21]

Trigeneration

Trigeneration or combined cooling, heat and power (CCHP), is a process by which some of the heat produced by a cogeneration plant is used to generate chilled water for air conditioning or refrigeration. An absorption chiller is linked to the combined heat and power (CHP) to provide this functionality.

Trigeneration systems present several benefits:

- Onsite, high efficiency production of electricity, heat, and cooling energy
- Reduced fuel and energy costs
- Lower electrical usage during peak summer periods
- Significant reduction in greenhouse gas emissions
- No harmful chemical pollutants since water is used as the refrigerant.

The conventional CHP produces electricity and, thanks to a heat recovery system, heat. The heat produced can be partially used to feed an absorption chiller, in blue in the image in the next page. The absorption chiller produces chilled water or very cold refrigerant fluid (like ammonia).

The absorption chiller can be fed by hot water, steam, or directly by the exhaust gases from the engine (without the heat recovery system).

The output of the chiller can be cold water at a temperature up to 4°C if the chiller works with a couple Lithium Bromide/Water as absorbent/refrigerant, or can be a fluid at very low temperature, up to -60°C if the working couple is Water/Ammonia.

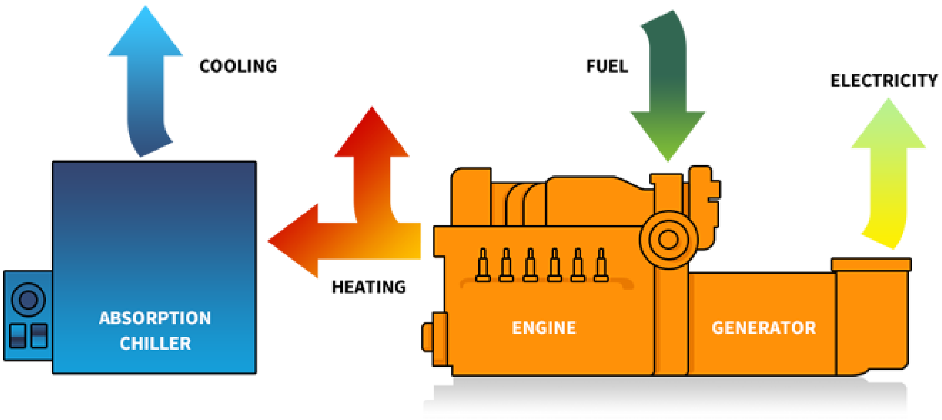

Figure 22: Sketch of a trigeneration system

The efficiency of the chiller is defined by the Coefficient of Performance (COP), the ratio between the output cooling energy and the input thermal energy. It varies between 0,7 and 1 according to the number of the stages of the cooling cycle, to the temperature of the heat source, to the temperature of the refrigerant and to other parameters.

The efficiency of an absorption chiller is lower with respect to that of a conventional compression chiller, but the energy source, heat is a less valuable energy with respect to electricity. The heat recovered in a CHP to feed an absorption chiller has a lower exergy content with respect to electricity.

A CCHP system presents higher efficiencies with respect to traditional power system because the energy of the fuel is exploited more.

Chiller

A chiller is a thermal machine that, thanks to the compression and expansion of a refrigerant fluid, cools down a heat transfer fluid (usually water or air).

Chillers may be classified on the basis of chilling capacity as small size, below 20 kW, medium size, up to 100 kW, and large size, above 100 kW.

It works following a refrigeration cycle. Similarly to the heat pump cycles, the refrigeration cycles allow to transfer heat from one location at a lower temperature to another location at a higher temperature. The aim of the chiller is to refrigerate or to cool the ambient.

Since heat cannot spontaneously flow from a colder location to a hotter area, to move it from the cold source to the hot sink, work is required.

Among the different cycles, the vapor-compression cycle and the vapor absorption cycle are the most used.

The vapor-compression cycle starts with the refrigerant that enters the compressor (1) as a low temperature and low-pressure saturated vapor. The compressor increases both the pressure and the temperature of the vapor, obtaining a superheated vapor (2). Then, the refrigeration fluid passes through a condenser and cools and condensate completely (saturated liquid (3)). The high-pressure liquid passes through the expansion valve which, reducing the pressure, decreases the temperature too (4). Finally, the low-pressure cold mixture (liquid and vapor) of refrigerant goes into the evaporator, where it vaporizes completely (1) collecting the heat from the heat transfer fluid. At this point, the cycle restarts.

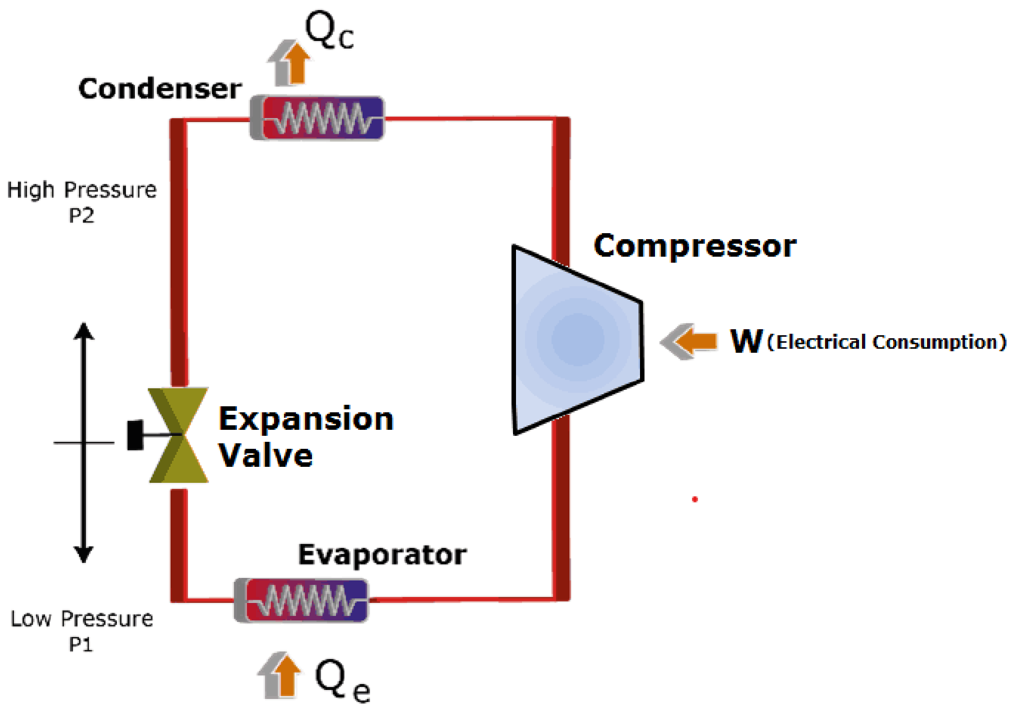

Figure 23: Vapor-compression refrigeration cycle [22]

The compressor can be of different types. To work, the compressor needs electricity, so an electrical energy consumption.

The expansion valve is an important device because it maintains a pressure difference between the low and the high-pressure levels, and because it regulates and controls the amount of liquid refrigerant entering the evaporator.

The condenser and the evaporator are two heat exchangers. They permit the heat transfer between the refrigerator circuit and the other two circuits. The first, in contact with the condenser, can be the external air or a water circuit (evaporative condenser). The second circuit hosts the heat transfer fluid (typically water, air, or glycol), that releases heat to let the refrigerant fluid vaporizes.

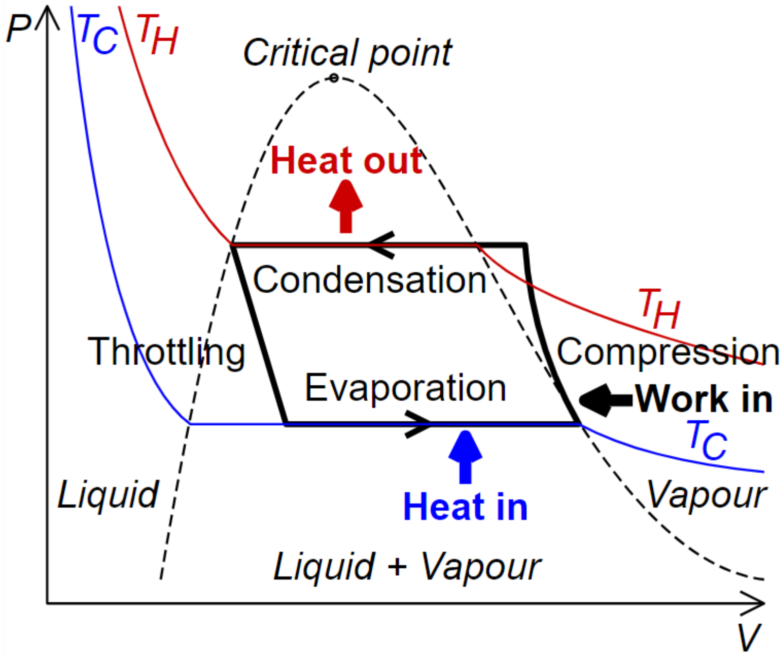

Figure 24: Vapor-compression refrigeration cycle – P-V diagram [23]

In the P-V diagram the cycle can be seen. The compression and the expansion are the vertical transformation (ideally, perfectly vertical), while the horizontal transformations are the evaporation and the condensation.

The cycle starts from the bottom right angle (T_c, low pressyre) and goes counter wise.

Even if the refrigerant fluids present dangerous aspects from the environmental point of view (toxicity and climate change), the vapor-compression cycle is the most used, mainly because the high COP (Coefficient of Performance) it can achieve.

The vapor absorption cycle is similar but presents different features. The biggest difference is in the compression stage. It doesn't need electricity as input energy, it works exploiting the energy from a thermal source. This means that an absorption chiller is a device that can be perfectly coupled with a cogenerating system or with solar thermal collectors (or with all the machines and devices that present waste heat).

The compressor is substituted by a *thermal compressor*, that is made of an absorber, a desorber (or generator), and a solution pump.

Absorption Chiller

The adoption of vapor absorption systems can be useful to reduce the electricity purchased, from the utility companies, to feed the conventional vapor compression refrigerators. The absorption refrigerators are powered by thermal energy, that can derive from waste heat. In addition, the absorption technologies help reduce problems related to CO2 emissions and increase the global efficiency of the energy consumption.

The refrigerant side of the absorption cycle essentially works under the same principle as the vapor compression cycle. However, the mechanical compressor used in the vapor compression cycle is replaced by the thermal compressor in the absorption cycle. The thermal compressor consists of an absorber, a generator, and a solution pump [24].

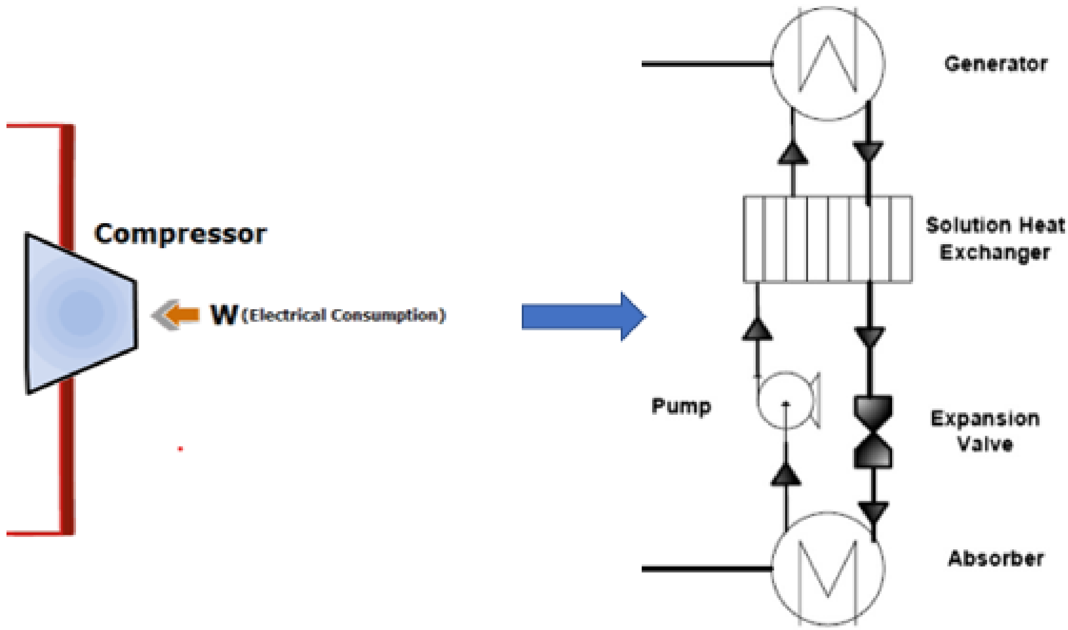

Figure 25: Electrical compressor of a vapor compression chiller (left) [22] and the thermal compressor of a absorption chiller (right) [24]

Absorption process

The working fluid in an absorption refrigeration system is a binary solution consisting of refrigerant and absorbent. Two evacuated vessels are connected to each other. The left vessel contains liquid refrigerant while the right vessel contains a binary solution of absorbent/refrigerant. The solution in the right vessel will absorb refrigerant vapor from the left vessel causing pressure to reduce. While the refrigerant vapor is being absorbed, the temperature of the remaining refrigerant will reduce as a result of its vaporization. This causes a refrigeration effect to occur inside the left vessel. At the same time, solution inside the right vessel becomes more dilute because of the higher content of refrigerant absorbed. This is called the “absorption process” [25].

The absorption process is an exothermic process. Heat is rejected out to the surrounding to maintain the absorption capability. When the absorption occurs, the solution gets more and more dilute until the saturation. The refrigerant must be separated from the diluted solution. The separation process is made using heat. It is applied to the right vessel in order to dry the refrigerant from the solution.

These processes are reported in the figure below.

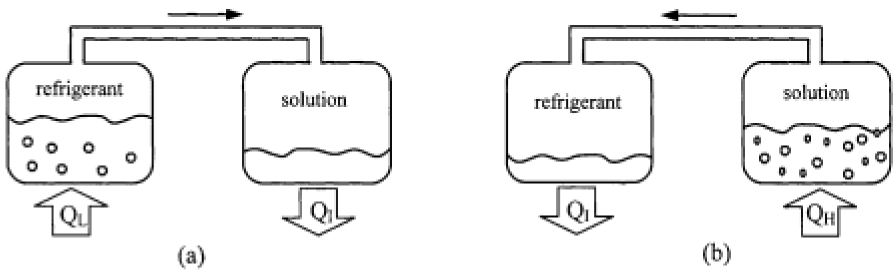

Figure 26: the absorption process (a) and the regeneration process (b) [25]

In figure 26 (a) it can be seen the absorption process occurring in the right vessel. As a consequence, there is a heat release from the vessel. On the contrary, since the temperature of the refrigerant decreases during the absorption, heat is absorbed by the left vessel.

In figure 26 (b) it can be seen the "regeneration" of the refrigerant and the solution. Heat is supplied to the right vessel, and the condensation of the refrigerant in the left vessel releases heat.

The absorption refrigeration cycle

The cooling effect cannot be performed continuously, since the absorption and the separation processes cannot be done simultaneously. To overcome this problem, and to perform continuously the cooling effect, a combination of these two processes is needed.

In the figure from Srikhirin et al. [25] the absorption refrigeration cycle is reported.

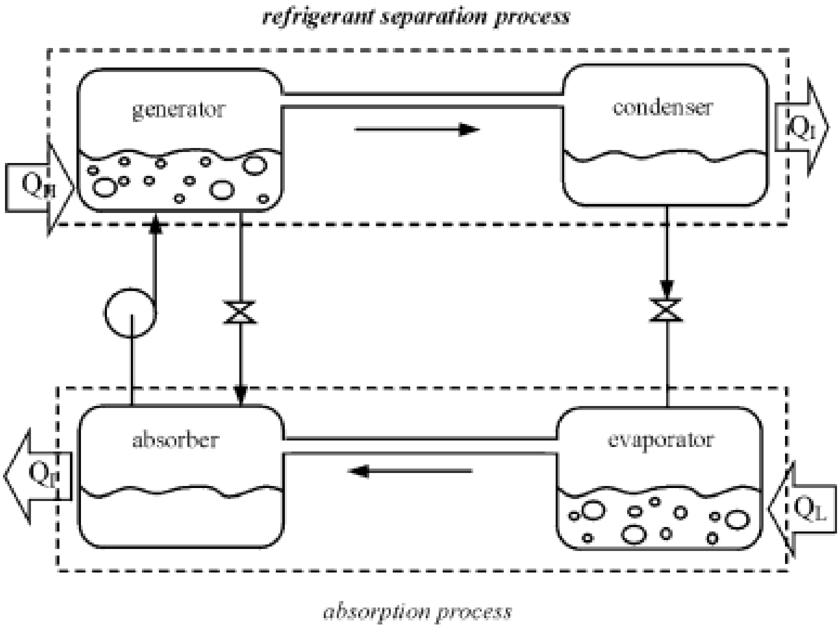

Figure 27: A continuous absorption refrigeration cycle [25]

In the figure 27, the lower part represents the absorption process, while the upper part represents the refrigerant separation process.

In the evaporator, bottom right vessel, there is cold low-pressure water. Low temperature heat (Q_L) is absorbed by the bottom right vessel. In this way the water starts to evaporate. The low temperature heat is the heat taken from the water (or the heat transfer fluid) that must be chilled.

The water vapor, from the evaporator goes to the absorber. In the absorber there is the liquid solution absorbent/refrigerant. The vapor is absorbed by the solution. Since the absorption process is exothermic, from the bottom left tank, the absorber, an equal amount of heat, as the low temperature heat, is rejected to the ambient at an intermediate level of temperature (Q_I).

The solution, absorbing the water vapor, becomes more and more diluted. To regenerate the solution, it is pumped to the generator, where a high temperature heat source (Q_H) is applied. The heat source allows the water to evaporate. The water vapor is separated from the solution and sent to the condenser. The regenerated absorbent/refrigerant solution is sent back to the absorber, passing through a valve.

The water vapor goes into the condenser. Here, there is a heat release (Q_I) to let condensate the vapor, obtaining water at the upper level of pressure and low temperature. The water is finally sent to the evaporator, passing through a lamination valve. The lamination valve reduces the pressure of the water and at the same time its temperature. The water inside the evaporator is at low pressure and low temperature, and it is able to absorb low temperature heat from the thermal fluid to be chilled and restarts the cycle.

Overall, the energies involved are the low temperature heat (Q_L), the heat absorbed by the refrigerant from the heat transfer fluid (water, glycol…), the high temperature level (Q_H), that is the heat that drives the system, and allows the solution to be regenerated. This heat is usually available from a cogenerating system, a solar thermal system, or from waste heat. The third energy involved is the intermediate temperature heat (Q_I), that is equal to the sum of the other two energies, and it is released thanks to an evaporative condenser.

Single-effect absorption

The single-effect absorption system is the simplest and most commonly used design.

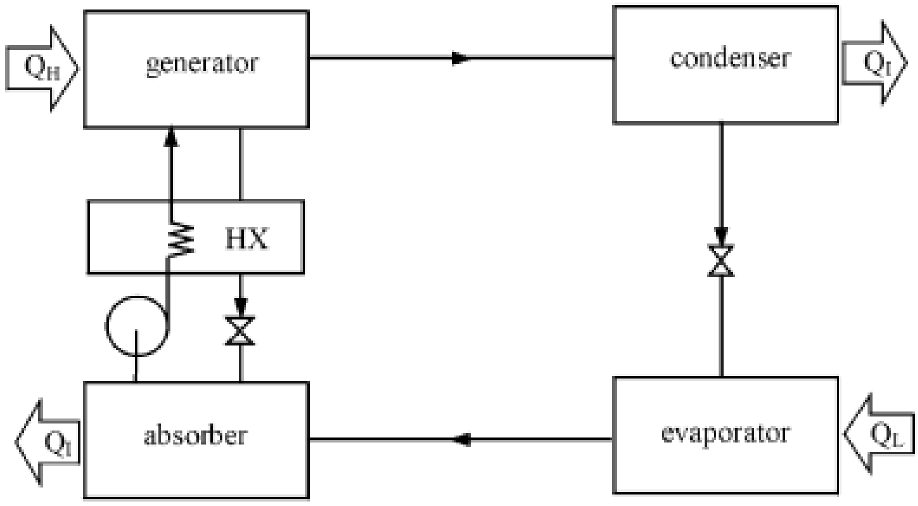

Figure 28: A single-effect LiBr/water absorption refrigeration system with a solution heat eschanger (HX) that helps decrease heat input at the generator [25]

Following the process described previously, the high temperature heat is supplied to the generator to evaporate the refrigerant out from the solution. The refrigerant condensate in the condenser and passes through an expansion valve. Then evaporate in an evaporator (subtract the low temperature heat), and goes into the absorber.

The heat exchanger allows the solution from the absorber to be preheated before entering the generator by using the heat from the hot solution leaving the generator. Therefore, the COP is improved as the heat input at the generator is reduced.

This is the scheme of a single-effect absorption system using a non-volatility absorbent. When volatility absorbents are used, the system requires an extra component called rectifier, which will purify the refrigerant before entering the condenser.

The efficiency of the chiller is evaluated using the COP (Coefficient of Performance). The COP takes into account the useful work, related to the low temperature heat extracted from the heat transfer fluid, and the work supplied to the chiller to obtain the refrigerant effect. It consists in both the high temperature heat and the electrical power supplied to the solution pump.

$$COP = \frac{Q_{COLD}}{Q_{HEAT} + W_{PUMP}}$$

Since W_{PUMP} is negligible with respect to Q_{HEAT}, the formula che be rewrite in this way:

$$COP = \frac{Q_{COLD}}{Q_{HEAT}}$$

Ideally, the COP can be expressed also according to the temperature of the heat sources and sinks:

$$COP_{IDEAL} = \frac{T_L}{T_H} * \frac{T_H - T_I}{T_I - T_L}$$

With the temperatures expressed in Kelvin.

As a consequence, the COP increases increasing T_L and T_H, and decreasing T_I.

The higher the temperature of the high temperature heat, the higher the COP. This means that the availability of hot water at 100°C allows to obtain higher efficiency with respect to systems fed by hot water at 90°C.

The higher the temperature of the low temperature heat, the higher the COP. Usually, the chilled water produced by the absorption chiller exits from the system at 7°C and returns at 12°C. Sometimes the temperature required for the chilled water is different. If it is higher, like 9°C, the system is able to work with a higher efficiency, conversely, if the temperature required il lower, like 5°C, the absorption chiller needs to be over-dimensioned, resulting in a lower efficiency system.

The lower the temperature of the intermediate temperature heat, the higher the COP. The intermediate temperature heat is the energy released by means of an evaporative condenser. Usually, the water flowing in the evaporative condenser circuit enters the absorption chiller at a temperature of 29°C and returns to the evaporative condenser at 34°C. different settings can be performed. Changing these parameters, the system must be designed in a different way, and so is able to reach different efficiencies. If the water arrives at 27°C the systems can work with higher efficiencies. It the water arrives at 31°C the system must be over-dimensioned, obtaining lower COPs.

Double-effect absorption

The main objective of a double-effect absorption cycle is to increase system performance when high temperature heat source is available. The cycle is configured in a way that heat rejected from a high-temperature stage is used as heat input in low-temperature stage for generation of additional cooling effect in the low-temperature stage.

High temperature heat from an external source supply to the first-effect generator. The vapor refrigerant generated is condensed at high pressure in the second-effect generator. The heat rejected is used to produce addition refrigerant vapor from the solution coming from the first-effect generator.

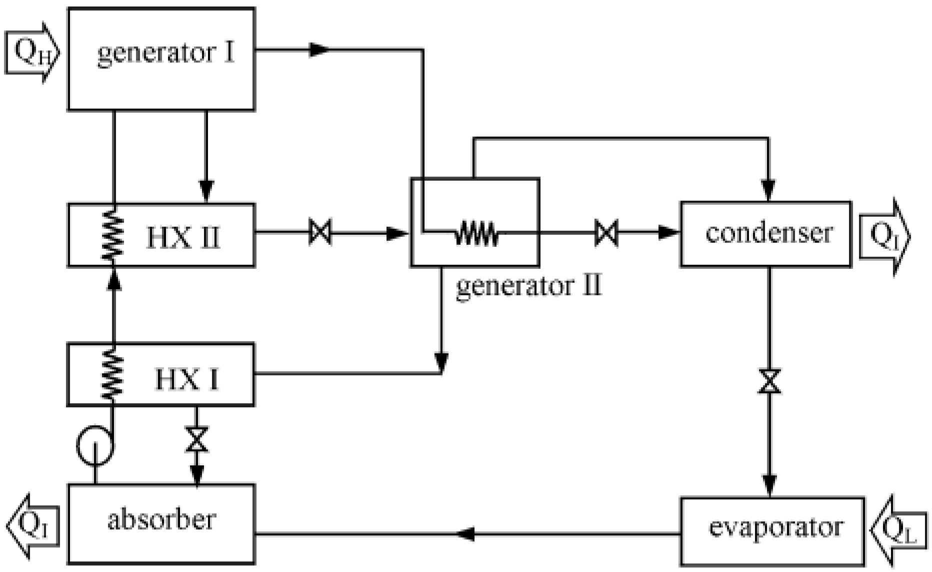

Figure 29: A double-effect LiBr/water absorption cycle [25]

This system permits to achieve higher COPs.

The double-effect absorption system is considered as a combination of two single-effect absorption systems.

If the heat supplied to a single-effect absorption system is A, the useful cooling power is:

$$Q_{C,Single\ Effect} = A * COP_{SINGLE}.$$

Since the heat rejected from the condenser can be assumed equal to the cooling capacity, the heat supply to the second generator of a double-effect cycle is equal to $A * COP_{SINGLE}$. The cooling effect produced from the second-effect generator is:

$$Q_{C,Second\ effect\ generator} = (A * COP_{SINGLE}) * COP_{SINGLE}.$$

Therefore, the COP of a double-effect absorption system is;

$$COP_{DOUBLE} = A * (COP_{SINGLE} + (COP_{SINGLE})^2).$$

Multi-effect absorption

The multi-effect absorption refrigeration cycle goal is to increase the system performance. The constrain to its work is the need of a high temperature heat.

In the following figure is represented a triple-effect absorption cycle. Heat of condensation from the higher-pressure stage is used for refrigerant separation in the lower-pressure stage.

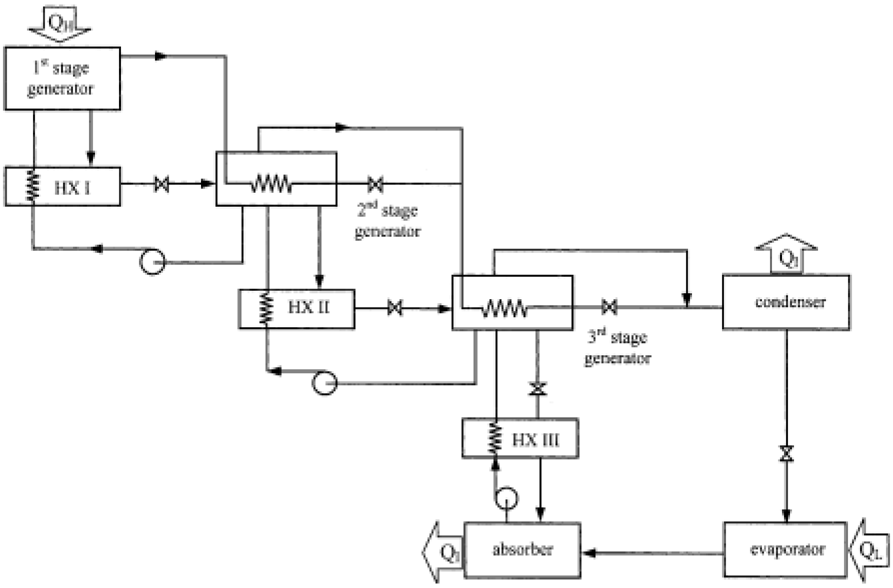

Figure 30: A triple-effect absorption cycle

$$COP_{TRIPLE} = A * (COP_{SINGLE} + (COP_{SINGLE})^2 + (COP_{SINGLE})^3)$$

Fixing the COP of a single stage equal to 0,60, the COPs for the multi-stage cycles are reported in the following table:

COP_{SINGLE}	0,60
COP_{DOUBLE}	0,96
COP_{TRIPLE}	1,18

Table 5: example of how the COP of an absorption chiller can vary according to the number of stages

Working fluid for absorption refrigeration systems

The performance and efficiency (COP) of absorption systems is directly correlated with the chemical, thermos-physical, and thermodynamic properties of the working fluid. The suitability of the absorbent/refrigerant pairs is determined by several necessary or desirable properties [3].

A fundamental requirement of absorbent/refrigerant combination is that, in liquid phase, they must have a margin of miscibility within the operating temperature range of the cycle [25].

- The elevation of boiling (the difference in boiling point between the pure refrigerant and the mixture at the same pressure) should be as large as possible and the refrigerant should be much more volatile than the absorbent in order to separate them easily.
- Refrigerant should have high heat of vaporization and high concentration within the absorbent in order to maintain low circulation rate between the generator and the absorber per unit of cooling capacity.
- Transport properties that influence heat and mass transfer, e.g., viscosity, thermal conductivity, and diffusion coefficient should be favorable
- Both refrigerant and absorbent should be non-corrosive, environmental friendly, and low-cost cycle [25].

However, the desirable properties are sometimes mutually exclusive, and it is very difficult (if not impossible) to find a working pair which fulfils all the requirements. More precisely, it is a matter of compromise [26].

Even if in several studies there are presented a lot of refrigerants and a lot of absorbers, the most common working fluids with practical application in absorption systems are NH_3-H_2O and H_2O-LiBr.

<u>Water-lithium bromide</u>

Lithium bromide is a salt and drying agent. The lithium ion (Li+) in the lithium bromide solution has a strong affinity to the water molecules, which is essential to produce absorption cooling effect. The advantages of this working pair include high safety, volatility ratio, affinity, stability, and latent heat. Water is the refrigerant, which evaporates at very low pressures producing the cooling effect. Since water freezes at below 0 °C, the minimum chilled water temperature in the absorption system with H_2O-LiBr is around 5 °C. This is the reason why these systems are used for air-conditioning applications and cannot be used for low temperature refrigeration. These systems operate under high vacuum pressures. The LiBr crystallization occurs at moderate concentrations. Normally, an internal control system is installed inside the absorption equipment to assure operation under predetermined range and to avoid crystallization. The lithium bromide solution is corrosive to some metals used for construction of absorption equipment (i.e. steel or copper). Corrosion inhibitors may be used to overcome this problem. These additives protect the metal parts and can improve heat and mass transfer performance [26].

Ammonia-water

Ammonia as the refrigerant offers the opportunity to operate with evaporating temperatures below 0 ºC. Generally, ammonia-water is used for refrigeration applications in the range from 5 ºC down to -60 ºC, as the freezing point of NH_3 is -77°C. The preferred heat source temperature for ammonia-water equipment is from 95 ºC to 180 ºC. The absorption systems with this working pair operate at moderate pressure and no vacuum is required till -30 ºC. The advantage of this working pair is that ammonia is completely soluble in water (at all concentrations), and therefore, there is no risk of crystallization. Ammonia is both toxic and flammable. Another disadvantage of ammonia is incompatibility with materials such as copper or brass. For that reason, steel is normally used as the construction material for ammonia-water absorption equipment. Finally, small temperature difference between the boiling points of the refrigerant and the absorbent requires an additional device to obtain a high purity vapor of the refrigerant. This device called rectifier cools the vapor produced in the generator, demanding more supply heat. The consequence is lower coefficient of performance (COP) [26].

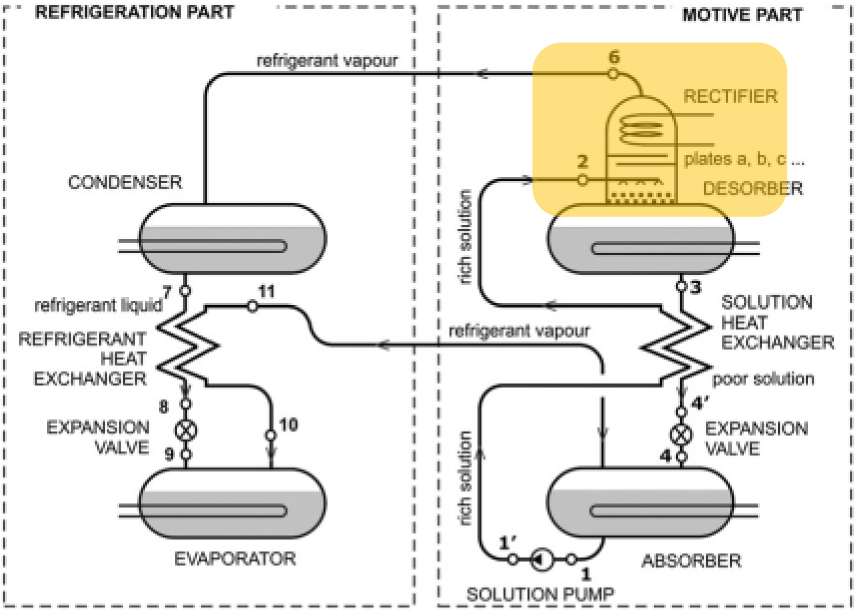

Figure 31: A water-ammonia refrigeration cycle – the rectifier [27]

The rectifier is positioned after the generator and before the condenser.

Absorption chiller components

<u>Evaporator</u>

The evaporator of an absorption chiller is the component that extracts heat from the heat transfer fluid (secondary circuit). It is a heat exchanger and puts in contact the refrigerant and the heat transfer fluid.

Generally, shell and tubes heat exchangers are used for this application. This type of heat exchanger is composed of a pressure vessel, the shell, in which passes a bundle of tubes. Inside the tubes there is the fluid that needs to be cooled, while in the shell there is the refrigerant.

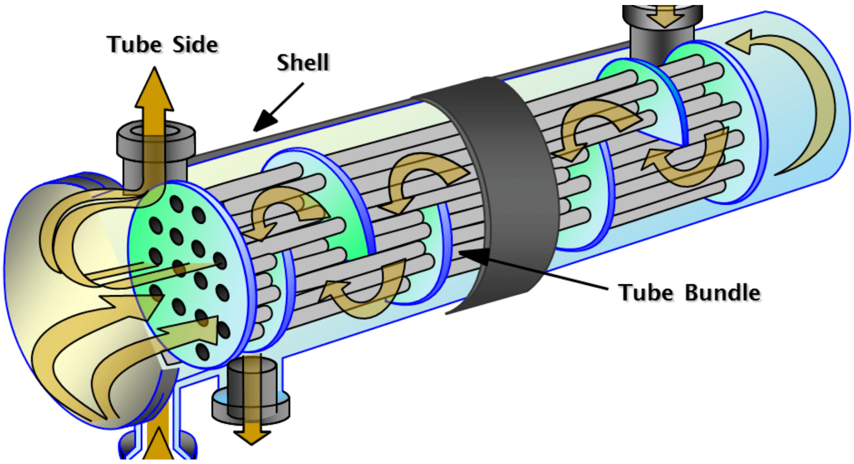

Figure 32: A shell and tubes heat exchanger [28]

Since the refrigerant entering the heat exchanger (shell side) is at low pressure, its boiling point is lower. This is to facilitate the evaporation of the refrigerant. During the evaporation the heat is absorbed from the other fluid passing in the heat exchanger, the fluid to be cooled. At the inlet of the heat exchanger there is a low pressure, low temperature refrigerator, and the heat transfer fluid (generally water or glycol). On the other side, at the outlet there is steam (due to the evaporation) and chilled water or glycol.

Absorber

In the absorber the steam exiting from the heat exchanger is absorbed by the absorber. During the absorption process (exothermic process) heat is rejected out to the surrounding to maintain the absorption capability.

During the absorption heat and mass transfer occur.

The most important thing necessary to have good performances of an absorber is its absorption surface, that should be as bigger as possible.

Different types of absorbers exist, with different shapes and characteristics.

- Falling film absorbers

Falling film exchangers are the most frequently used today in absorption systems. This technology consists in generating a stable film over a heat exchange surface, usually at low flow regimes to avoid heat and mass transfer resistance due to the increase in film thickness. The exchange surface can be a horizontal tube or a vertical surface. The horizontal tube baffle structures have been historically the predominant technology in commercial absorption machines thanks to their versatility and simplicity of functioning. However, plate heat exchangers are now replacing them given their advantages in terms of compactness and low cost [29].

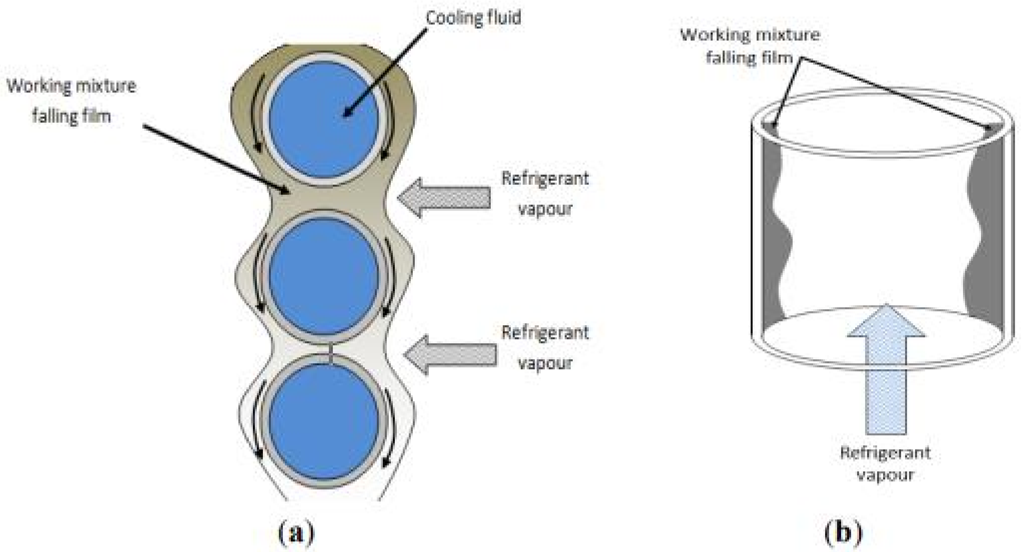

Figure 33: Falling film absorber with horizontal tubes (a) and vertical tubes (b) [29]

With horizontal tube falling film exchangers, a solution distributor is located on top of the exchanger to let the solution flow down over the horizontal tubes, where the heat and mass transfer processes take place. The heat and mass transfer of falling films over tubes is a complex phenomenon influenced by the flow regime of the solution which can take different forms between the tubes such as drops, columns, or entire sheets, depending on the solution flow rate. The performance increases as the tube diameter decreases. Another enhancement method is the corrugation and surface modification.

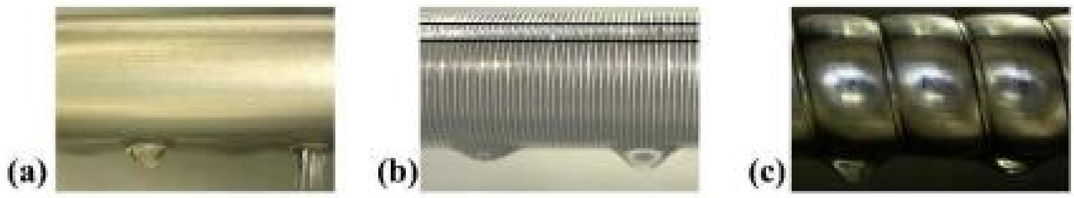

Figure 34: Falling film absorber with horizontal tubes - enhancement method: surface modification. Smooth tube (a), integral-fin tube (b), and turbo helix tube (c) [29]

In the previous image three different configuration of the horizontal tube are reported:

a) Smooth tube
b) Integral-fin tube
c) Turbo helix tube.

The falling film on vertical tubes can be inside or outside the tube; this choice does not seem to impact the exchanger performance. The choice relies only on the desired application. An enhancement for the vertical tubes is an internally micro finned tube. Vertical tubes are a good choice for air-cooled absorbers owing to the easy addition of fins on their external surface. However, the required heat exchange area is from two to three times that of water-cooled heat exchangers for similar conditions.

Commercial plate heat exchangers operate in falling film mode at low flow regimes. Their main advantages are their low cost, flexibility, easy maintenance, and high performance. Regarding their fabrication method, they can be gasketed or brazed. The heat exchange surface can be smooth or corrugated, in which case, the turbulent flows generated enhance the transfers and reduce the fouling effect thanks to its self-cleaning nature. To improve the performance of plate falling films, a fin structure can be installed on the flat plate. In the image below there is reported the comparison of wetting rate for a flat plate and a patterned surface.

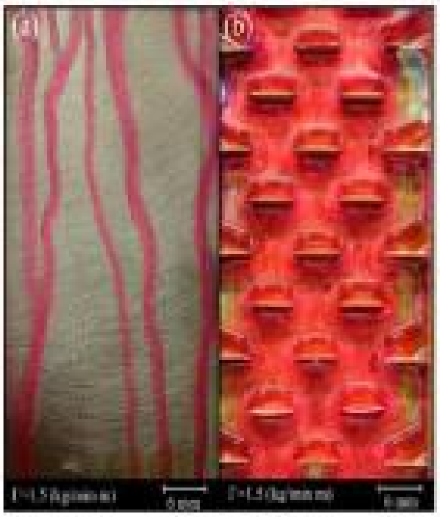

Figure 35: Comparison of wetting rate for a flat plate and a patterned surface [30]

- Adiabatic absorbers

Adiabatic absorbers separate the heat and mass transfer processes. The heat transfer occurs in an external conventional single-phase heat exchanger, which allows reducing its size and cost, as a commercial model can be used. Usually, mass transfer limits the absorption rate, being the liquid molecular diffusion the factor that controls the absorption process [31].

- Bubble absorbers

Bubble type absorbers provide better heat and mass transfer coefficients, and also good wettability and mixing between the liquid and the vapor. Bubble absorption is in general more efficient than falling-film absorption, especially for low solution flow rates.

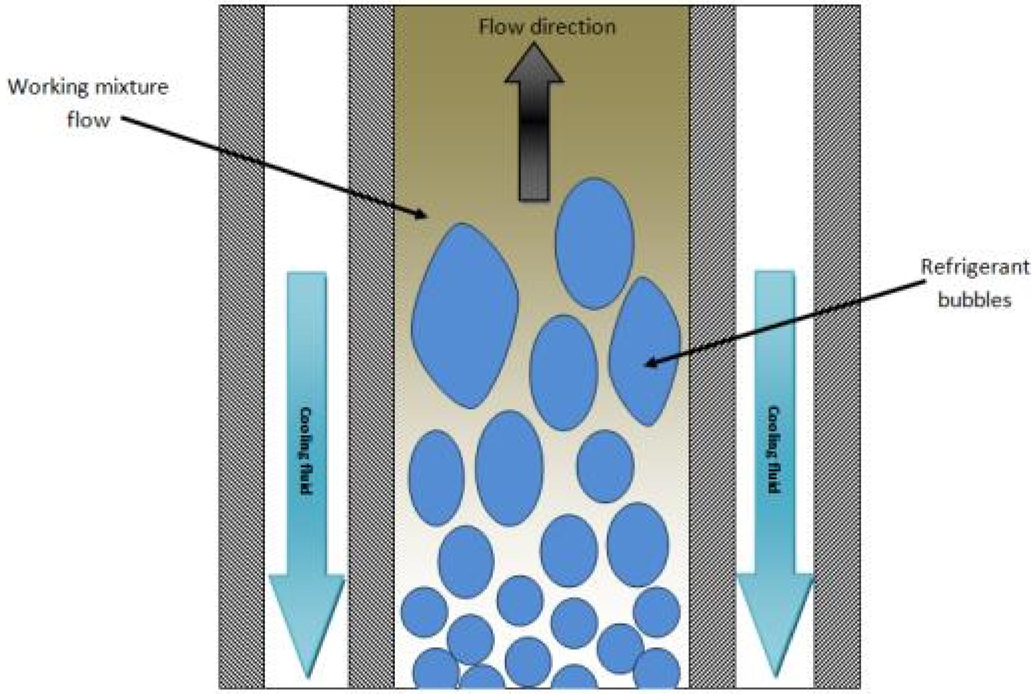

Figure 36: Sketch of a bubble absorber [31]

The heat exchanger was formed by four plates with three channels. The upflow of solution in the central channel was cooled by the downflow of water in the two external channels [31].

<u>Generator</u>

The main goal of the generator is to separate the refrigerant from the absorbent. It is a tank that contains the solution. Thanks to the heat supply, the refrigerant is evaporated and separated. The more volatile components evaporate, while the others remain in the liquid phase.

If the substances that compose the solution have a similar volatility, another component must be added to completely separate them, a distillation column. Heat is supplied to the column from the lower part. The steam goes up while the liquid goes down. The column is made of different plates that put in contact the steam (from the bottom) and the liquid (from the upper part). The contact between these permits a first evaporation of the more volatile components. The plates of the column can be positioned in different ways.

<u>Heat exchanger</u>

The heat exchanger positioned between the absorber and the generator is a component that permits an energy recovery. Thanks to it the rich solution coming from the absorber to the generator is preheated by the warmer solution coming from the generator to the absorber.

Condenser

The condenser, similarly to the evaporator, is a heat exchanger. Its goal is to cool down the steam. The cold stream could be water or air. At the inlet there is hot and high-pressure steam, while at the outlet there is cold and high-pressure solution of liquid and steam.

Lamination valve

The lamination valve is positioned between that components that have a big pressure difference, for example the condenser and the evaporator. The valve presents a big diameter variation. Thanks to this variation, the flow velocity at the exit of the valve increases a lot, reducing the pressure, and consequently the temperature (and the boiling temperature too). This component is crucial for the absorption cycle because it regulates and maintains the pressure differences.

Martini&Rossi

Martini & Rossi is an Italian multinational spirits company founded in 1863 in Turin for the production of the Martini vermouth. Since 1993 it is part of the Bacardi-Martini Group.

Figure 37: Martini & Rossi Logo

Today Martini & Rossi has two plants, the main one is located in Pessione (TO), with the headquarter of the company and the other in Santo Stefano Belbo (CN), dedicated to the harvest of grapes for sparkling wine.

Pessione is the cradle of Martini and the producer of flagship brands within the Bacardi-Martini portfolio. Center of excellence and proficiency for production, development and industrialization of vermouth, sparkling wine and spirits bottling.

The production is divided in three macro groups of products:

- Vermouth
- Sparkling wine
- Spirit

Figure 38: Martini products – Vermouth

Figure 39: Martini products – Sparkling wine

Figure 40: Pessione plant products - Spitit

The yearly production of the site is over 20 million of nine-liter cases, corresponding to over 200 million of bottles and 170 million of liquid, exporting more than 100 countries all around the world. More than 400 employees are working in the Pessione site, on 7 bottling lines and 3 bulk departments dedicated to each type of products.

Energy infrastructure and consumption

The two main energy vectors used in the Pessione plant are electricity and steam.

The electricity is both purchased and self-produced thanks to a cogenerating system.

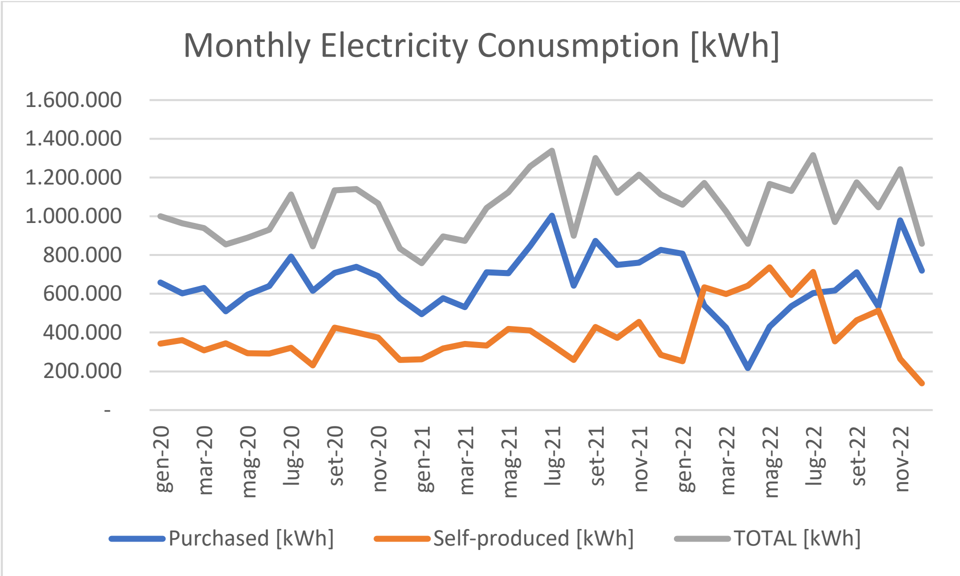

Figure 41: Monthly electricity conusmption trend. Purchased and self-produced electricity in the Martini & Rossi Pessione plant

The steam is produced thanks to three boilers, the thermal recovery of the cogenerating system, and a solar thermal field (during the summer period). A part for the solar thermal resource, the other systems are fed by natural gas from the grid.

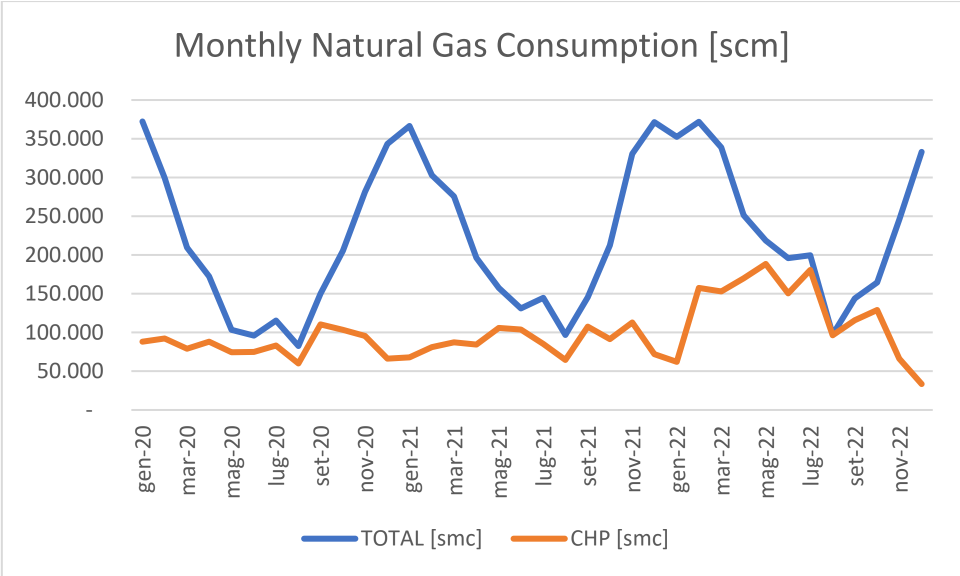

Figure 42: Monthly natural gas consumption trend. Total consumption and cogenerating system consumption in the Martini & Rossi Pessione plant

Solar field

On the rooftop of Tinaggio 92 (highlighted in yellow in the image below) there are installed 298 high vacuum solar panels manufactured by TVP Solar, with a gross area of 596 m^2 and a net aperture area of 584 m^2.

Physical Characteristics		
Dimensions	see diagram for details	
Gross Area	1.95 m^2	21 sq. ft.
Aperture Area	1.84 m^2	20 sq. ft.
Weight	52 Kg	114 lb
Volume of HT fluid	1.3 L	44 fl. oz.
Heat Absorber-Pipe	Al sheet + Cu pipe	
Absorber Coating	Alanod Mirotherm 1300R	
Back-plate	441 stainless steel	
Glass Coating	Single-sided anti-reflective (interior face)	
Connecting Ports	TVP proprietary	
Operating Conditions		
Stagnation Temperature	310 °C	590 °F
Max. Operating Pressure	16 bar	232 psi
Pressure Drop H_2O @ 260 l/h, 100°C	0.7 kPa	14.6 lb/sq. ft.

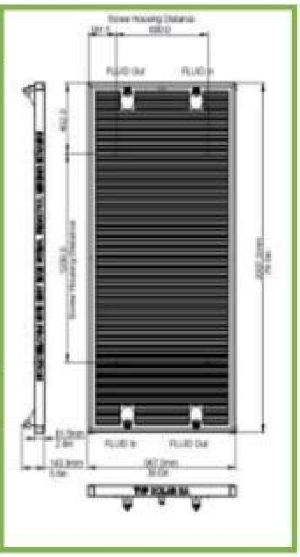

Figure 43: Solar collectors specs [8]

Figure 44: Martini & Rossi Pessione plant – aerial view

The installed peak power is 327 kW_t and the gross heat production per year is equivalent to 349 MWh_t, with a yearly global efficiency of around 44%. The panels are able to reach a maximum temperature of 177°C, generating steam up to 3,7 bar. The panel's tilt angle is equal to 35°, to maximize the average yearly solar fraction, according to the local latitude (N 44°58'5") while the azimuth is slightly lower than 0° (-5°) (almost South-facing).

Figure 45: The solar thermal filed above the Tinaggio 92

In order to find the best matching possible between the potential energy production of the solar field, and the plant energy needs, together with the available space in the plant, and the external weather conditions, two different operation modes were identified.

Winter mode, chosen for the periods with the lowest irradiation, driving the solar field to produce energy for heating the environment of the Tinaggio 92, the main vermouth tank farm production department in Pessione, standing below the solar roof.

During this operation mode, the installation works between a temperature range of 60 °C and 120 °C fueling two new unit heaters installed in the area.

For the period with the highest irradiation, the Summer mode was designed. It drives the flow up to 177°C producing 3.7 bar saturated steam.

The heat produced by the solar panels is made available to an indirect steam generator through a second circuit about 400 m long and an additional heat exchanger was needed to transfer the heat from the solar field to the steam network.

All the system, with the pipes and the various components is represented in the following P&ID.

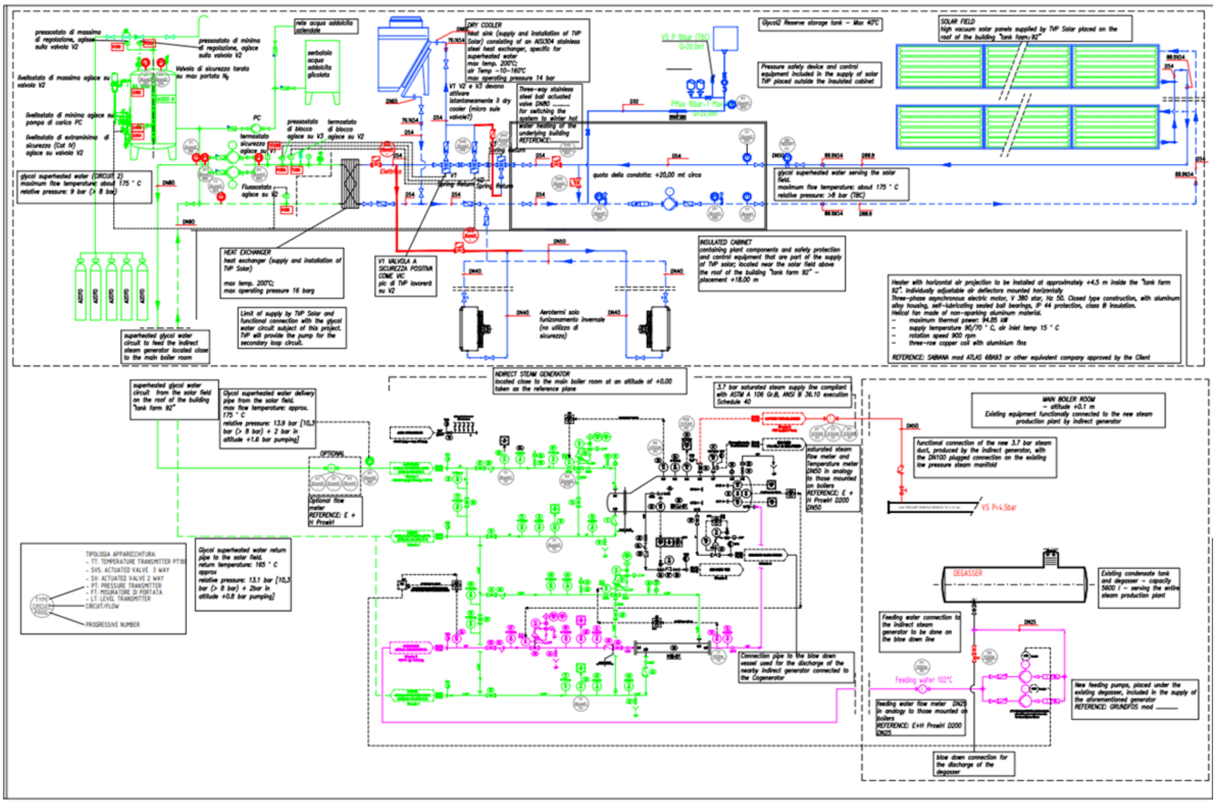

Figure 46: Solar thermal field P&ID

The control logic operation of TVP's solar thermal systems is based on a simple switching on different modes, depending on the working fluid temperature during the day. The principal operation logic that allows the solar field to work optimally are outlined below. It is possible to manage the relevant parameters by the Human Machine Interface (HMI) of the PLC Cabinet.

(i) Warm Up Mode

The system will automatically start-up operation once the solar radiation read by Pyranometer is above an editable setpoint value (Irradiation >= Threshold [W/m^2]) and the time is between Sunrise and Sunset). Once these conditions are verified, the main pump starts with a fixed frequency until the temperature transmitter reaches the next setpoint value. As soon as this is achieved the start-up and preheating mode is completed.

Then, the system is able to run in two different operating modes depending on the settings (see below 'application mode' and 'fixed mode').

(ii) Application Mode

When the circuit is preheated, the system switches to this mode when the temperature transmitter reaches the desired temperature to start thermal transfer with the heat exchanger. This operation mode stop working as soon as the Temperature Transmitter reaches the settable value of stop. In this mode, the fluid starts to circulate in the heat exchanger and the flowrate is regulated by an algorithm that optimizes speed pump according to the solar irradiation measured by the pyranometer to reach the nominal temperature.

(iii)Fixed Mode

The second scenario involving the 'Fixed mode' operation that can be considered as "transitional", as it occurs at the moment when there are no warm and no application mode conditions. In this mode, the pump operates at a fixed frequency in order to reach the conditions for application mode activation or, in case of problems or absence of application, waiting for the dry cooler mode described in the next point below.

(iv)Dry Cooler Mode

This is an emergency operation which starts automatically when the temperature transmitter reads a temperature equal to a security threshold set point of start and automatically stop when the temperature transmitter reads a temperature equal to a set point of stop.

(v) Defreezing Mode

This mode prevents the fluid inside the system from freezing. If the temperature of the system is lower than a set value, the pump switches on and starts working at a fixed frequency. When the temperature system reaches an upper value, the pump switches off.

(vi) Auto load Mode

This mode prevents the system from running out of heat transfer fluid (HTF) in the event of a leak. If the pressure of the system is lower than a set value, the valve is totally opened and the pump start working if the level of HTF into the refill tank is enough. Once the upper limit value is reached the valve closes.

(vii) Manual Mode

In this mode, the user must be near the HMI screen to drive the operations. In this mode the operator can chose all working parameters. TVP recommends the use of this mode to expert users only and takes no responsibility under this mode of operation.

	Setpoint
Warm Up Mode	Starts when: >200 W/m2 (time between sunrise and sunset)
Pressure circuit 1	Between 2.5 and 7 bar
Filling Pump circuit 1	Starts: < 2 bar ; Stops: > 2.5 bar
Defreezing Mode	Starts: < 1 °C ; Stops: > 3 °C
	WINTER MODE
Application Mode	Starts: > 90 °C ; Stops: < 70 °C
Dry Cooler Mode	Starts: > 130 °C ; Stops: < 120 °C
	SUMMER MODE
Application Mode	Starts: > 70 °C ; Stops: < 60 °C
Dry Cooler Mode	Starts: > 177 °C ; Stops: < 160 °C
Pressure circuit 2	Between 7.5 and 9.5 bar

Table 6: Solar thermal field operation modes

The solar field is designed to work in relation to the solar irradiation. During the nights and below 200 W/m^2 the circulation pump of circuit 1 is stopped. Only when the external temperature decreases below 1°C the defreezing mode is active, and the pump drives the flow until the temperature reaches 3°C to prevent the ice formation inside the pipes.

The minimum pressure of the circuit 1 is 2,5 bar and it is possible from the PLC to activate a function for automatic filling. In this way the system drives a second filling pump to refill the circuit once the pressure drops below 2 bar to restore it at 2.5 bar.

The pressure variation due to the temperature increase is handled by the three expansion vessels of 100L each installed in circuit 1, next to the thermal block.

Winter Mode

In the first hours of the morning, until the circuit 1 reaches 70°C, the two two-way valves (2W001 – 2W002) open the solar field loop, excluding the thermal block and allowing a quicker increase of the temperature.

Once the system reaches the minimum temperature, the flow is driven to the unit heaters providing heat to the department standing below the solar roof.

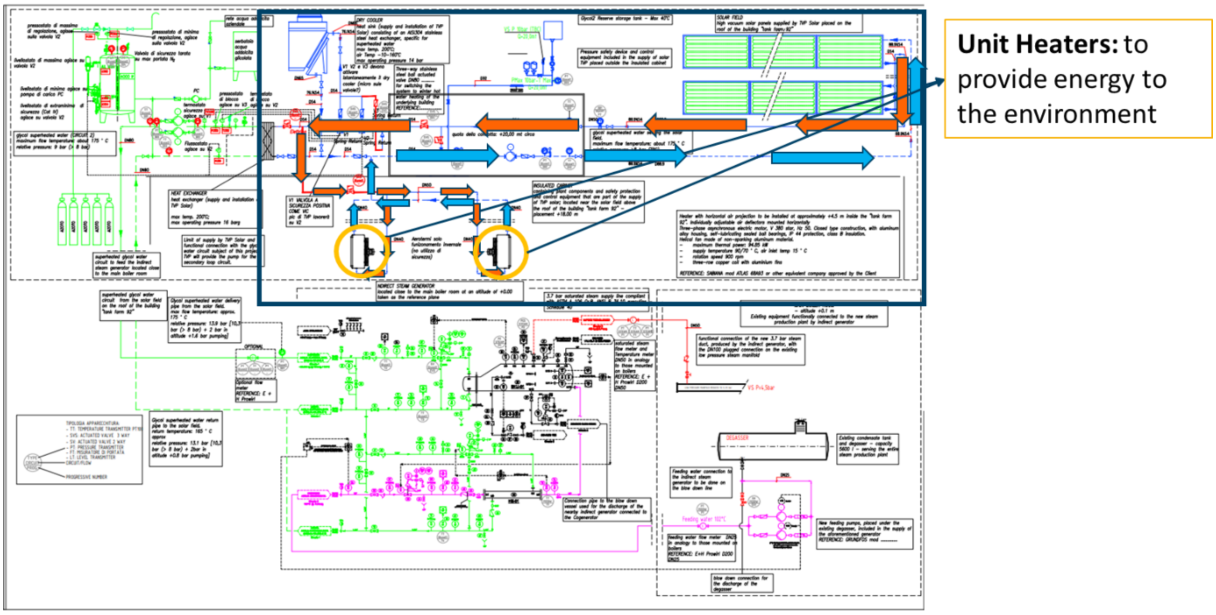

Figure 47: Solar thermal field P&ID – Winter mode – Application mode

All the parameters remain in such conditions, until reaching 130°C when, for safety conditions, the flow is driven to the Dry Cooler. It dissipates the excess of energy until the temperature drops below 120 °C.

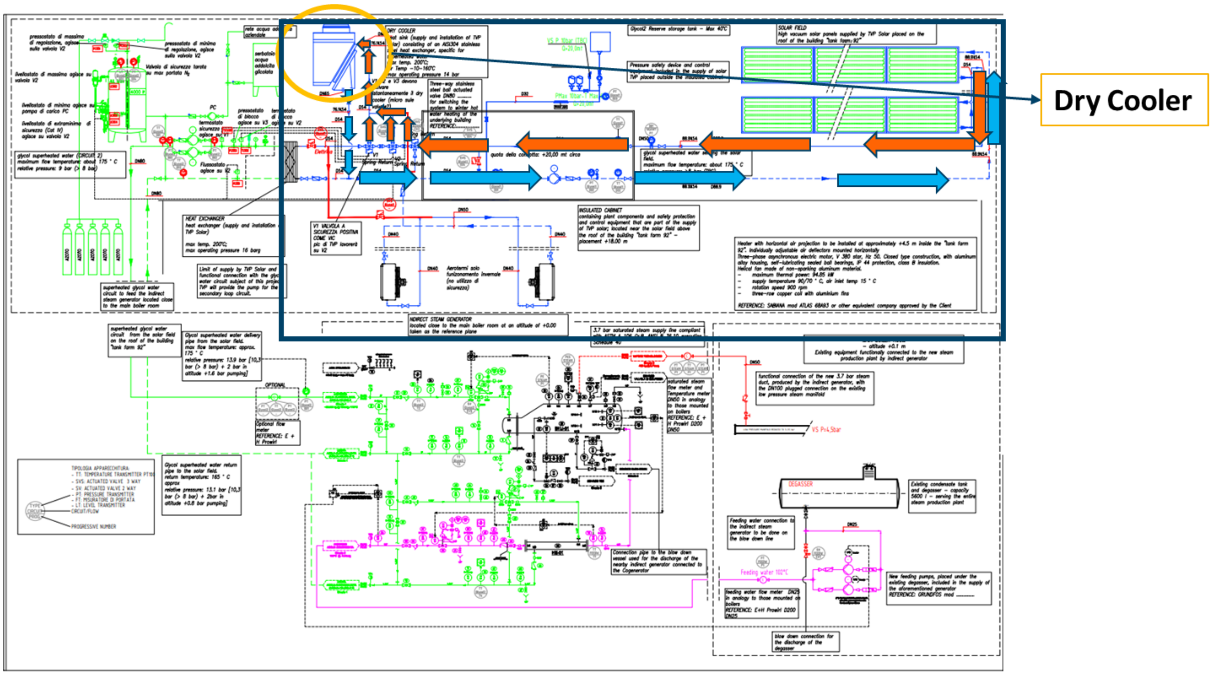

Figure 48: Solar thermal field P&ID – Winter mode – Dry cooler mode

During a typical operating day, the circuit 1 pressure stands between 2,5 bar and 7 bar.

Summer Mode

During the Summer Mode, the circuit 1 works to fuel a second circuit, circuit 2.

This is about 400 m long and brings the energy produced by the solar field to the Indirect Steam generator (ISG).

The temperature above which the valves allow the circuit to reach the heat exchanger, enabling the energy transmission between the two circuits, is 70°C.

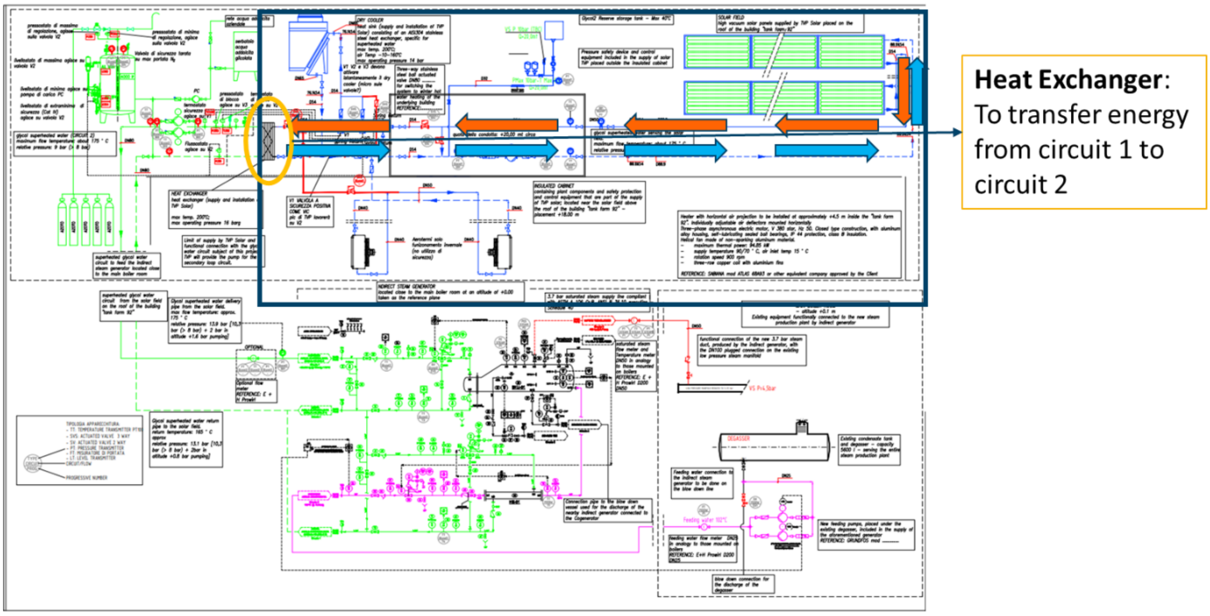

Figure 49: Solar thermal field P&ID – Summer mode – Primary circuit

The circuit 2 is responsible for driving the flow to the indirect steam generator, it happens when the circuit 1 temperature stands between 70°C to 177 °C.

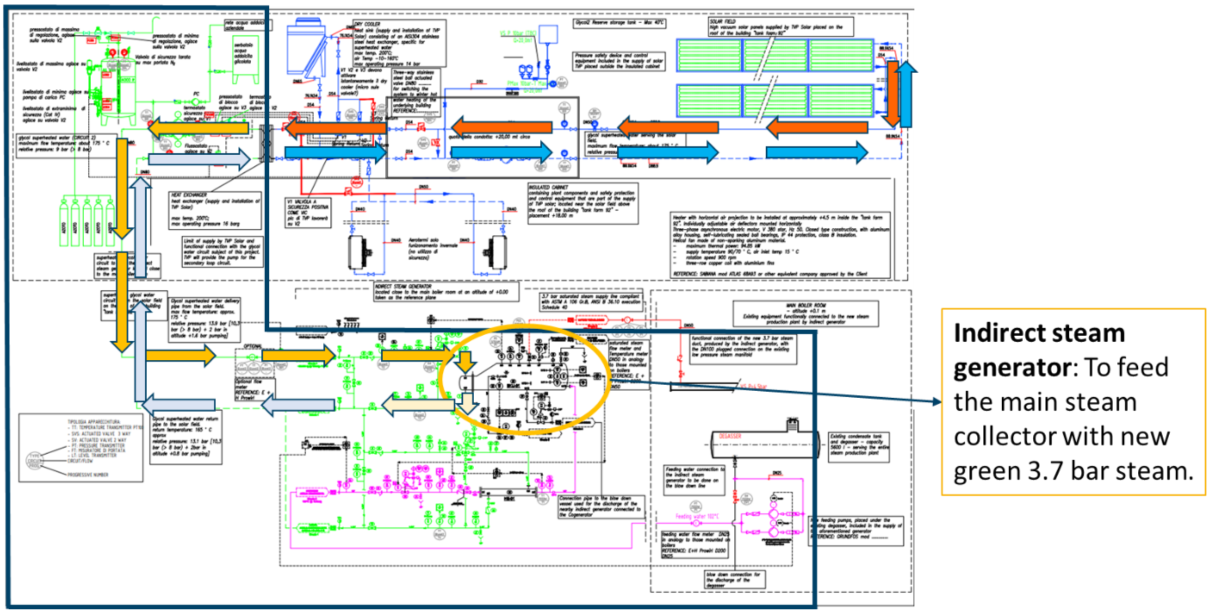

Figure 50: Solar thermal field P&ID – Summer mode – Secondary circuit

If this temperature is exceeded the system drives the flow to the Dry Cooler, following the same procedure described for the winter mode. The only difference is linked to the minimum temperature that allows the system to exchange again energy with circuit 2, in Summer Mode it is set to 160 °C.

Focusing on the indirect steam generator, it is fed with water exiting the existing degasser, with a temperature of 104°C. The feeding pump are controlled with a level switch installed in the ISG.

The steam produced by the solar field enters the main steam collector where it is driven directly to the steam demanding processes.

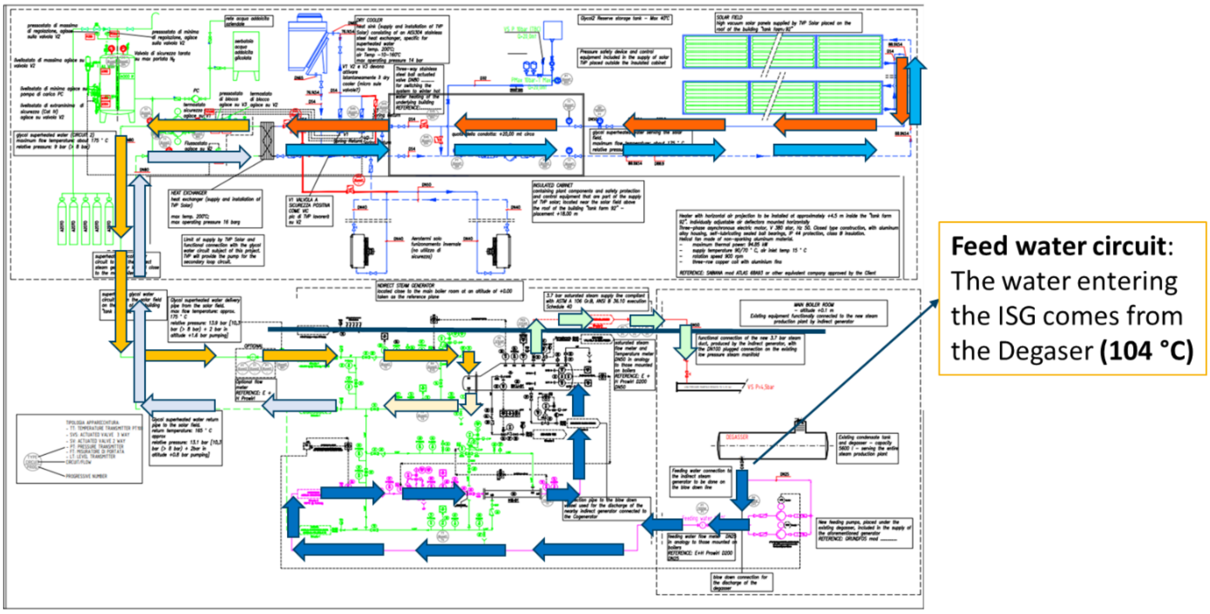

Figure 51: Solar thermal field P&ID – Summer mode – Indirect steam generator

In the image above, there are reported colored arrows representing the different circuits and flows of the solar system during the summer mode. The primary circuit is represented by the red arrows (exiting from the solar field) and the blue arrows (returning to the solar field). The primary circuit, by means of a heat exchanger, exchanges heat with the secondary circuit, represented with orange arrows (hotter side) and light blue arrows (colder side). The secondary circuit exchanges heat, by means of a second heat exchanger, with the indirect steam generator. In the indirect steam generator, the entering flow of water, form the degasser, is represented by dark blue arrows. The steam produced by the indirect steam generator, that goes to the main steam collector, is represented by light green arrows.

In order to allow an increase in overall efficiency, a pre-heat exchanger was added. Thanks to it, the feed water is pre-heated before entering the ISG by the return of circuit 2.

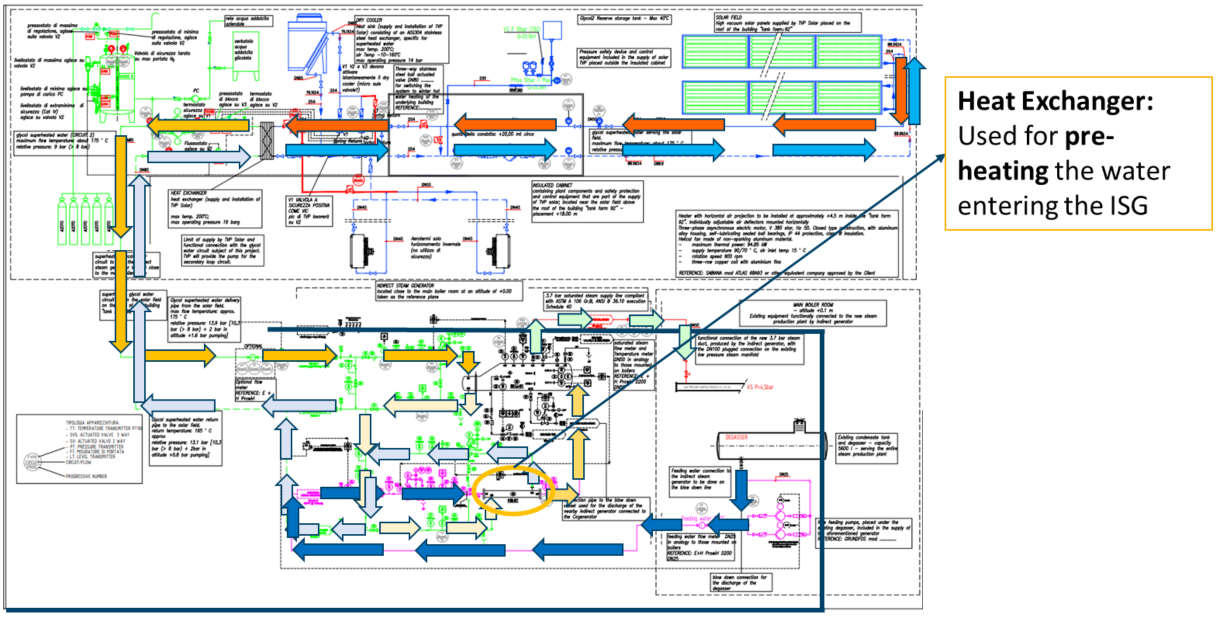

Figure 52: Solar thermal field P&ID – Summer mode – Pre-heating of the feedwater

The circuit 2 pressure is controlled with an expansion vessel pre-charged with nitrogen. The circuit 2 pressure stands between 7,5 and 9,5 bar.

Solar resource in Pessione

The solar radiation data measured by M&R are available thanks to a pyranometer installed on the top of the roof of the Tinaggio 92.

Considering the data of solar irradiance along an entire year, Pessione presents an annual irradiation of 1.797 kWh/m^2.

In the graph below there are three curves, for three different days (one in January, one in March, and one in June), representing the hourly average solar radiation in completely sunny days. It can be easily seen the bell shape of the curves. The maximum is between 12:00 and 13:00. The yellow curve (June) presents the highest values and the highest aperture. It means that the day duration is longer and that the solar irradiation is higher. Conversely, the blue curve (January) presents the lowest values.

During the summer period and around midday, in sunny conditions, the solar radiation reaches and overcomes 1000 W/m^2.

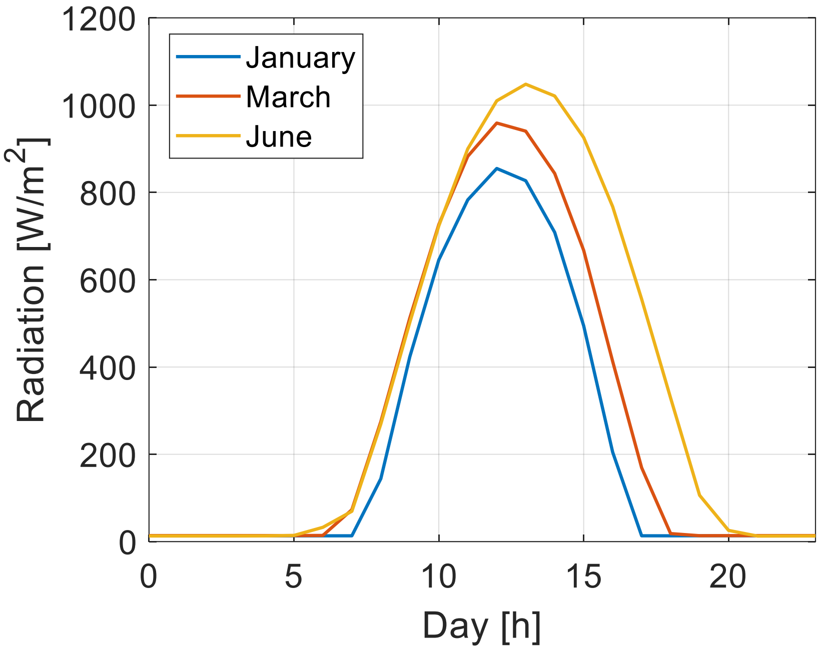

Figure 53: Solar resource in Pessione – Radiation variation during a sunny day for three different periods of the year

The graphs below present a carpet plot and two details of the behavior of the solar irradiance during the year and the day.

On the X-axis of the carpet plot there are the 52 weeks of the year. On the Y-axis there is the day subdivided in part of 15 minutes. The color of the cells represents the intensity of the solar irradiance. Dark blue means low irradiance, below 30 W/m^2 (night). Then light blue and green represent intermediate values, between 100 and 600 W/m^2. Orange and yellow represent high values of solar irradiance, higher than 700 W/m^2.

In the second graph there is the weekly average irradiance reported for the 52 weeks of the year. The central weeks, in the summer period, presents the higher values in comparison to the winter weeks.

Similarly, the third graph reports the 15 minutes average solar irradiance during the day. As expected, we can appreciate the bell shape of the curves and the different heights achieved by the curves relative to different days in the year.

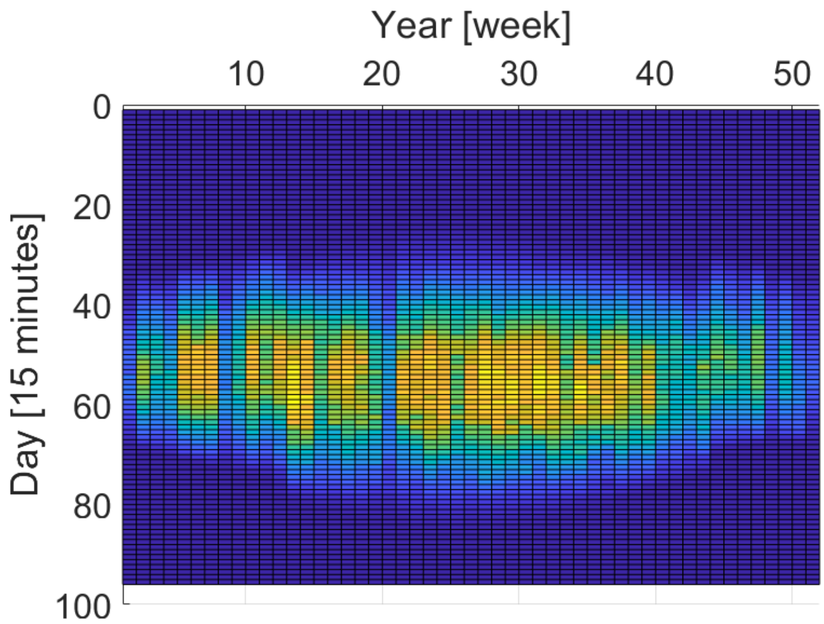

Figure 54: Solar resource in Pessione – Carpet plot

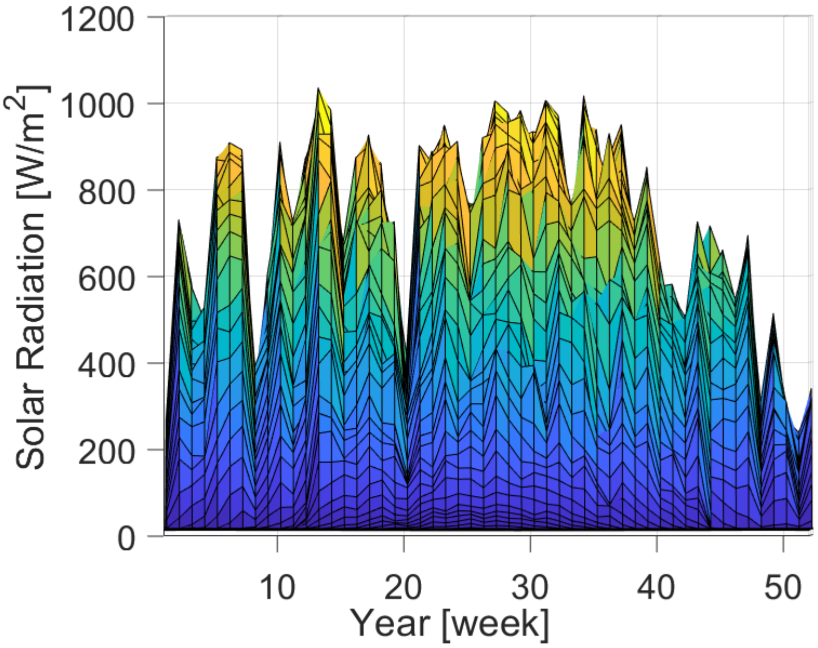

Figure 55: Solar resource in Pessione – Weekly average

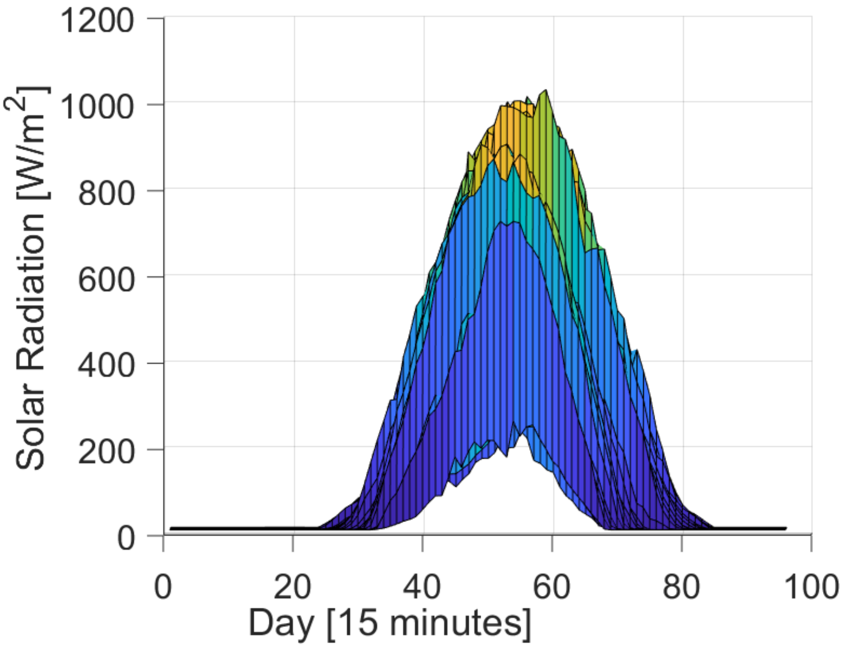

Figure 56: Solar resource in Pessione – Daily trend

Overall, the solar resource in Pessione seems to be sufficient to obtain relatively good efficiencies for both the solar photovoltaic and the solar thermal technologies.

Solar Field data

Winter mode

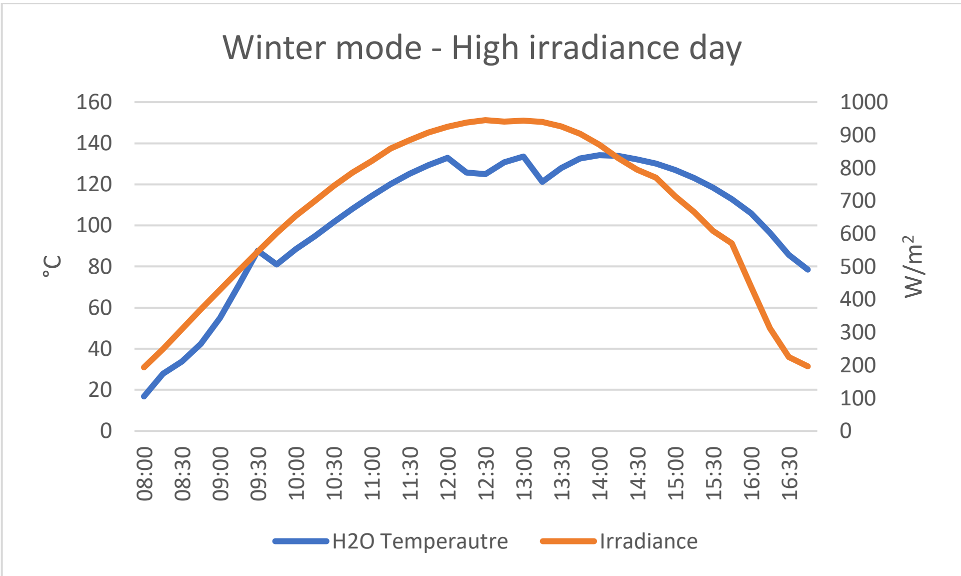

Figure 57: Solar thermal field – winter production

In a sunny winter day, the pump starts to work around the 8:00 AM, when the irradiance overcomes 200 W/m^2. The water inside the panels is heated up reaching very high temperatures.

From the graph it can be seen that around 12:00 and 13:00 the dry cooler started twice, because the temperature of the water reached 130°C.

In winter period the solar field works very well, reaching the expected temperatures and powers.

Summer mode

For the scope of this text, it is better to go in deep for the summer mode of the solar field. Actually, the aim of the system is to produce saturated steam at 3,7 bar.

Two different problems have been faced:

- The secondary circuit is too long, and the water flowing in it decreases its temperature. This means that the circuit takes more time to charge the indirect steam generator (to reach the desired temperature)
- When the indirect steam generator is ready to produce steam, sometimes there is not a steam demand (low steam demand during the afternoons of the summer months). This results in an increase of the pressure inside the steam collector, decreasing the steam production of the solar field.

Mainly for these two reasons, the solar field, With the system to produce steam, presents a low efficiency when it works in the summer mode.

Below, a table resuming the energy at three different levels and the corresponding efficiency. The data are referred to a period of 15 minutes and consider a sunny day.

	SUN	**FIELD**	**STEAM**	**FIELD**	**STEAM**	**TOTAL**
	Energy [KWh]	**Energy [KWh]**	**Energy [kWh]**	**Efficiency**	**Efficiency**	**Efficiency**
08:30	37,4	8,8	-	23,4%	-	-
08:45	45,0	8,2	-	18,3%	-	-
09:00	52,9	12,0	-	22,6%	-	-
09:15	60,4	15,4	-	25,5%	-	-
09:30	68,4	18,9	-	27,7%	-	-
09:45	76,2	22,7	-	29,8%	-	-
10:00	83,8	26,5	-	31,6%	-	-
10:15	91,2	28,9	-	31,7%	-	-
10:30	98,3	32,4	-	33,0%	-	-

10:45	105,2	35,7	-	34,0%	-	-
11:00	111,8	38,7	-	34,6%	-	-
11:15	118,2	40,3	-	34,1%	-	-
11:30	123,7	42,0	-	34,0%	-	-
11:45	128,8	43,1	-	33,5%	-	-
12:00	133,1	43,5	-	32,6%	-	-
12:15	137,7	44,5	-	32,3%	-	-
12:30	140,8	43,7	-	31,1%	-	-
12:45	142,6	47,7	8,0	33,4%	16,8%	5,6%
13:00	144,5	54,7	27,8	37,9%	50,8%	19,2%
13:15	146,1	57,6	29,5	39,4%	51,1%	20,2%
13:30	146,1	59,0	30,3	40,4%	51,4%	20,7%
13:45	145,4	59,6	29,6	41,0%	49,7%	20,4%
14:00	143,9	57,2	29,8	39,8%	52,0%	20,7%
14:15	143,5	56,7	28,9	39,5%	50,9%	20,1%
14:30	141,9	54,8	28,3	38,6%	51,5%	19,9%
14:45	138,1	52,8	26,6	38,2%	50,4%	19,3%
15:00	135,0	50,6	25,1	37,4%	49,7%	18,6%
15:15	130,9	48,3	23,8	36,9%	49,3%	18,2%
15:30	126,5	44,9	20,8	35,5%	46,3%	16,4%
15:45	122,0	38,7	18,6	31,7%	48,1%	15,2%
16:00	115,9	36,0	10,1	31,1%	28,1%	8,7%
16:15	108,6	31,8	6,2	29,3%	19,3%	5,7%
16:30	102,3	27,7	1,5	27,0%	5,5%	1,5%
16:45	96,0	22,8	-	23,8%	-	-
17:00	88,7	17,3	-	19,5%	-	-
17:15	81,4	14,2	-	17,4%	-	-
17:30	74,2	9,1	-	12,3%	-	-
	TOTAL	**TOTAL**	**TOTAL**	**AVERAGE**	**AVERAGE**	**AVERAGE**
	4.086	1.347	344.862	31,4%	18,1%	6,8%

Table 7: Solar thermal field – Summer production (Energy and efficiency)

The efficiency of the solar field has an average value of 31,4%, with a maximum of around 41%. The indirect steam generator has a daily average efficiency equal to 18,1%. This value is strongly influenced by the charging time of the generator, during which, obviously, the efficiency is null. When the generator is working, its efficiency is around 50%. The total efficiency of the solar field plus the indirect steam generator averagely, in a day, is 6,8%, and is strongly influenced by the functioning of the indirect steam generator.

To exploit in a better way the energy produced by the solar field, an absorption chiller could be a good idea. Since the temperatures of the water exiting from the solar field reach very high values, it can be analyzed both the ambient cooling and the refrigeration.

CHP

The cogenerating system installed in the Pessione plant of Martini&Rossi is an ECOMAX®12 NGS manufactured by AB ENERGY SPA.

The engine model is J 416 GS-B406 and is fueled by natural gas. The power input of the fuel is equal to 2.880 kW (+-5%), while the mechanical power output is 1.234 kW, with a specific fuel consumption of 2,33 kWh/kWh (+-5%) and the electrical power output is 1.203 kW, with an electrical efficiency of 41,8%.

The system has two different scopes:

- Low voltage electricity production
- Thermal energy production.

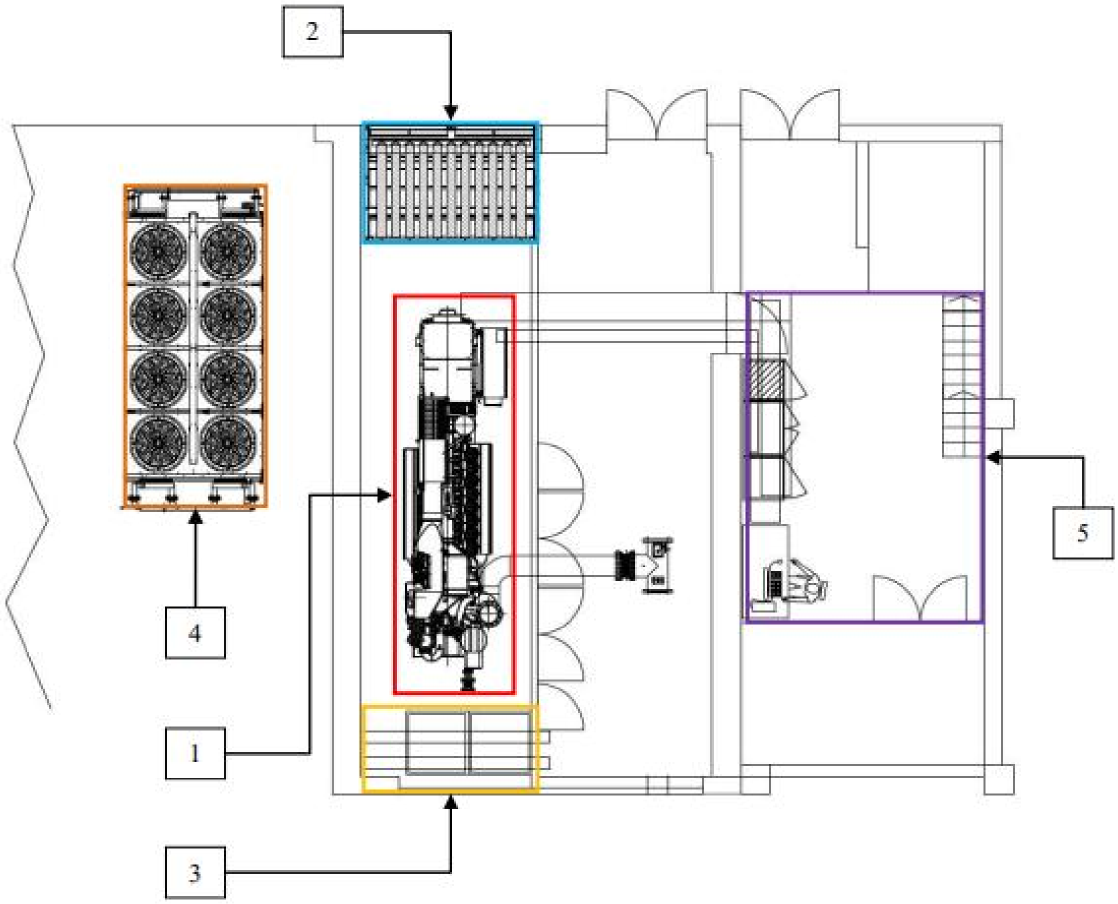

Figure 58: Cogenerating system scheme

The entire system is represented in the figure above.

1) Engine and alternator

The cogeneration unit is made of a direct coupling between the internal combustion engine and the alternator. The engine is the component where the chemical power of the fuel is transformed into mechanical power, used by the alternator to produce electricity, and into thermal power, that can be used by the heat transfer fluid. The alternator is the component that transforms the mechanical power into electrical power (400V and 50Hz).

2) Air suction box

This is a very important component of the system. It enters a flow of air inside the engine room.

3) Air expulsion box

It has the opposite purpose of the air suction box. It expels the air from the engine room.

4) Dissipator

Its purpose is to dissipate the heat absorbed by the engine cooling fluid. It dissipates to the ambient the stored heat so that the fluid returns to an acceptable temperature. The dissipator is composed of a hydraulic circuit, in which cooling water flows, and some fans to generate a flow of air to remove heat from the water.

5) Control room

Hydraulic circuits

In the cogenerating system there are several hydraulic circuits:

- Engine water circuit

The water flowing in this circuit cools the lubricant oil, the mixture air-gas after the first stage of compression and engine cooling jacket.

The heat absorbed by the water can be transferred to another circuit, the utility hot water circuit, thanks to a heat exchanger. If the temperature of the water is still to high it is cooled down passing through the dissipator.

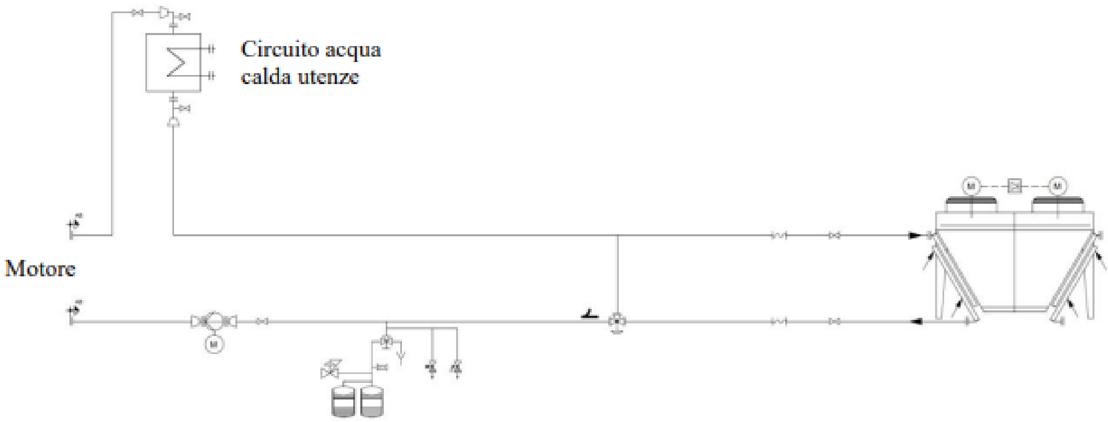

Figure 59: Cogenerating system – Engine water circuit P&ID

- Intercooler water circuit

The water flowing inside this circuit is responsible for the cooling of the mixture air-gas after the second stage compression. To dissipate the heat absorbed by the water, the circuit goes into the dissipator.

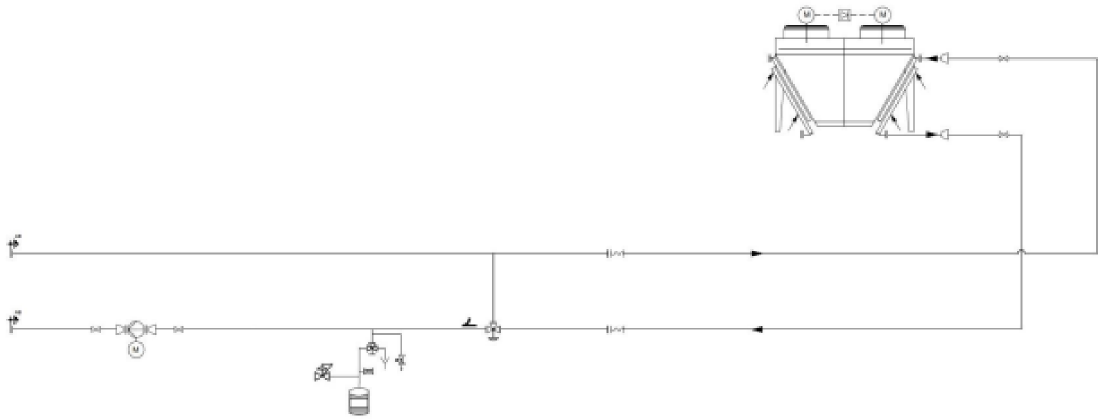

Figure 60: Cogenerating system – Intercooler water circuit P&ID

- Exhausts circuit

The exhaust gases produced by the combustion are sent to the atmosphere after a treatment to decrease the pollutant content. the most important pollutants that are controlled in this process are carbon monoxide and unburned hydrocarbons.

- Lubricant oil circuit

This circuit is responsible for the oil that lubricates the engine. The circuit is fed by new oil, and it produces exhaust oil, and is composed of two main elements: the refill tank and the engine oil pan. It is possible to refill the refill tank or directly the engine oil pan (this, only in two cases: before the first start, or in the case the entire oil of the circuit is replaced).

During the normal operation the oil from the engine oil pan is consumed and replaced. It is refilled thanks to the refill tank. When the level of the oil in the refill tank goes below a certain threshold, it is refilled by an external tank.

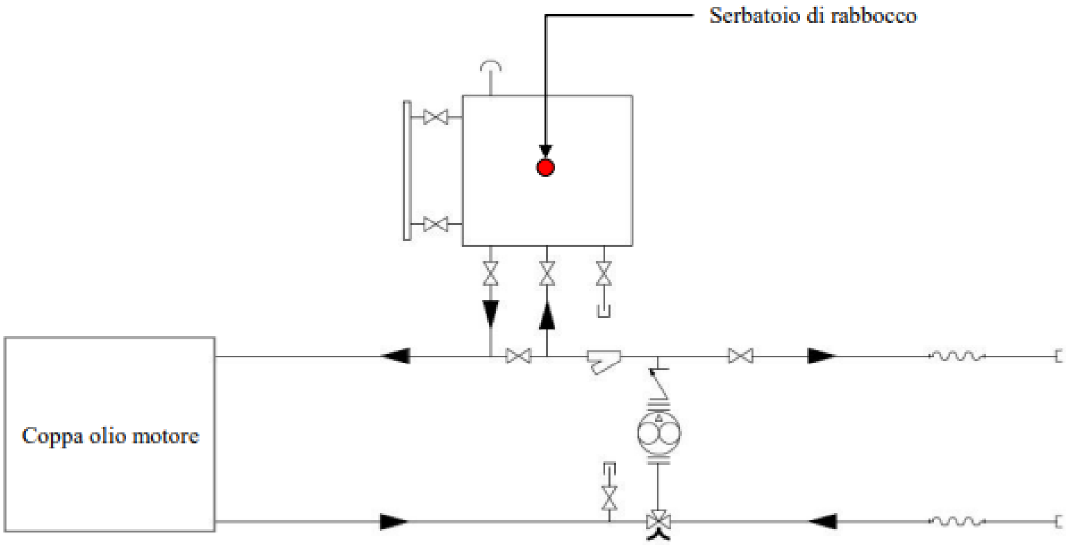

Figure 61: Cogenerating system – Lubricant oil circuit P&ID

- Utility hot water circuit

This circuit is a closed loop that is in contact with two heat exchangers. The first one is a heat exchanger that heats up the temperature of the water flowing in the circuit. The heat is provided by the engine water circuit. This heat is released, thanks to the other heat exchanger, to a hot water circuit that feeds two tanks.

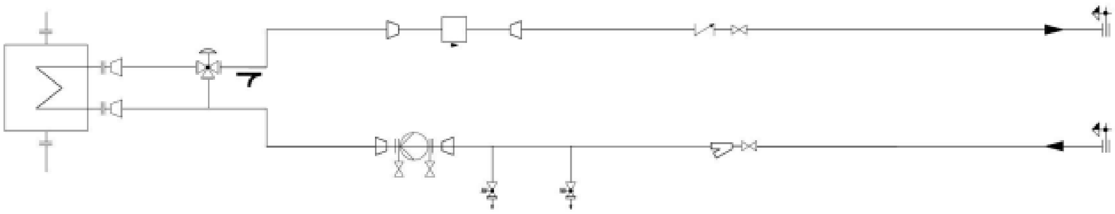

Figure 62: Cogenerating system – Utility hot water circuit P&ID

Energy production

The installed cogenerating system presents four different ways to produce energy.

It produces electricity, as a normal generator, with an installed power equal to 1,2 MW. It produces hot water, thanks to the utility hot water circuit. It produces steam, thanks to a boiler fed by exhaust gases, and it produces hot water thanks to the exhaust gases exiting from the boiler to produce steam.

The operation of the system is ruled by a software named GEM COGE by Energenius, that maximizes the economic return of the system. It considers the electricity price, the natural gas price, the plant energy needs, and what can be produced by the system (electricity, steam, and hot water). For this reason, it doesn't operate every working day, but its functioning depends on the parameters above mentioned.

In the following charts some data about the CHP are reported. The gas consumption, the energy production, and the efficiency of the system. The charts report the data in a monthly basis.

The two tables below report the annual values registered in 2022 about the CHP system.

Electricity	H2O Engine	H2O Second Stage	Steam	Fuel Energy
MWh	MWh	MWh	MWh	MWh
5.979	1.453	232	1.422	14.442

Table 8: Cogenerating system – Energy consumption and production

EE Eff	TH Eff	Total Eff	CO2 emission
			ton
41,2%	22,6%	63,8%	2.843

Table 9: Cogeneratin system – Electrical and thermal efficiencies

Since the CHP is ruled according to the economic return, from the gas consumption chart it can be seen that the usage of the CHP system is variable during the year, according to the relative variations in price of the methane and the electricity.

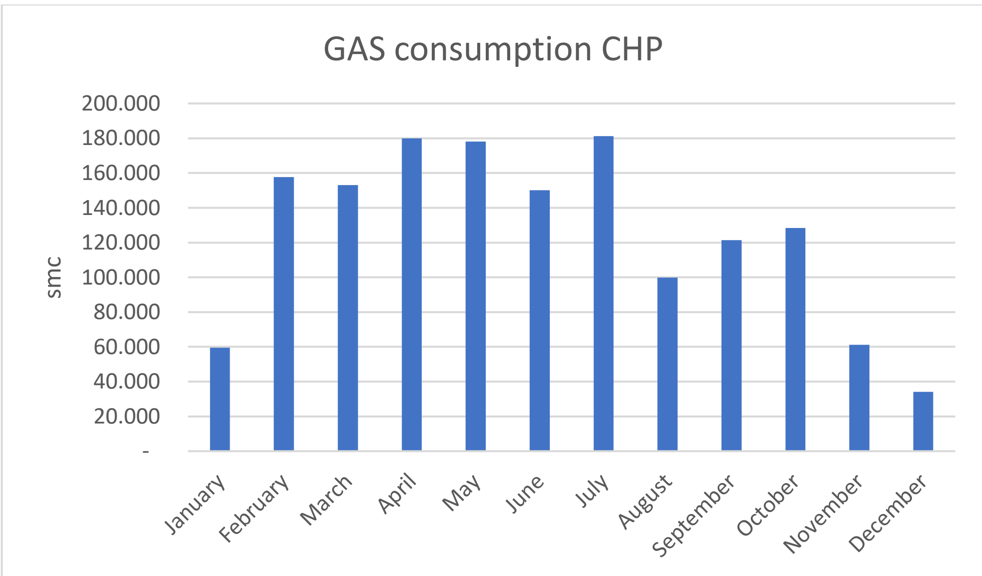

Figure 63: Cogenerating system – gas consumption trend

Usually, the methane price increases a bit during the winter months due to an increase demand of thermal energy for heating. In the graph, the winter months present the lowest consumption (lowest usage of the CHP). On the contrary, during summer months, the CHP was used a lot, and the gas consumption reached 180.000 smc per month. From the graph it can be seen a limit of the algorithm that stands below the CHP system. Usually, the thermal demand is higher during winter, and falls in summer. This doesn't allow the CHP to reach the maximum allowable performances. The installation of an absorption chiller would allow to exploit the thermal energy recovered during the summer months, increasing the overall performances of the system.

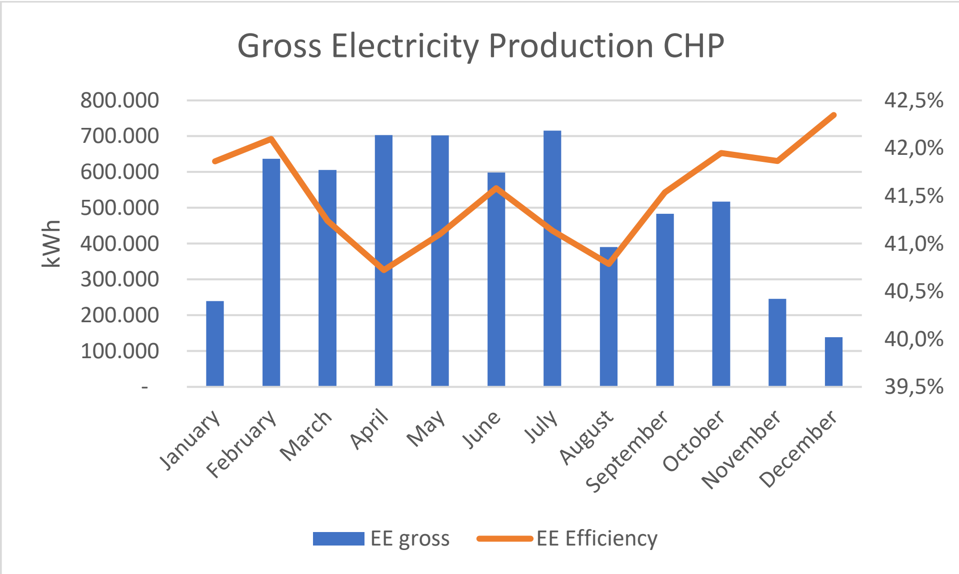

Figure 64: Cogenerating system – Electricity production and efficiency trend

From the electricity production point of view, the cogenerator is working very well. The efficiency is quite stable and near the nominal value, around 41%. Considering the absolute values, from February to July, the electricity production was between 600.000 and 700.000 kWh.

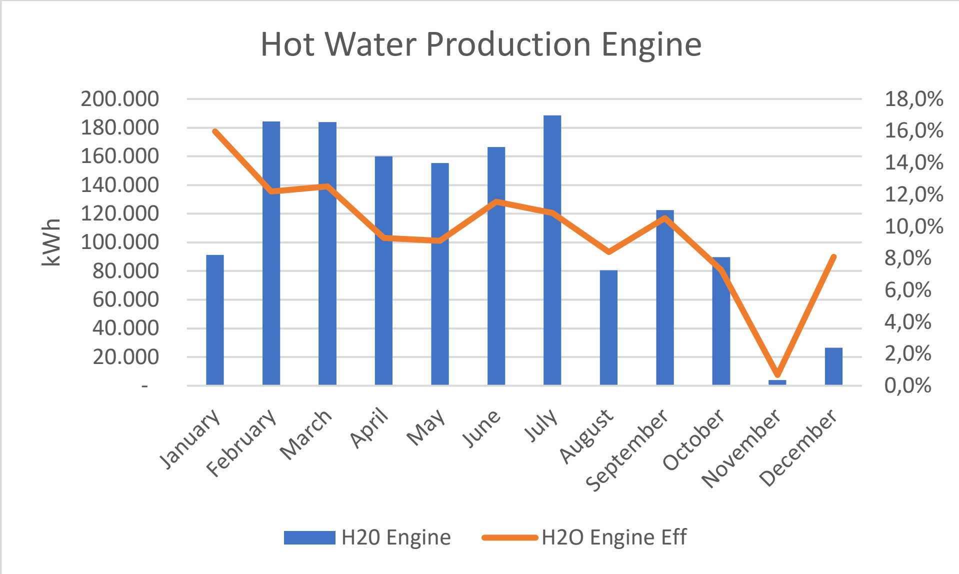

Figure 65: Cogenerating system – Hot water (engine recovery) production and efficiency trend

The hot water production, recovered from the cooling circuit of the engine, presents an efficiency around 10 to 13%, with a maximum in January (16%), and a minimum in November (lower than 1%).

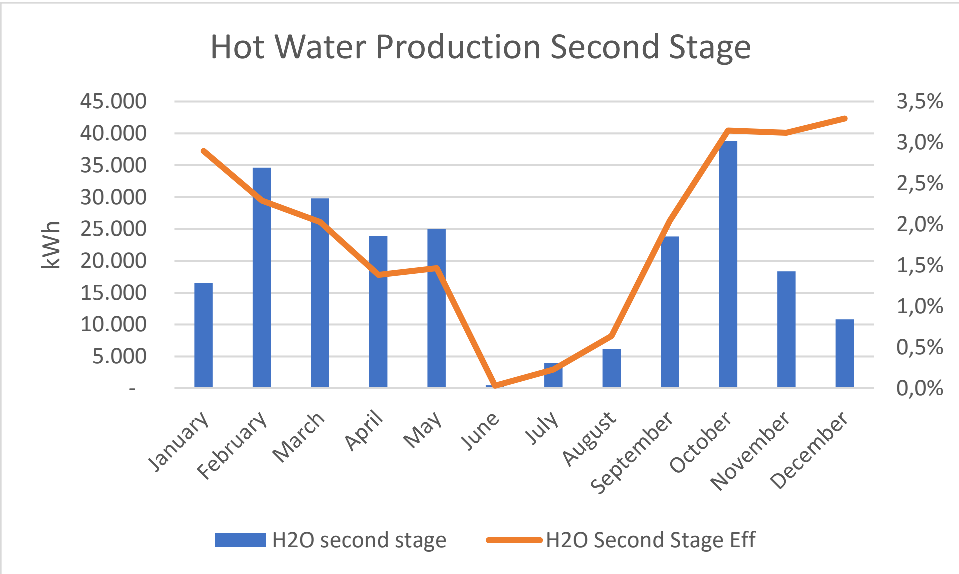

Figure 66: Cogenerating system – Hot water (second stage recovery) production and efficiency trend

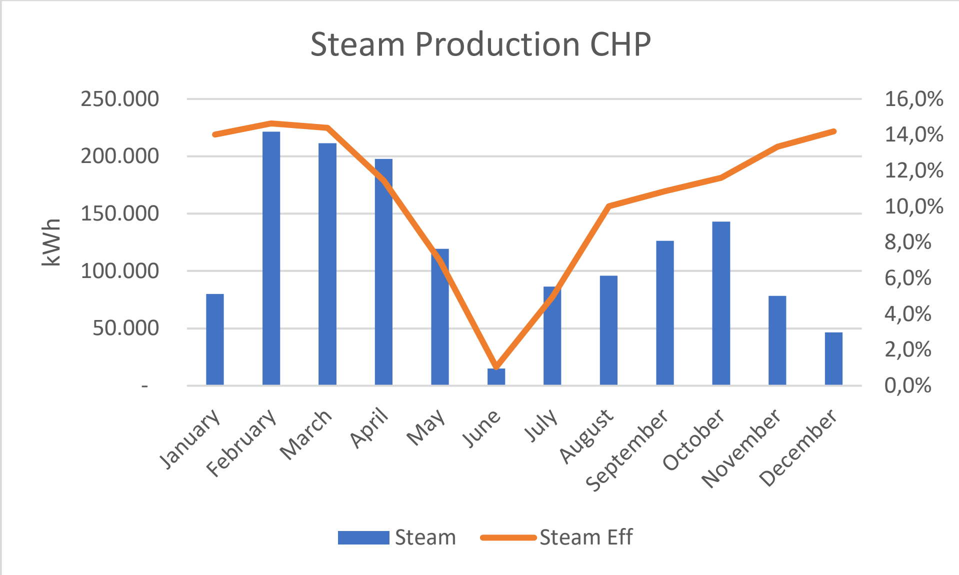

Figure 67: Cogeneration system – Steam production and efficiency trend

The water production from the second stage of the exhaust gases recovery and the steam production present similar trends. The efficiency is strongly influenced by the seasonality of the thermal demand. In fact, during summer months the efficiency registered was very low.

Overall, the efficiency of the CHP system varies during the year, as previously said, depending on the thermal needs of the plant. The lowest value registered in 2022 was around 55%, in June, while the maximum one was in January, around 75%. The efficiency could be increased during the summer months thanks to an absorption chiller that would exploit in a better way the thermal recovery of the cogenerating system.

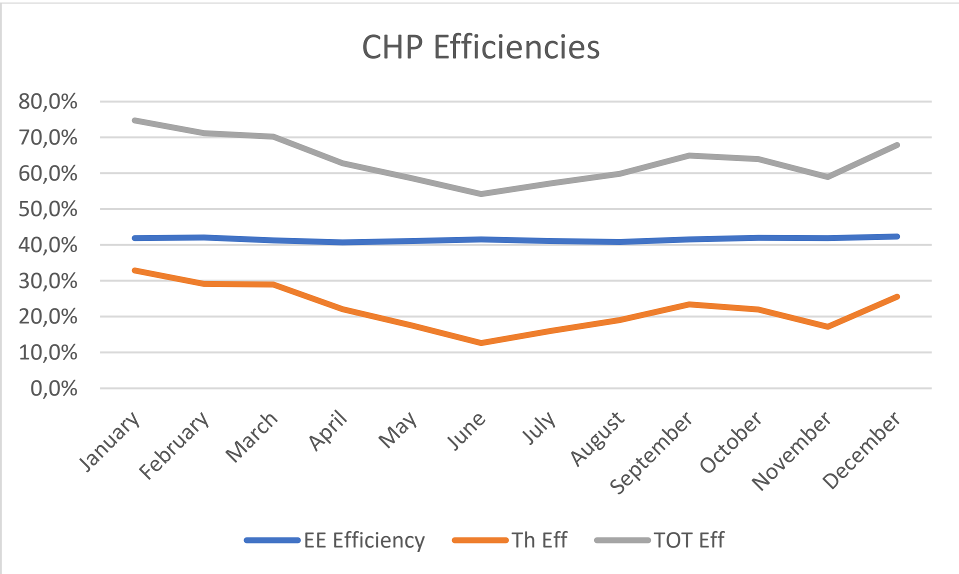

Figure 68: Cogenerating system – efficiencies trends

Case study – Cooling Energy

An absorption chiller allows to use a thermal source to produce chilled water. These types of chillers are usually employed to cool down the temperature of the buildings during summer periods, but can also be used for the refrigeration, and so entering in the manufacturing process.

The first case study regards the adoption of an absorption chiller used for the ambient cooling. Different possibilities are evaluated, and so, different suppliers.

The second case study, conversely, is about an absorption chiller with ammonia as refrigerant, that could be used to refrigerate the vermouth during the tartaric stabilization.

Before the analysis of the two case studies, an overview of the thermal resources is reported here.

- Cogenerating system

Thermal recovery from the engine water circuit:

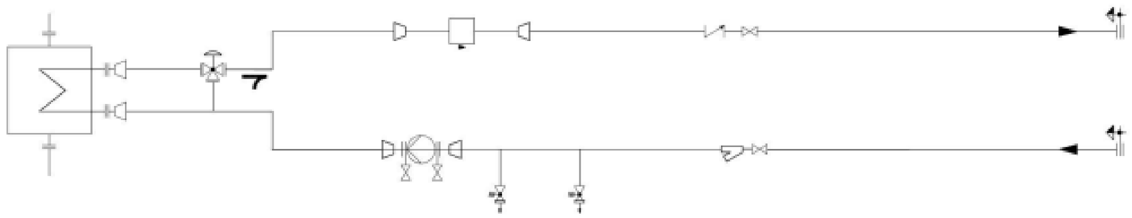

Figure 69: Cogenerating system – Engine water circuit P&ID

The hot water circuit is heated up by a heat exchanger where the engine water circuit passes. This has an inlet temperature of 93°C, an outlet temperature of 80°C, and a volumetric flowrate equal to 53,8 m^3/h.

The hot water circuit has an inlet temperature of 70°C, an outlet temperature of 80°C, and a volumetric flowrate equal to 64,6 m^3/h. The useful power is equal to 745 kW_t.

Actually, the hot water circuit, by means of a second heat exchanger, heats up another hot water circuit, containing the hot water used in the plant.

Hot water:

Temperature IN	80	°C
Temperature OUT	70	°C

Volumetric flow rate	64,6	m^3/h
Power	745	kW_t

Table 10: Hot water (engine recovery) specs

From the cogenerating system is recovered an additional amount of thermal energy. This amount is recovered through the hot exhaust gases, that entering in a heat recovery system, produce low pressure steam (3,5 bar). The exhausts exiting from the recovery system have a temperature of 164°C.

These hot exhausts pass through a second heat exchanger (second stage) and produce an additional amount of hot water. The exhaust gases enter at 164°C and exit at 57°C, with a volumetric flow rate equal to 5.420 Nm^3/h. The hot water enters at 50°C and exits at 70°C, with a flow rate equal to 17 m^3/h. the useful power is around 200 kW_t. This hot water, by means of another heat exchanger, heats up the hot water circuit containing the hot water used in the plant.

Hot water:

Temperature IN	70	°C
Temperature OUT	50	°C
Volumetric flow Rate	17	m^3/h
Power	200	kW_t

Table 11: Hot water (second stage recovery) specs

Exhausts:

Temperature IN	164	°C
Temperature OUT	57	°C
Volumetric flow rate	5420	Nm^3/h
Power	200	kW_t

Table 12: Exhausts (second stage recovery) specs

- Solar field

The solar field has an installed power equal to 327 kW_t.

It is made of two different circuits. The first one is directly in touch with the solar collectors, while the second one is fed by the primary circuit by means of a heat exchanger.

Inside the primary circuit the mixture is made of water (70%) and glycol (30%). In the secondary circuit the mixture is similar, but with different ratios: water (60%) and glycol (40%).

In the following part, in the analysis of the first option of the first case study, some graphs reporting the behavior of the solar field at different ambient conditions are represented and discussed.

Ambient cooling

In this case the absorption chiller used is a typical H2O-LiBr chiller, able to produce chilled water at 7°C.

First of all, the cooling needs of the different departments must be addressed.

In this analysis three different departments are taken into account. These, are the three bottling departments.

- Vermouth bottling department

Actually, the cooling needs of the department are satisfied by two identical machines, two DATATECH OEDA 95.2 CO from BlueBox.

Each has a refrigerant installed capacity of 95,4 kW_c, two compressors with a nominal power of 22,6 kW_e and three fans that absorb 4,2 kW_e. The maximum power absorbed by the compressors is equal to 33,8 kW_e.

Considering the previous data, the energy efficiency ratio (EER) (similar to the COP) is 3,56.

The refrigerant used in the cycle is the R410A.

Overall, the cooling needs of the department are equal to 190,8 kW_c, with an absorbed electrical power of 70 kW_e.

- Rum bottling department

The cooling of the department is made thanks to a traditional compression chiller that cools down water. Then, thanks to a distribution net, the water goes into 10 cooling units for the ambient cooling. The chiller is a Klimatechnik JWA 172 S/K/P SI/PS/CC/IM. It has a colling capacity equal to 178 kW_c and at nominal operation it absorbs 58,2 kW_e. Its EER is 3,06.

- Sparkling wine bottling department

The sparkling wine bottling department is the most difficult department to cool down in the summer period. This is mainly due to the machineries that are inside the building and to the fact that there is a steam consumption during all the year for the heating of the bottles after their filling, to perform the labelling. The wine is cold and enters in the bottles at low temperature. This creates condensate on the walls of the bottles. If the bottles are not heated up the condensate remains on the walls and make impossible the gluing of the labels.

The department is subdivided in two main area, the line 13 and the line 24.

The line 13 area is cooled by an air treatment unit with a cooling capacity of 160 kW_c. The air treatment unit can work both in the summer and in the winter period. The pipes entering to the unit are connected to two heat exchangers, and thanks to different valves hot water or cold water can enter to the unit. For the winter operation there is a heat exchanger water-water. The primary circuit hot water comes directly from the boiler room. For the summer operation the heat exchanger works with glycol-water. The cold glycol comes from the refrigeration system of the sparkling wine bulk department.

The line 24 is cooled by three units. These units are equal to the units present in the vermouth bottling department, the DATATECH OEDA 95.2 CO. Overall, the cooling needs of the area are equal to 283,5 kW_c (with a maximum electricity absorption of 105 kW_e and a nominal EER of 3,56).

The following image represents the aerial photo of the Martini&Rossi S.P.A. Pessione plant. Among the others, underlined, there are the vermouth bottling department (in orange), the rum bottling department (in blue), and the sparkling wine bottling department (in green).

In addition, two flags are reported: one for the solar field, located above the Tinaggio 92 building, and one for the cogenerating system, located near the boiler room.

Figure 70: Pessione plant – underlined the bottling departments and the solar field and the CHP system

The table below reports the main data of the cooling systems of the three departments. Considering the number of hours during which the systems are turned on, an estimation of the energy consumption can be made. In addition, considering an electricity price equal to 225€/MWh$_e$, the yearly costs can be evaluated too. These data are referred to a year of utilization.

	Maximum Power [kW$_e$]	Cooling Power [kW$_c$]	Hours per season	Energy [kWh]	k€
VTH	70	191	2.100	147.000	33,1
RUM	60	178	2.700	162.000	36,5
SPW L24	105	286	4.000	420.000	94,5
SPW L13 – ATU	70	160	400	28.000	6,3

Table 13: Cooling needs of the bottling departments

Option 1 – Solar field

The first option considers installing an absorption chiller directly in contact with the solar field, linked to the primary circuit. This would allow to remove the secondary circuit and to obtain higher efficiency of the entire system. Since the solar field peak power is 327 kW_t, considering the cooling needs, and the location of the departments inside the plant, the only department that can be cooled is the vermouth bottling department.

To estimate the feasibility of the project, two different suppliers have been contacted. To define the size of the chiller three different days have been analyzed: a sunny day, a cloudy day, and a variable weather day.

In the chart below, to better understand the differences between the three selected days, the solar irradiance is reported.

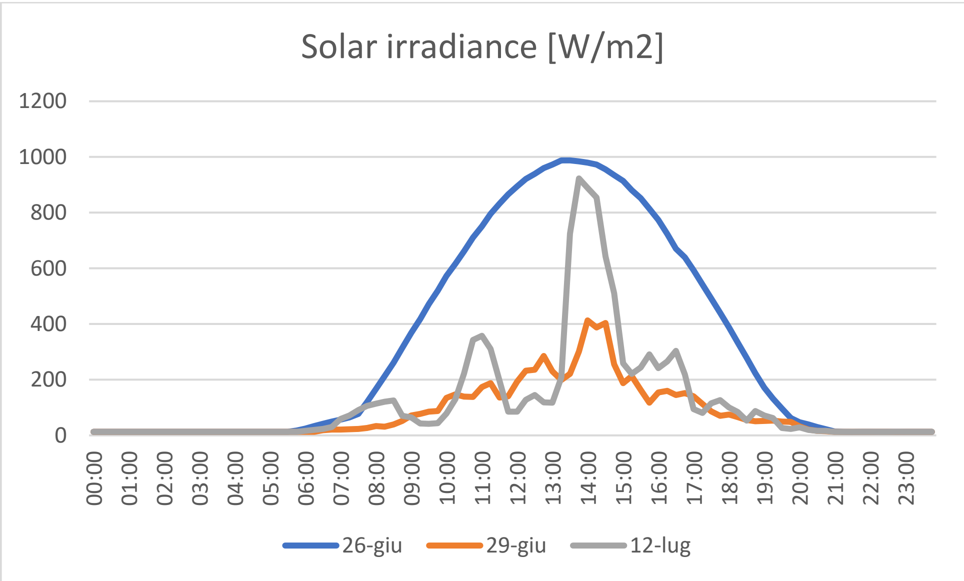

Figure 71: Solar irradiance variation during the day - Three different days: sunny, cloudy and variable weather conditions

Then, the water temperature and the available power are analyzed. These data are evaluated for both the primary and the secondary circuits.

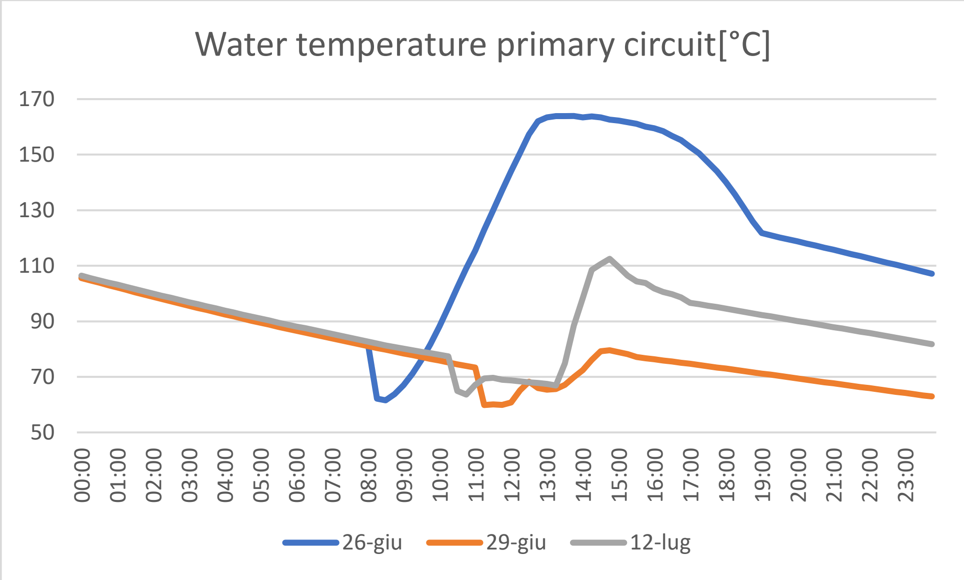

Figure 72: Hot water temperature of the primary circuit of the solar thermal filed – Three different days: sunny, cloudy, and variable weather conditions

The water temperature in the primary circuit reaches very high values during the sunny day. The solar irradiance overcomes 200 W/m^2 at the 8:00 AM, and as a consequence the temperature of the water decreases, since there is a mixing of all the water through the entire piping. Then, after this first transient, the primary circuit starts to be heated up by the incoming sun rays. The maximum temperature is reached at 1:15 PM, with a value higher than 163 °C. Then, at a reduction of the solar radiation, corresponds a reduction of the temperature of the water. Around the 7 PM the pump stops to work, and the temperature of the water start to decrease in a linear way, depending to the thermal losses due to conduction and convection through the pipes.

In the variable weather day, it can be noted a different, but similar trend. Due to the variability of the weather the temperature of the water starts to increase after the 1 PM, then it reaches the maximum just before the 3 PM, overcoming 110 °C, and then, since the pump stops working at 16:45 (200 W/m^2), starts to decrease almost linearly. On the other hand, for the cloudy day, the temperature of the water is not sufficiently high to feed an absorption chiller. The maximum temperature reached in this condition is lower than 80°C.

Similarly, but with slightly lower values, the water temperature values for the secondary circuit are reported in the following chart. In the secondary circuit the three phases of the temperature variation, similarly to what happen in the primary circuit, can be appreciated too.

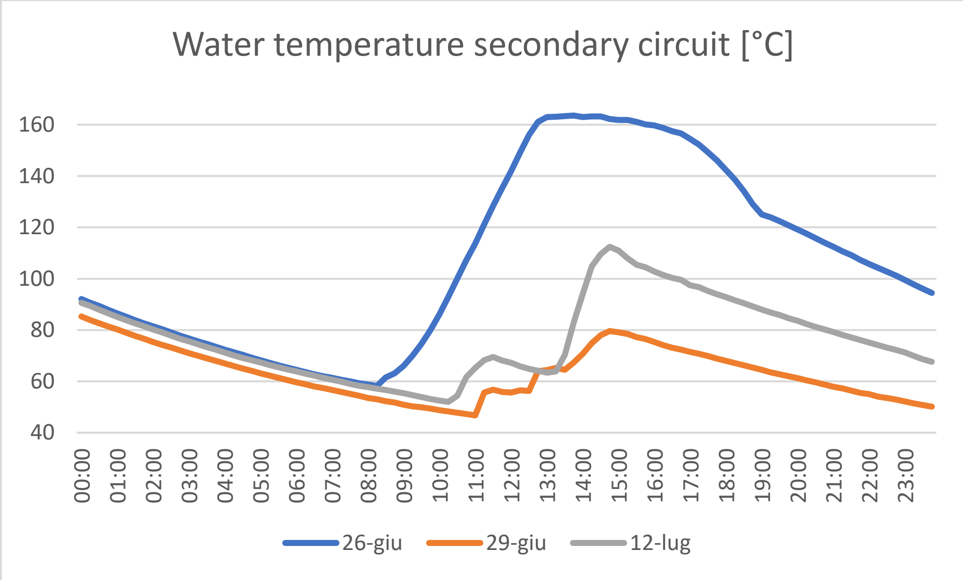

Figure 73: Hot water temperature of the secondary circuit of the solar thermal field – Three different days: sunny, cloudy, and variable weather conditions

Finally, coupling the temperature of the water with the flowrate available, the power trend of the hot water for the three days and for the two circuits is reported in the two following graphs.

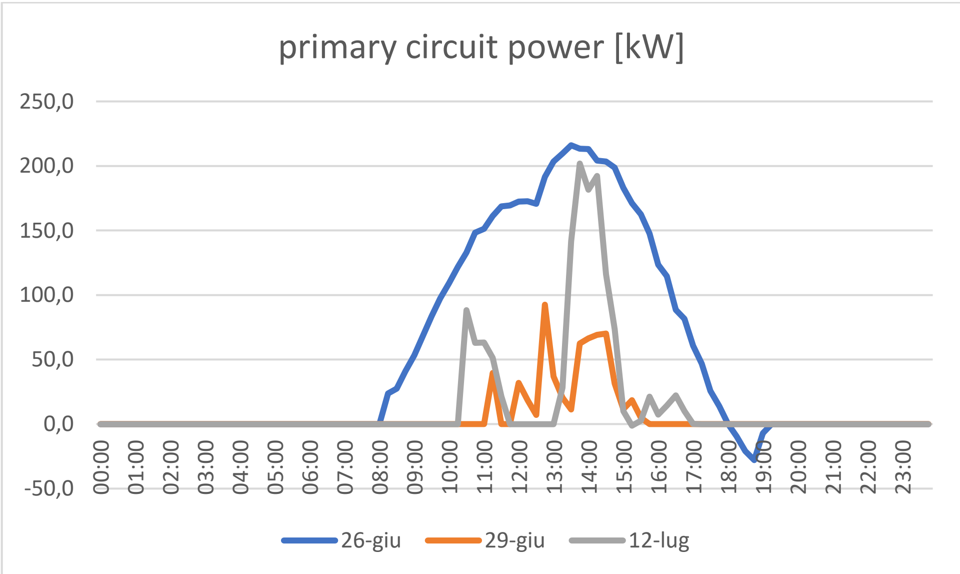

Figure 74: Primary circuit power – Three different days: sunny, cloudy, and variable weather conditions

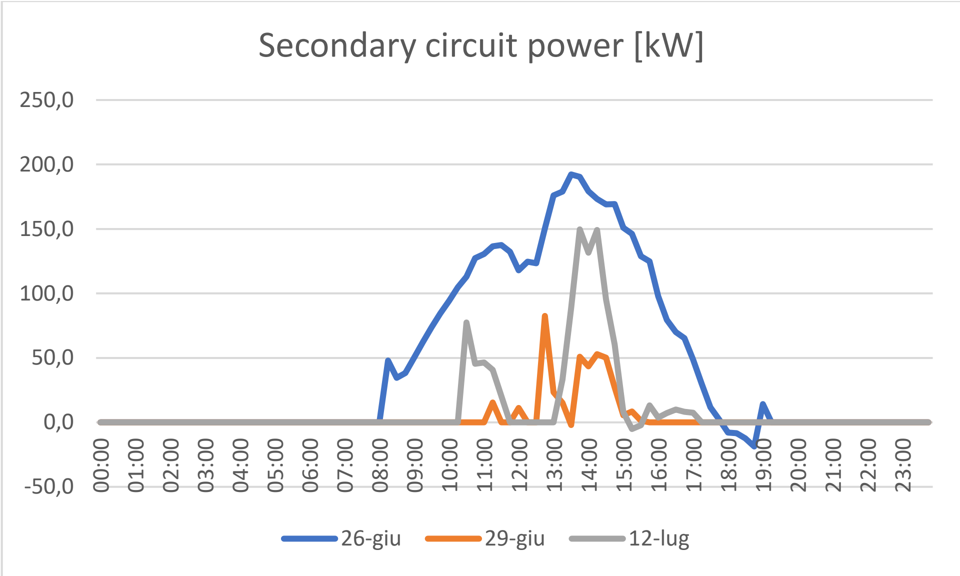

Figure 75: Secondary circuit power – Three different days: sunny, cloudy, and variable weather conditions

The trends regarding the useful thermal power of the hot water inside the primary and the secondary circuits for the three different days are similar, but with lower values for the secondary circuit with respect to those of the primary circuit. This is due to the fact that passing from the primary to the secondary circuit some losses are added.

It can be seen that for the sunny day the power has acceptable values for most of the day. On the other hand, for the other two days analyzed the power is not constant or very low.

Considering these data two different chillers have been dimensioned and analyzed.

The useful power produced by the solar field is directly related to the solar radiation. Higher the temperature, higher the exergy content of the thermal energy produced by the collectors.

The useful power is related to the solar irradiance by means of the efficiency of the solar field. The nominal value of efficiency is around 44%, but the registered average value in sunny conditions is around 35%.

Starting from this value it is possible to evaluate the available useful power starting from the solar irradiance:

Solar Irradiance	**Useful Power Nominal**	**Useful Power Registered**
[W/m^2]	kW_t	kW_t
200	52,4	41,7
400	104,9	83,4
580,0	**152,1**	**121**
600	157,3	125,2
762,7	**200**	**159,1**
800	209,8	166,9
958,8	**251,4**	**200**
1000	262,2	208,6

Table 14: Solar field useful power production according to the input solar irradiance

The useful power has been evaluated considering the following equation:

$$P_u = GA_{coll}\eta_{coll}$$

With a collectors' area equal to 596 m^2 and an efficiency equal to 35%.

It is important to notice that, considering the measured average efficiency, the solar field, during the summer operation mode, is able to produce 200 kW_t of thermal power only when the solar irradiance overcomes 958,8 W/m^2. On the other hand, only 762,7 W/m^2 are sufficient to produce 200 kW_t considering the nominal average efficiency.

To better dimension the absorption chiller, a daily average (between 9 AM and 6 PM) solar irradiance has been evaluated. This value, for sunny days, is around 580 W/m^2, with a maximum reaching 790 W/m^2. Considering the average value, the useful power produced by the solar field is equal to 121 kW_t.

Option 1.1 121 kWt

This system takes into account the average value of solar irradiance reached every day. Starting from a value of 580 W/m^2, the absorption chiller has been dimensioned, resulting in a system able to receive 121 kW_t from the solar field. The temperatures involved are 80-70°C for the heat source, 7-12°C for the chilled water, and 29-34°C for the cooling water. According to these parameters, the chiller has a nominal COP equal to 0,824, resulting in a cooling power of 100 kW_c.

In the table below the main characteristics of the absorption chiller are reported.

Thermal power	kW_t	121
Cooling power	kW_c	100
COP		0,824
Chilled water temperature	°C	7 – 12
Chilled water volumetric flowrate	m^3/h	17,2
Cooling water temperature	°C	29 – 34
Cooling water volumetric flowrate	m^3/h	38,3
Hot water-glycol (40%) temperature	°C	80 – 70
Hot water-glycol (40%) volumetric flowrate	m^3/h	11,6

Table 15: Option 1.1 Absorption chiller specs

The flow rates are evaluated starting from the powers involved and the temperature differences.

In addition, some parameters have been fixed:

Chilled water specific heat	kJ/kgK	4,191
Chilled water denisty	Kg/m^3	999
Cooling water specific heat	kJ/kgK	4,176
Cooling water denisty	Kg/m^3	995
Hot water specific heat	kJ/kgK	4,189
Hot water denisty	Kg/m^3	972
Hot water-glycol (40%) specific heat	kJ/kgK	3,680
Hot water-glycol (40%) denisty	Kg/m^3	1.021

Table 16: Water properties (specific heat and density)

$$P = mC_p\Delta T$$

and

$$V = \frac{m}{\rho}$$

Where P is the power, m is the mass flowrate, C_p is the specific heat, ΔT is the temperature difference, V is the volumetric flowrate, and ρ is the density.

This results in:

$$V = \frac{P}{\rho C_p \Delta T}$$

Attention, it must be taken into account the conversion factor 3.600 to shift from kJ to kW.

The cooling water flows in a circuit linked to the evaporative condenser, that is dimensioned summing the thermal and the cooling powers (221 kW) and adding a 5%. In this way, the evaporative condenser would dissipate a power equal to 232 kW.

Other data of interest for the feasibility are the dimensions of the chiller:

Length	mm	2.669
Depth	mm	1.536
Height	mm	1.810

Table 17: Option 1.1 Absorption chiller dimensions

Finally, to drive the chilled water to cool down the ambient, a distribution system made of pumps and piping, and the units to move the air chilled by the water are needed.

Actually, in the vermouth bottling department, there is not the distribution system, nor the cooling (or heating) units. This because the air heaters use steam.

The price of this chiller is 82.000 €, that of the evaporative condenser is near 20.000 €.

Absorption chiller	82.000 €
Evaporative condenser	20.000 €

Table 18: Option 1.1 Absorption chiller and evaporative condenser prices

This option is rejected because is not able to satisfy completely the cooling demand of the vermouth bottling department. It is technically feasible, but it is not economically feasible. This because this system would be put in parallel to the existing cooling system.

Option 1.2 200 kWt

The second option takes into account a thermal power equal to 200 kW. This seems to be an over-dimension of the system. The solar field is able to produce 200 kW_t, nominally up to 327 kW_t, but averagely it produces a lower amount of power. This results in a more frequent partial loads functioning of the absorption chiller.

The temperatures considered are the same as before, a part for the hot water temperature, that in this case is 95-85°C. considering these data, the selected chiller is able to produce 158 kW_c, with a nominal COP equal to 0,79.

In the table below the main characteristics of the absorption chiller are reported.

Thermal power	kW_t	200
Cooling power	kW_c	158
COP		0,79
Chilled water temperature	°C	7 – 12
Chilled water volumetric flowrate	m^3/h	27,2
Cooling water temperature	°C	29 – 34
Cooling water volumetric flowrate	m^3/h	62,0
Hot water-glycol (40%) temperature	°C	95 – 85
Hot water-glycol (40%) volumetric flowrate	m^3/h	19,2

Table 19: Option 1.2 Absorption chiller specs

The cooling water flows in a circuit linked to the evaporative condenser, that is dimensioned summing the thermal and the cooling powers (358 kW) and adding a 5%. In this way, the evaporative condenser would dissipate a power equal to 376 kW.

The dimensions of the chiller are reported in the table below:

Length	mm	3.200
Depth	mm	1.400
Height	mm	2.100

Table 20: Option 1.2 Absorption chiller dimensions

The price of this chiller is 75.000 €, that of the evaporative condenser is 24.000 €.

Absorption chiller	75.000 €
Evaporative condenser	24.000 €

Table 21: Option 1.2 Absorption chiller and evaporative condenser prices

This system would, nominally, almost satisfy the cooling needs of the department. This is true especially if the distribution system is well designed.

Since this project is technically feasible, an economic analysis will be performed in the next section.

Option 2 – Cogenerating system

The second option considers the usage of the hot water recovered from the CHP. Only that recovered from the engine cooling circuit can be used. This because the hot water recovered from the second stage of the exhaust gases has a temperature that is too low.

Considering an almost fixed functioning of the CHP in the summer months, as before said during the CHP analysis, the hot water recovered sent to the chiller has a thermal power equal to 745 kW.

Even for the second option two different suppliers have been contacted. The two proposed two similar solutions making different assumptions.

Option 2.1 745 kWt – 614 kWc

The first option considers a thermal source with a power equal to 745 kW_t. The temperatures involved are 80-70°C for the hot water, 7-12°C for the chilled water, and 29-34°C for the cooling water. The chiller dimensioned has a quite high efficiency, equal to 0,824, resulting in a cooling capacity of 614 kW_c.

Thermal power	kW_t	745
Cooling power	kW_c	614
COP		0,824
Chilled water temperature	°C	7 – 12
Chilled water volumetric flowrate	m^3/h	105,6
Cooling water temperature	°C	29 – 34
Cooling water volumetric flowrate	m^3/h	235,5
Hot water temperature	°C	80 – 70
Hot water volumetric flowrate	m^3/h	65,9

Table 22: Option 2.1 Absorption chiller specs

The cooling water flows in a circuit linked to the evaporative condenser, that is dimensioned summing the thermal and the cooling powers (1.359 kW) and adding a 5%. In this way, the evaporative condenser would dissipate a power equal to 1.427 kW.

The dimensions of the chiller are reported below:

Length	mm	4.872
Depth	mm	2.138
Height	mm	2.346

Table 23: Option 2.1 Absorption chiller dimensions

The price of this chiller is 187.000 €, that of the evaporative condenser is 51.000 €

Absorption chiller	187.000 €
Evaporative condenser	51.000 €

Table 24: Option 2.1 Absorption chiller and evaporative condenser prices

Since the chilled water produced has a power equal to 614 kW, this chiller could satisfy the cooling demand of the two lines of the sparkling wine bottling department and the rum bottling department. A further economic analysis is performed in the next section.

Option 2.2 745 kWt – 580 kWc

The second option considers the same parameters, but takes into account a lower efficiency chiller. The nominal COP is equal to 0,779, resulting in a cooling capacity of 580 kW_c.

Thermal power	kW_t	745
Cooling power	kW_c	580
COP		0,779
Chilled water temperature	°C	7 – 12
Chilled water volumetric flowrate	m^3/h	99,7
Cooling water temperature	°C	29 – 34
Cooling water volumetric flowrate	m^3/h	229,6
Hot water temperature	°C	80 – 70
Hot water volumetric flowrate	m^3/h	65,9

Table 25: Option 2.2 Absorption chiller specs

The cooling water flows in a circuit linked to the evaporative condenser, that is dimensioned summing the thermal and the cooling powers (1.325 kW) and adding a 5%. In this way, the evaporative condenser would dissipate a power equal to 1.391 kW.

The dimensions of the chiller are presented below:

Length	mm	4.700
Depth	mm	2.000
Height	mm	2.900

Table 26: Option 2.2 Absorption chiller dimensions

The price of this chiller is 146.000 €, that of the evaporative condenser is 44.000 €.

Absorption chiller	146.000 €

Evaporative condenser	44.000 €

Table 27: Option 2.2 Absorption chiller and evaporative condenser prices

In this case the chilled water is not able to completely satisfy the cooling needs of both the two lines of the sparkling wine bottling department and the rum bottling department (624 kW_c), but considering a more efficient distribution system the size of the absorption chiller previously described could be sufficient to cover the actual cooling demand.

Another option could be to cool down only the sparkling wine department. To better evaluate this solution, it is better to consider a smaller absorption chiller, nearer to the real cooling needs. This is necessary to understand better the costs, and the thermal power required by the system.

For the reasons above mentioned, the cooling system to cool down both the sparkling wine bottling department and the rum bottling department only will be analyzed also form the economic point of view.

Option 3 – Solar field plus cogenerating system

This option considers the usage of all the thermal power available to feed a single absorption chiller. In this option, such as for the previous one, the hot water produced by the second stage of the exhaust gases is not considered.

The overall thermal power available is around 950 kW_t, considering both the CHP recovery and the solar field.

It is important to underline that in this case an additional heat exchanger must be positioned after the secondary circuit of the solar field. The heat exchanger would allow the heating up of a third circuit, containing water. The heated water would be mixed with the hot water produced by the CHP.

Even in this case, different suppliers have been contacted to compare their proposals.

Option 3.1 – 950 kWt

The first proposal consists in an absorption chiller with a thermal power request equal to 950 kW_t. The temperatures involved are 80-70°C for the hot water, 7-12°C for the chilled water, and 29-34°C for the cooling water. These data allow to obtain a chiller with a nominal COP equal to 0,775, and a cooling power of 736 kW_c.

Thermal power	kW_t	950
Cooling power	kW_c	736
COP		0,775
Chilled water temperature	°C	7 – 12
Chilled water volumetric flowrate	m^3/h	126,6
Cooling water temperature	°C	29 – 34
Cooling water volumetric flowrate	m^3/h	290,8
Hot water temperature	°C	80 – 70
Hot water volumetric flowrate	m^3/h	84,0

Table 28: Option 3.1 Absorption chiller specs

The cooling water flows in a circuit linked to the evaporative condenser, that is dimensioned summing the thermal and the cooling powers (1.686 kW) and adding a 5%. In this way, the evaporative condenser would dissipate a power equal to 1.770 kW.

Length	mm	5.400
Depth	mm	2.100
Height	mm	3.000

Table 29: Option 3.1 Absorption chiller dimensions

The price of this chiller is 179.000 €, that of the evaporative condenser is 67.000 €

Absorption chiller	179.000 €
Evaporative condenser	67.000 €

Table 30: Option 3.1 Absorption chiller and evaporative condenser prices

This absorption chiller could almost satisfy all the cooling demand of the bottling departments.

This proposal is further analyzed in the next section also considering an economic evaluation.

Option 3.2 – 1.000 kWt

This second proposal considers a thermal power equal to 1.000 kW_t. This is an assumption that considers using all the thermal available from the CHP and that from the solar field, mixing the different hot water streams, obtaining a higher amount of thermal power. This can be obtained because the hot water from the engine of the CHP is at 80°C, the hot water from the second stage of the exhaust gases is at 70°C and the hot water from the solar field is at a temperature higher than 90°C. Mixing them it is possible to obtain a thermal source of more than 1000 kW_t, with an average temperature of 80°C.

The temperatures involved are the same as the option described before. In this case the COP is a bit lower, with a nominal value of 0,739, and the cooling power is equal to 739 kW_c.

Thermal power	kW_t	1.000
Cooling power	kW_c	739
COP		0,739
Chilled water temperature	°C	7 – 12
Chilled water volumetric flowrate	m^3/h	127,1
Cooling water temperature	°C	29 – 34
Cooling water volumetric flowrate	m^3/h	301,3
Hot water temperature	°C	80 – 70
Hot water volumetric flowrate	m^3/h	88,4

Table 31: Option 3.2 Absorption chiller specs

The cooling water flows in a circuit linked to the evaporative condenser, that is dimensioned summing the thermal and the cooling powers (1.739 kW) and adding a 5%. In this way, the evaporative condenser would dissipate a power equal to 1.826 kW.

The dimensions of the machine are reported in the table below.

Length	mm	5.420
Depth	mm	2.350
Height	mm	2.860

Table 32: Option 3.2 Absorption chiller dimensions

The price of this chiller is 149.000 €, that of the evaporative condenser is 69.000 €.

Absorption chiller	149.000 €
Evaporative condenser	69.000 €

Table 33: Option 3.2 Absorption chiller and evaporative condenser prices

This system is able to satisfy almost all the cooling needs of the three bottling departments (815 kW). This is true also considering that a new and more efficient distribution system, with new cooling units would be installed, decreasing the actual cooling needs.

For this proposal an economic analysis is performed and represented in the next section.

Distribution system

In addition to the absorption chillers, a distribution system must be considered. In fact, the chillers produce chilled water, but the water must be distributed through the departments to be cooled down. Pumps and piping must be dimensioned and quoted to perform the economic analysis.

For the vermouth bottling department and for the sparkling bottling department the cooling unit needs to be added. Only the rum bottling department present a cooling system made with chilled water.

The assumptions made, considering data available from previous projects are:

- Cooling units

Each cooling unit has a cooling power equal to 87 kW_c, and costs 6.500 €.

- Pumps

A 36 m3/h 5 bar pump costs 3.800 €. For different sizes pumps a scalability factor equal to 0,8 is considered.

The cost of different size pumps is estimated according to the following formula:

$$\frac{C_1}{C_2} = \left(\frac{S_1}{S_2}\right)^{0,8}$$

Where C represents the cost and S the size (volumetric flow rate) of the pumps.

Size [m^3/h]	Cost [€]
27,2	3.100
99,7	8.600
105,6	9.000
126,6	10.400
127,1	10.500

Table 34: Pump prices

- Piping

The piping is made of a tube and a layer of insulation. The tube is made of stainless steel, with a diameter equal to 80 mm and a thickness equal to 2 mm. The tube costs 90 €/m.

The insulation layer has a thickness of 40 mm and costs 40 €/m.

Overall, each meter of the piping costs around 130 €/m.

Considering these data, it is possible to estimate the distribution system related costs for each department, a part for the pumps, that are dimensioned according to the volumetric flow rate of the fluid passing through the chiller.

The new cooling units needed to cool down the bottling departments are two units for the vermouth bottling department, and five units for the sparkling wine bottling department (three units for the line 24 and two units for the line 13.

For the vermouth bottling department, considering the Option 1 (solar field alone), the piping starts from the solar field, and has a length of around 400 m. considering the Option 3 (solar field coupled with the CHP), the piping starts from the boiler room, and has a length of around 320 m.

For the sparkling wine bottling department, in any case the piping starts from the boiler room, and has a length equal to around 430 m.

The rum bottling department already has a chilled water distribution system, but a link between the new system and the old one should be taken into account. In this way, a piping of around 50 m is needed.

Below, two tables report the main results regarding the distribution system costs:

Department	Number of cooling unit	Cost [€]
Vermouth	2	13.000
Sparkling Wine	5	32.500
Rum	0	0

Table 35: Number of cooling units to be purchased for each bottling department

Department	Length [m]	Cost [€]
Vermouth (Option 1)	400	52.000
Vermouth (Option 3)	320	41.600
Sparkling Wine	430	55.900
Rum (link)	50	6.500

Table 36: Piping costs for each bottling department

Refrigeration

The absorption chiller can work also with other mixtures, not only with Water-BrLi. The most used, a part Water-BrLi, is NH_3-Water. Since the refrigerant is ammonia, the temperature of the fluid exiting the chiller could reach a value far below 0°C.

Thanks to this different mixture, the absorption chiller can also be integrated inside the manufacturing process.

Absorption chillers working with ammonia need a higher temperature thermal source, so for the analyzed case, only the solar field would be suitable (only in determined hours of the day, in a sunny day). The higher the temperature of the feed water, the higher the efficiency of the chiller is. Globally, a chiller working with ammonia-water has a lower COP in comparison to a chiller working with water-BrLi. This is due also to the temperature of the chilled fluid that must be reached.

In this case, the temperature that must be reached is -11°C, the temperature of the glycol used to cool down the vermouth during the tartaric stabilization.

Actually the glycol is cooled down by a conventional compression refrigeration cycle. The system is made of four CWRW-163/145/36 by Gaudino installed in 2011. The refrigerant used is the R507. Each compressor has an electrical power absorption equal to 119,5 kW_e and e cooling power production equal to 330,71 kW_c, with a COP of 2,767.

Overall, the entire refrigeration system of the vermouth has an installed cooling capacity equal to 1.322,84 kW_c.

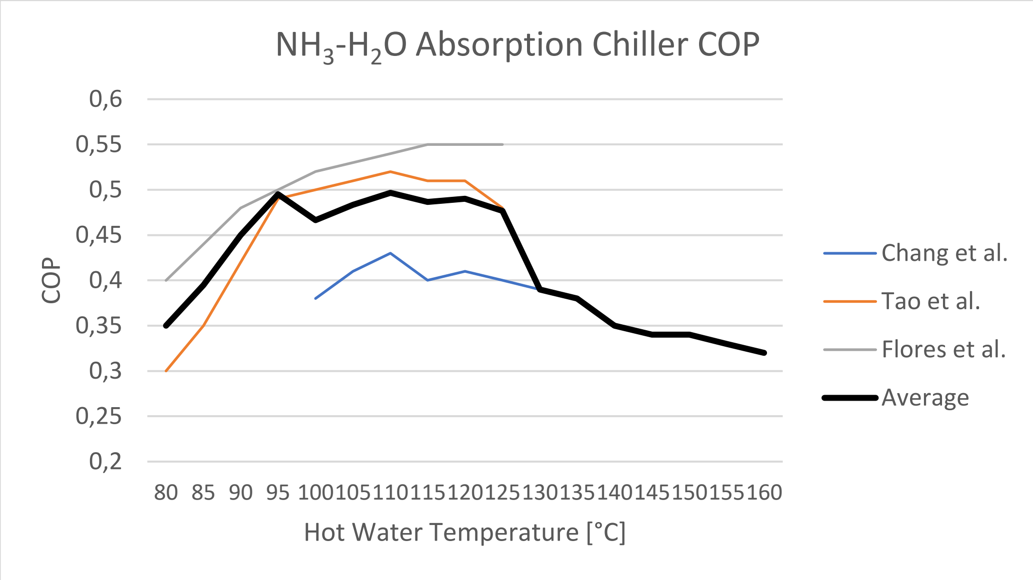

Figure 76: NH_3-H_2O Absorption chiller coefficient of performance

In the graph above there are reported four different COP trends of an absorption chiller with ammonia. The temperature range goes between 80 and 160°C.

Three curves, the blue one, the orange one, and the grey one, are referred to three different studies. The blue one is referred to the study of Chang et al. [32], the orange one is referred to the study of Tao et al. [33], and the grey one is referred to the study of Flores et al. [34].

The black curve is the average of the three curves introduced above. The result is that the COP is between 0,3 and 0,5. It reaches its maximum for values of temperature between 95 and 125°C. for temperature lower than 95°C and higher than 125°C the COP decreases (below 0,4).

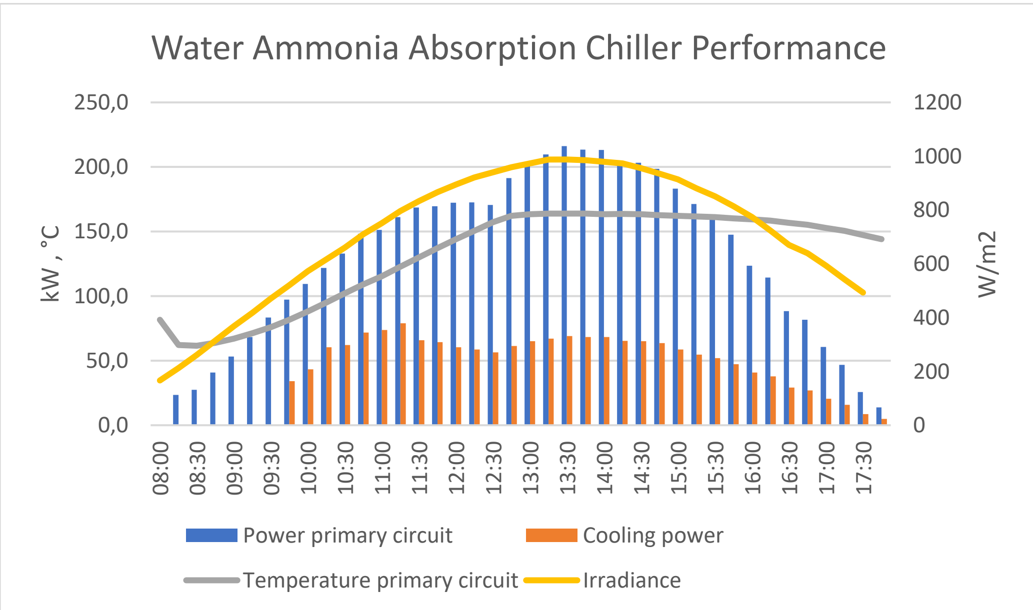

Figure 77: Water ammonia absorption chiller performances during a sunny day

Starting from the data referred to a sunny day (high irradiance), it can be seen the trend of the temperature of the water flowing in the primary circuit. Considering the temperature and the flowrate, the thermal power is evaluated. Then, to obtain the cooling power, it must be coupled the thermal power produced by the hot water at a certain temperature and the coefficient of performance of the absorption chiller at that temperature. Integrating the cooling power over the day it is obtained the cooling energy produced in one sunny day.

The production during the day reaches 430 kWh of cooling energy.

Considering a period of functioning of the summer mode between May and September, and that the days that have a sufficient solar availability to firstly drive the solar filed, and then the absorption chiller, are around the 70%, the total cooling energy production per year is about:

$$E_{cooling} = 153\ days * 0{,}70 * 430 \frac{kWh}{day} = 46.053\ kWh_c$$

Obviously, the absorption chiller analyzed for the refrigeration purpose would be installed in series to the actual refrigeration system. this because alone, the chiller coupled with the solar field is note able to satisfy the cooling demand required during the process of the tartaric stabilization.

In addition, considering the COP of the existing system, 2,767, the electricity that would be saved is equal to:

$$E_e = \frac{E_c}{COP} = \frac{46.053}{2{,}767} = 16.644\ kWh_e$$

Considering the electricity price as equal to 225 €/MWh, the economic saving per year would be equal to:

$$Saving\ [€] = 16{,}644 * 225 = 3.745\ €$$

Since an absorption chiller with NH_3-water is more expensive than an absorption chiller with water-BrLi, the saving obtained is negligible with respect to the initial investment (with a payback time higher than the life of the system).

Economic analysis

To define the economic performance of the project, different calculations have been made and some data are required.

First of all, the duration of the investment is set equal to 10 years. It is important to have the values of the capital expenditure and of the annual savings.

Considering the capital expenditure and the duration of the investment, the annual depreciation is evaluated:

$$Depreciation = \frac{CAPEX}{n°years}$$

The depreciation value is subtracted from the saving to evaluate the taxes:

$$Taxes[€] = Tax[\%] * (Revenues - Depreciation)$$

Setting the Tax equal to 27,9%.

After the evaluation of the taxes to be paid, the net annual cash flow can be computed:

$$Net\ Cash\ Flow = Revenues - Taxes$$

Adding the interest rate it is possible to evaluate the discounted net cash flow:

$$Discounted\ Net\ Cash\ Flow = Net\ Cash\ Flow * \frac{1}{(1+i)^n}$$

Where i is the interest rate, set equal to 7,50%, and n is the year.

In this way it is possible to evaluate the net present value, starting from the capital expenditure and summing, annually, the discounted net cash flow.

Thanks to this analysis it is possible to evaluate three indicators of the investment:

- Rate of return (ROR)
- Payback time (PBT)
- Internal rate of return (IRR)

Option 1.2

The option 1.2 is about the usage of the solar field to feed an absorption chiller that cools down the ambient temperature of the vermouth bottling department.

The overall electricity consumption to cool down the department is equal to 147.000 kWh. This value regards the entire day, and not only the hours between the 8 AM and the 6 PM. The electricity consumption of the actual cooling system during the hours when the solar field is working is equal to the 49,32% of the total consumption. Thanks to this percentage it is possible to obtain the electricity saving that would bring the adoption of this system.

$$Electricity\ saving = 147.000 * 49{,}32\% = 72.500\ kWh$$

Considering an electricity price equal to 225 €/MWh, the electricity saving in monetary terms becomes 16,3 k€ per year.

In the table below the main data for the economic evaluation are reported:

Description	€
Absorption Chiller	75.000
Evaporative condenser	24.000
Pump	3.100
Pipings	52.000
Air coolers	13.000
Total CAPEX	**167.100**
Annual Savings	**16.313**

Table 37: Option 1.2 – Costs and savings

Year	CAPEX	Revenues	Discounted net cash flow	NPV
0	-167.100 €	0	-167.100 €	-167.100 €
1	0	16.313 €	15.175 €	-151.925 €
2	0	16.313 €	14.116 €	-137.809 €
3	0	16.313 €	13.131 €	-124.678 €
4	0	16.313 €	12.215 €	-112.462 €
5	0	16.313 €	11.363 €	-101.099 €
6	0	16.313 €	10.570 €	-90.529 €
7	0	16.313 €	9.833 €	-80.697 €
8	0	16.313 €	9.147 €	-71.550 €
9	0	16.313 €	8.509 €	-63.041 €
10	0	16.313 €	7.915 €	-55.126 €

Table 38: Option 1.2 – Net Present Value

This is not sustainable from the economic point of view. The NPV after ten years is negative.

Option 2.1

The option 2.1 is about the usage of the thermal power recovered from the water of the engine cooling circuit. The chiller dimensioned according to this power has a cooling capacity equal to 614 kWc. Thanks to this capacity, the system would be able to cool down the entire sparkling wine bottling department and the rum bottling department.

Since the CHP works almost constantly, the production of chilled water would be constant during the day. This result in the complete substitution of the existing cooling system, that in a year consumes more than 600.000 kWh for the ambient cooling of the two departments. In monetary terms this means an annual saving higher than 135 k€.

Description	€
Absorption Chiller	187.000
Evaporative condenser	51.000
Pump	9.000
Pipings	62.400
Air coolers	32.500
Total CAPEX	**341.900**
Annual Savings	**137.300**

Table 39: Option 2.1 – Costs and savings

Year	CAPEX	Revenues	Discounted net cash flow	NPV
0	-341.900 €	0	-341.900 €	-341.900 €
1	0	137.300 €	100.960 €	-240.940 €
2	0	137.300 €	93.917 €	-147.023 €
3	0	137.300 €	87.364 €	-59.659 €
4	0	137.300 €	81.269 €	21.610 €
5	0	137.300 €	75.599 €	97.209 €
6	0	137.300 €	70.325 €	167.534 €
7	0	137.300 €	65.418 €	232.952 €
8	0	137.300 €	60.854 €	293.807 €
9	0	137.300 €	56.609 €	350.415 €
10	0	137.300 €	52.659 €	403.075 €

Table 40: Option 2.1 – Net Present Value

ROR	1,17
PBT [year]	4
IRR	29,31%

Table 41: Option 2.1 – Economic indicators

From the economic point of view this project seems to be feasible, with a payback time lower than 4 years (and a simple payback time equal to 2,49 years).

Option 2.2

The option 2.2, a part for the different chiller, considers the same data s the option 2.1. the chiller would cool down the sparkling wine bottling department and the rum bottling department. The annual saving is higher than 135 k€.

Description	€
Absorption Chiller	146.000
Evaporative condenser	44.000
Pump	8.600
Pipings	62.400
Air coolers	32.500
Total CAPEX	**293.500**
Annual Savings	**137.300**

Table 42: Option 2.2 – Costs and savings

Year	CAPEX	Revenues	Discounted net cash flow	NPV
0	-293.500 €	0	-293.500 €	-293.500 €
1	0	137.300 €	99.704 €	-193.795 €
2	0	137.300 €	92.748 €	-101.047 €
3	0	137.300 €	86.277 €	-14.770 €
4	0	137.300 €	80.257 €	65.487 €
5	0	137.300 €	74.658 €	140.145 €
6	0	137.300 €	69.449 €	209.595 €
7	0	137.300 €	64.604 €	274.200 €
8	0	137.300 €	60.097 €	334.297 €
9	0	137.300 €	55.904 €	390.201 €
10	0	137.300 €	52.004 €	442.205 €

Table 43: Option 2.2 – Net Present Value

ROR	1,51
PBT [year]	4
IRR	34,65%

Table 44: Option 2.2 – Economic indicators

From the economic point of view this project seems to be feasible, with a payback time lower than 4 years (and a simple payback time equal to 2,14 years). The economic results of the option 2.2 are even better than those of the option 2.1.

Option 3.1

The option 3.1 considers the installation of a chiller able to satisfy almost all the cooling needs of the three bottling departments. This allows to obtain an annual saving equal to around 170 k€.

Description	€
Absorption Chiller	179.000
Evaporative condenser	67.000
Pump	10.400
Pipings	104.000
Air coolers	65.000
Total CAPEX	**425.400**
Annual Savings	**170.400**

Table 45: Option 3.1 – Costs and savings

Year	CAPEX	Revenues	Discounted net cash flow	NPV
0	-425.400 €	0	-425.400 €	-425.400 €
1	0	170.400 €	125.327 €	-300.073 €
2	0	170.400 €	116.584 €	-183.489 €
3	0	170.400 €	108.450 €	-75.039 €
4	0	170.400 €	100.884 €	25.845 €
5	0	170.400 €	93.845 €	119.690 €
6	0	170.400 €	87.298 €	206.988 €
7	0	170.400 €	81.207 €	288.196 €
8	0	170.400 €	75.542 €	363.737 €
9	0	170.400 €	70.271 €	434.009 €
10	0	170.400 €	65.369 €	499.377 €

Table 46: Option 3.1 – Net Present Value

ROR	1,17
PBT [year]	4
IRR	29,23%

Table 47: Option 3.1 – Economic indicators

From the economic point of view this project seems to be feasible, with a payback time lower than 4 years (and a simple payback time equal to 2,50 years).

Option 3.2

The option 3.2 considers the same data as the option 3.1. this means that the annual savings that could be done are around 170 k€.

Description	€
Absorption Chiller	149.000
Evaporative condenser	69.000
Pump	10.500
Pipings	104.000
Air coolers	65.000
Total CAPEX	**397.500**
Annual Savings	**170.400**

Table 48: Option 3.2 – Costs and savings

Year	CAPEX	Revenues	Discounted net cash flow	NPV
0	-397.500 €	0	-397.500 €	-397.500 €
1	0	170.400 €	124.603 €	-272.897 €
2	0	170.400 €	115.910 €	-156.986 €
3	0	170.400 €	107.823 €	-49.163 €
4	0	170.400 €	100.301 €	51.138 €
5	0	170.400 €	93.303 €	144.441 €
6	0	170.400 €	86.794 €	231.234 €
7	0	170.400 €	80.738 €	311.973 €
8	0	170.400 €	75.105 €	387.078 €
9	0	170.400 €	69.865 €	456.943 €
10	0	170.400 €	64.991 €	521.934 €

Table 49: Option 3.2 – Net Present Value

ROR	1,31
PBT [year]	4
IRR	31,52%

Table 50: Option 3.2 – Economic indicators

From the economic point of view this project seems to be feasible, with a payback time lower than 4 years (and a simple payback time equal to 2,33 years). The results obtained by the option 3.2, from the economic point of view, are even better than those obtained by the option 3.1.

Conclusions

Considering the results obtained in the economic analysis, the installation of an absorption chiller to cool down the bottling department in the Pessione plant of Martini & Rossi seems to be feasible. The feasibility of the system mainly depends on the size of the system itself, in fact, according to the different proposals, the absorption chiller specific cost changes a lot, starting from more than 800 €/kW for chiller smaller than 200 kW, and reaching a specific cost of around 200 €/kW for chiller with a thermal inlet power equal to 1000 kW.

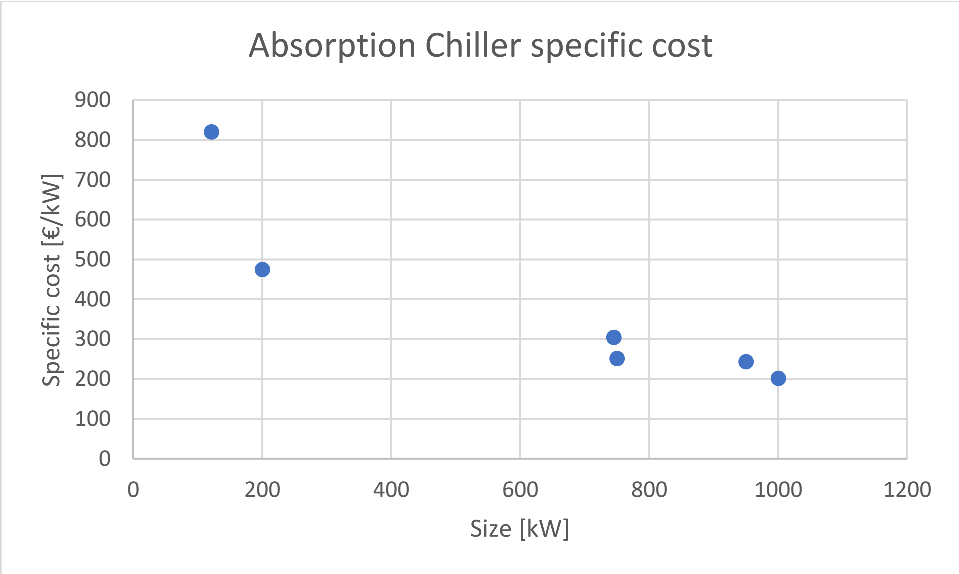

Figure 78: Absorption chiller specific cost

In addition, attention must be paid on the fact that the chiller represents only a portion of the total investment, typically around the 40-45%.

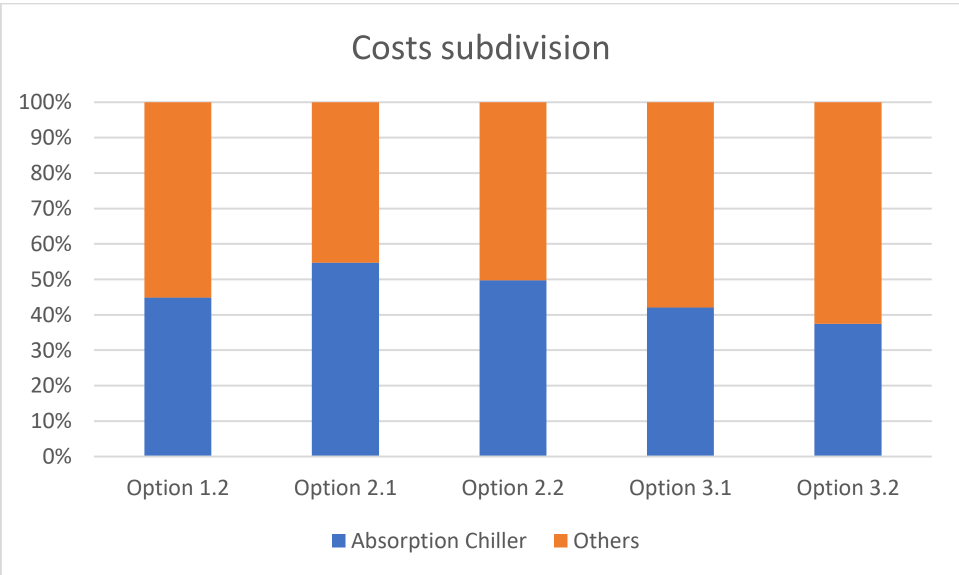

Figure 79: Costs subdivision

Summing up these points, the results demonstrate that an absorption chiller connected with the solar field alone is not economically feasible, on the other hand, a chiller fed by the CHP system, or by the combination of the CHP system and the solar field has very good economic indicators, with payback period even lower than 3 years.

The analysis carried out presents very good results also because the “heat producers” are already installed. Considering also the installation and the economic analysis of an entire new system would bring to different results not examined in this text. What can be assumed is that the costs related to a new solar thermal field would be very high, and probably not economically sustainable.

The advantage of an absorption chiller is the possibility to reuse waste heat or a heat that is not completely exploited. The constrain is that typically heat is produced burning fossil fuels, like methane in the cogenerating system, and that a renewable heat production is very expensive. A different alternative could be a traditional chiller with a mechanical compressor fed by electricity, that is cheaper in comparison to an absorption chiller and has higher efficiencies, but uses a higher quality source of energy, that is electricity. In this case the advantage should be that electricity could be more easily produced from a renewable resource reducing the environmental impacts.

It seems a bit strange from the energy point of view, but nowadays the cogenerating systems, that are usually fed by methane, are no more seen like a sustainable way for the energy production. From the chapter of the CHP systems, it is clear that a cogenerating system has very high efficiencies and is able to produce different energy vectors. The problem stands in the fact that it burns fossil fuels. Starting from this consideration, many companies are switching off their CHP systems, and are shifting to different renewable solutions to produce energy, first of all photovoltaic systems. This is a big problem for the absorption chiller systems sector. As said before, a renewable heat production is very expensive. This would bring to a massive usage of the traditional vapor compression chiller for air cooling instead of the innovative absorption chiller systems.

Finally, it can be said that, up to now, considering both the technical and the economic point of views, the absorption chiller systems are feasible and bring different savings. Considering a “greener” view, and all the effects that it could bring, there is no space for absorption chillers in the future of air cooling in industry since the costs for both the chiller and the heat producer are high.

Annex

The Sun-Earth relations

In this section, the definitions and the aspects of some relevant data for the calculation of the solar resource on the Earth are reported. First of all, the solar constant and the solar spectrum, to better understand how the solar radiation reaches the Earth. Then, the angles that compose the astronomical relationship between the Sun and the Earth are briefly described. Finally, there are reported the main relevant data of an inclined surface. These are very important since they affect a lot the energy production.

In the second part the definition of irradiance and irradiation are reported, with some formulas to obtain them, following the ASHRAE Model of clear sky.

The solar constant

The *solar constant,* according to *Encyclopedia Britannica [35]* is the total radiation energy received from the Sun per unit of time per unit of area on a theoretical surface perpendicular to the Sun's rays and at Earth's mean distance from the Sun.

It's not a true constant, it fluctuates just slightly over periods of years.

$$Solar\ minimum\colon\ I_{SC} = 1361\,\frac{W}{m^2}$$

$$Solar\ maximum\colon\ I_{SC} = 1362\,\frac{W}{m^2}$$

The solar spectrum

The spectral distribution of radiation arriving at the surface of the Earth is a function of Sun's radiation extraterrestrial distribution and atmospheric constituents.

The black line reported in the following figure represents the spectrum of a blackbody at 5250°C.

The yellow area represents the spectrum of the Sunlight at top of the atmosphere.

The red area represents the radiation at sea level. It is lower with respect to that at top of the atmosphere because the constituents of the atmosphere reflect, absorb, and scatter the sun rays.

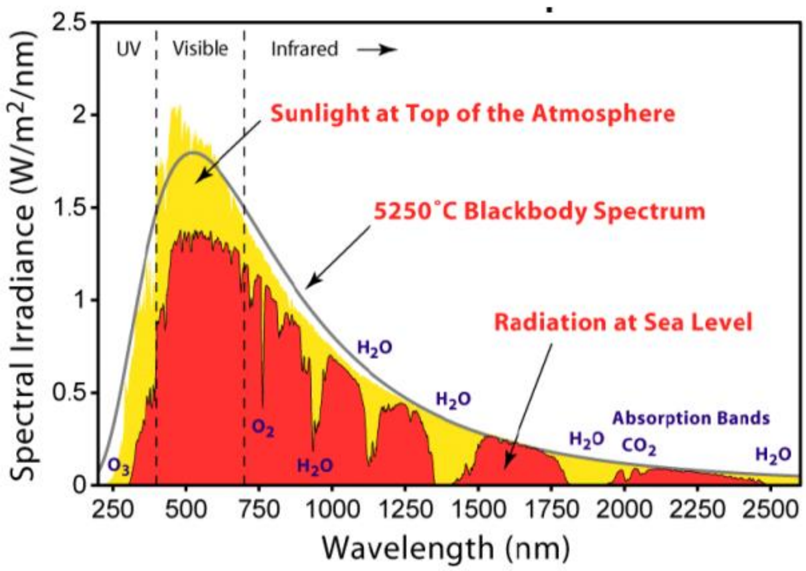

Figure 80: The solar spectrum

Starting from the figure above it can be noted that about half of the solar energy lies in the visible region (390-770 nm), and almost the same amount in the infrared (>770 nm).

Considering a different classification, most of the spectrum lies in the thermal region, with 99% in the range 250-4000 nm (short wavelength).

Sun-Earth astronomical relationships

The position of the Sun in the sky depends mainly on two different variables, time and geographical location of observation.

Sun-Earth distance

The Earth revolves in a counterclockwise direction around the Sun in an elliptical orbit with the Sun at one of the foci. The mean distance between the Sun and the Earth is one *astronomical unit* (AU).

The minimum distance is 0,983 AU. It is named *Perihelion* and occurs on the 3rd of January.

The maximum distance is 1,017 AU. It is named Aphelion and occurs on the 4th of July.

To evaluate the Sun-Earth distance of any day, different formulas has been made. The *eccentricity correction factor* E_0 is the square of the ratio between one AU and the Sun-Earth distance.

For sake of simplicity, only the formulas for "engineering" applications will be reported.

$$E_0 = \left(\frac{r_0}{r}\right)^2 = 1 + 0{,}033\cos\left(\frac{2\pi d_n}{365}\right)$$

In this formula the angle is expressed in radians, and d_n is the day number in the year.

Solar declination

The solar declination, δ, is the angular position of the Sun at solar noon relative to the plane of the equator. It varies between -23.45° and 23.45°.

This angle is due to the inclination of the polar axis, that is inclined at approximately 23.5° from the normal to the ecliptic plane, the plane of revolution of the Earth around the Sun.

This angle causes seasonal changes in solar radiation.

Period	Solar declination [°]
Equinoxes	0
Summer solstice	+23,45
Winter solstice	-23,45

Table 51: Solar declination values

The solar declination can be evaluated numerically according to the day number in the year.

$$\delta = \sin^{-1}\left\{0{,}4\sin\left[\frac{360}{365}(d_n - 82)\right]\right\}$$

Solar time

Two different times can be defined: the local apparent time (LAT) and the true solar time (TST). Solar radiation data are often referred to the TST.

The solar time is linked to the solar day. The solar day is the interval of time as the Sun appears to complete one cycle about a stationary observer on Earth. Its length varies through the year.

$$TST = LMT + ET = (LST + longitude\ correction) + ET$$

LMT: Local Mean Time

LST: Local Standard Time (Winter hour)

ET: Equation of Time

LST is obtained starting from the LMT thanks to the longitude correction. It is related to the standard meridian of the local time zone (multiple of 15°, both positive (East) and negative (West) starting from Greenwich, England).

$$TST = LST + \frac{4}{60}(\lambda - \lambda_0) + \frac{1}{60}ET \quad [hours]$$

λ: local longitude [°] (east positive, west negative)

λ_0: standard meridian longitude [°]

$$ET = [0{,}000075 + 0{,}001868 cos\Gamma - 0{,}032077 sin\Gamma - 0{,}014615\cos(2\Gamma) - 0{,}04089\sin(2\Gamma)]229{,}8\ [min]$$

Γ: day angle

$$\Gamma = \frac{2\pi(d_n - 1)}{365} \quad [rad]$$

<u>Zenith angle and solar altitude</u>

The zenith angle, θ_z, is the angle between the local zenith and the line joining the observer and the Sun. it can have values between 0 and 90°.

$$cos\theta_z = sin\delta sin\Phi + cos\delta cos\Phi cos\omega$$

Φ: latitude [°]

ω: hour angle [°]

The solar altitude, α, is the solar angular height above the observer's celestial horizon.

$$sin\alpha = cos\theta_z$$

It is the complement of the zenith angle: $\alpha = 90 - \theta_z$

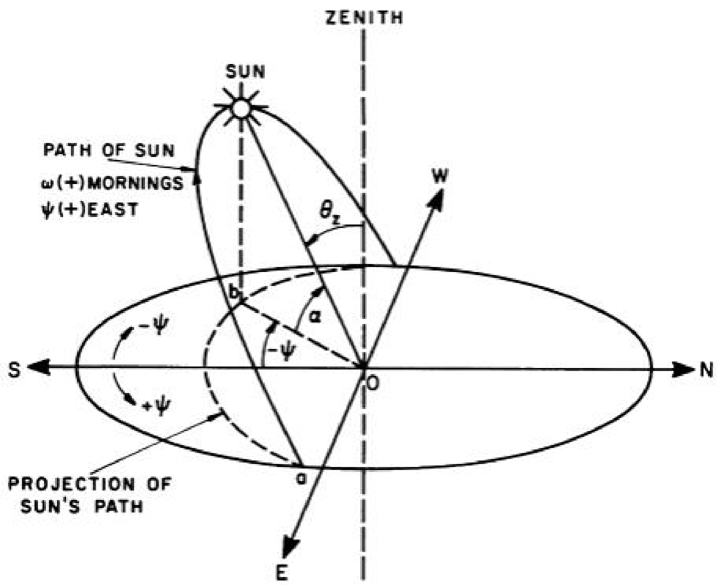

Figure 81: Zenith angle and solar altitude

Solar azimuth

The solar azimuth, ψ, is the angle at the local zenith between the observer's meridian and the plane containing the zenith and the Sun. it varies between -180° (East) and +180° (West). During the morning it has positive values, while during the afternoon it has negative values. During the noon, when the Sun is in the south, it's values is 0°.

$$cos\psi = (sin\alpha sin\Phi - sin\delta)/cos\alpha cos\Phi$$

Geographic latitude

The geographical latitude, Φ, is the angle between the plane of the earth's equator and the line perpendicular to the standard spheroid at a given point on the earth's surface [36]. Its value can vary between -90° (South Pole) and +90° (North Polw). It is 0° on the Equator.

Hour angle, sunrise and sunset and length of the day

The hour angle, ω, is a measure of the angular distance between the Sun at the local solar time and the Sun at solar noon [37].

$$\omega = 15(12 - TST) \quad [°]$$

It changes 15° per hour.

The sunrise hour angle can be evaluated fixing the zenith angle equal to 90°.

As a result: $\omega_{sr} = \cos^{-1}(-tan\Phi tan\delta)$

Similarly, the sunset hour angle (θ_z=-90°): $\omega_{ss} = -\cos^{-1}(-tan\Phi tan\delta)$

The sunset hour angle is equal to the sunrise one, except for the sign. So, the length of the day is the double of the sunrise angle:

$$N_d = \frac{2}{15}\cos^{-1}(-tan\Phi tan\delta) \quad [hour]$$

Inclined surfaces

Usually, the solar collectors and the solar panels are inclined and oriented with different angles. It is important to fix these angles during the design phase because the production of the solar collectors is strictly correlated to them.

- Slope of the surface β, measured from horizontal position.
- Surface azimuth angle γ, deviation of the normal with respect to the local meridian (positive values for East oriented collectors).

- Angle of incidence θ, the angle between normal to the surface and the Sun-Earth vector).

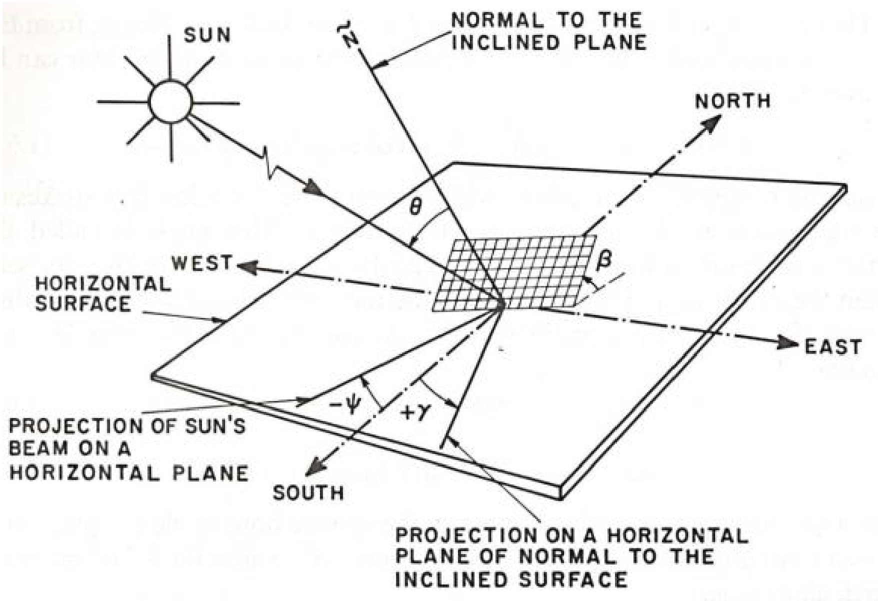

Figure 82: Solar angles for inclined surfaces

Irradiance and irradiation

Irradiance, G [W/m2]: it is the rate at which radiant energy is incident a surface per unit area of surface.

Irradiation, H [kWh/m2]: it is the incident energy per unit area on a surface, found by integration of irradiance over a specific period (hour, day, year…).

Beam, Diffuse and Total irradiance

- BEAM irradiance (G_b): it is the solar radiation received by a unit surface directly from the Sun without having been scattered by the atmosphere.
- DIFFUSE irradiance (G_d): it is the solar radiation received by a unit surface from the Sun after its direction has been changed by atmospheric scattering.
- TOTAL irradiance (G): it is the sum of the beam and the diffuse solar radiation on a surface.

Extra-atmospheric irradiance

The variation of extraterrestrial radiation flux depends on the variation of the Earth-Sun distance.

Extra-atmospheric irradiance incident on the plane normal to the irradiance on a day of the year:

$$G_{0n} = G_{sc}\left(1 + 0{,}033\cos\left(\frac{360d_n}{365}\right)\right)$$

Extra-atmospheric irradiance on a horizontal surface, it is equal to that incident on the plane normal to the irradiance multiplied by the zenith angle:

$$G_0 = G_{0n}\cos(\theta_z) = G_{sc}\left(1 + 0{,}033\cos\left(\frac{360d_n}{365}\right)(cos\Phi cos\delta cos\omega + sin\Phi sin\delta)\right)$$

Daily extraterrestrial irradiation on a horizontal surface

The value of the daily extraterrestrial irradiation on a horizontal surface is obtained integrating the irradiance over the period from sunrise to sunset:

$$H_0 = \frac{24}{1000\pi}G_{sc}\left(1 + 0{,}033\cos\left(\frac{360d_n}{365}\right)(cos\Phi cos\delta sin\omega_s + \omega_s sin\Phi sin\delta)\right)$$

Where the sunset hour angle is expressed in radians.

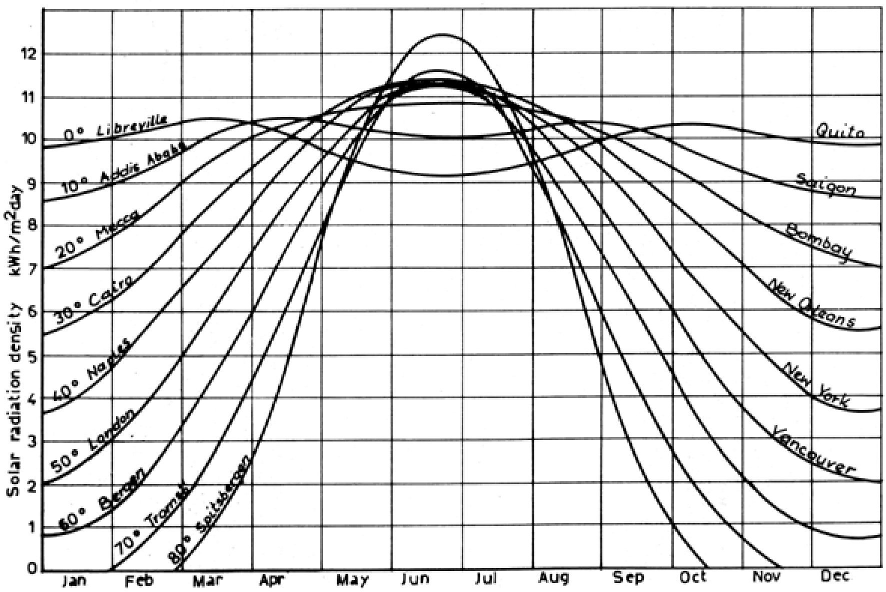

Figure 83: Extraterrestrial irradiation [38]

Thanks to the previous formula it can be evaluated how the extraterrestrial irradiation varies according to both the latitude and the day of the year (the image above represents only the northern hemisphere).

It can be seen that the nearer the Equator, the smaller the variation during the year is. Directly on the opposite side, the nearer the Pole, the bigger the variation during the year is. This is true for both the northern and the southern hemisphere.

Considering the absolute values of irradiance, in winter the radiation is higher in locations near to the Equator, while in summer it has its maximum in location near to the Pole. This is true only for the northern hemisphere. The shape of the irradiation curve for latitudes in the southern hemisphere is the same, but shifted of six months.

ASHRAE Model Clear Sky

Thanks to this model we can define the total irradiance reaching a surface in a perfectly clear sky condition.

The beam irradiance reaching a surface perpendicular to sun rays and the diffuse irradiance over a horizontal surface are evaluate with the following formulas:

$$G_{b,n} = G_0 \left(e^{-\tau_b m^b} \right)$$

$$G_{d,h} = G_0 (e^{-\tau_d m^d})$$

Where τ_b and τ_d, and b and d are coefficients related to the model:

$$b = 1{,}219 - 0{,}043\tau_b - 0{,}151\tau_d - 0{,}204\tau_b\tau_d$$

$$d = 0{,}202 - 0{,}852\tau_b - 0{,}007\tau_d - 0{,}357\tau_b\tau_d$$

(Milan)	Jan	Feb	Mar	Apr	May	Jun	Jul	Aug	Sep	Oct	Nov	Dec
τ_b	0,340	0,395	0,499	0,561	0,579	0,578	0,515	0,495	0,504	0,495	0,392	0,338
τ_d	2,248	1,977	1,693	1,588	1,596	1,640	1,818	1,876	1,799	1,759	2,036	2,261

Table 52: ASHRAE model coefficients

m is the air mass, evaluated as follow:

$$m = \frac{1}{\sin\alpha}$$

Irradiance over an inclined surface

The beam irradiance over an inclined surface is calculated starting from the beam irradiance over a surface perpendicular to the sun rays and multiplied by a geometric parameter R_b

$$R_b = \frac{cos\theta}{cos\theta_z}$$

The diffuse irradiance over an inclined surface is calculated thanks to the view factor:

$$G_{d,c} = G_{d,h} \cos^2(\frac{\beta}{2})$$

To define the global irradiance reaching an inclined surface, a reflected irradiance must be considered. The reflected component is defined considering the reflectivity of the ground (assumed equal to 0,3)

$$G_{r,c} = \rho\left(G_{b,n} sin\alpha + G_{d,h}\right) \sin^2\left(\frac{\beta}{2}\right)$$

The global irradiance reaching the inclined surface is the sum of the three components:

$$G_{tot} = G_{b,c} + G_{d,c} + G_{r,c}$$

Calculations and results

In the tables are reported the days considered in the analysis and some factors obtained following the formulas previously written.

Day	Month	d_n	B_n	ET	δ	b	d
20	Jan	20	-60,164	-10,973	-20,373	0,6119	0,2031
14	Feb	45	-35,507	-14,591	-13,675	0,6471	0,2459
22	Mar	81	0,000	-7,530	-0,075	0,6725	0,3137
8	Apr	98	16,767	-2,193	6,690	0,6763	0,3508
3	May	123	41,425	3,152	15,453	0,6675	0,3542
16	Jun	167	84,822	-0,390	23,346	0,6560	0,3446
20	Jul	201	118,356	-5,991	20,683	0,6342	0,2938
8	Aug	220	137,096	-5,358	16,040	0,6279	0,2791
16	Sep	259	175,562	5,835	1,925	0,6436	0,2951
2	Oct	275	191,342	11,454	-4,500	0,6574	0,3006
7	Nov	311	226,849	16,105	-17,025	0,6348	0,2368
11	Dec	345	260,384	6,048	-23,099	0,6105	0,2013

Table 53: ASHRAE model – overview on the days considered

20 Jan	ω	α	I	I_{bN}	I_{dh}	cosθ	R_b	I_{bc}	I_{dc}	I_{rc}	ASHRAE
8	55,58	7,44	181,70	55,40	6,04	0,50	3,85	213,18	5,33	0,46	218,97
9	40,58	14,97	362,42	166,39	18,79	0,68	2,63	437,79	16,60	2,17	456,55
10	25,58	20,66	494,97	260,14	30,77	0,81	2,30	599,23	27,18	4,30	630,70
11	10,58	23,99	570,35	316,21	38,37	0,89	2,19	690,96	33,89	5,85	730,69
12	-4,42	24,58	583,41	326,08	39,74	0,90	2,17	706,87	35,09	6,15	748,10
13	-19,42	22,35	533,27	288,42	34,57	0,85	2,24	645,82	30,53	5,05	681,40
14	-34,42	17,57	423,34	208,58	24,06	0,74	2,46	512,07	21,25	3,05	536,37
15	-49,42	10,73	261,10	100,84	11,04	0,58	3,11	313,17	9,75	1,04	323,97

16	-64,42	2,35	57,61	5,23	0,78	0,37	9,10	47,64	0,69	0,03	48,36
14 Feb	**ω**	**α**	**I**	**I_{bN}**	**I_{dh}**	**cosθ**	**R_b**	**I_{bc}**	**I_{dc}**	**I_{rc}**	**ASHRAE**
8	56,49	12,31	296,81	101,38	16,47	0,51	2,41	244,80	14,54	1,33	260,68
9	41,49	20,40	485,37	222,17	37,44	0,71	2,02	449,59	33,06	4,03	486,68
10	26,49	26,67	625,05	321,93	56,27	0,85	1,89	607,17	49,69	7,04	663,89
11	11,49	30,48	706,34	382,64	68,29	0,93	1,83	700,60	60,31	9,20	770,10
12	-3,51	31,31	723,72	395,82	70,95	0,95	1,82	720,71	62,66	9,70	793,06
13	-18,51	29,04	675,99	359,78	63,72	0,90	1,85	665,58	56,27	8,35	730,21
14	-33,51	24,00	566,41	279,27	48,07	0,79	1,94	540,52	42,45	5,67	588,64
15	-48,51	16,80	402,44	166,56	27,51	0,62	2,15	358,19	24,29	2,65	385,14
16	-63,51	8,06	195,24	47,73	7,92	0,41	2,94	140,25	6,99	0,51	147,76
22 Mar	**ω**	**α**	**I**	**I_{bN}**	**I_{dh}**	**cosθ**	**R_b**	**I_{bc}**	**I_{dc}**	**I_{rc}**	**ASHRAE**
6	84,72	3,76	89,84	3,98	1,68	0,09	1,41	5,61	1,48	0,07	7,16
7	69,72	14,23	336,34	93,29	24,25	0,35	1,41	131,33	21,42	1,65	154,40
8	54,72	24,16	559,94	225,32	59,55	0,58	1,41	317,22	52,59	5,32	375,12
9	39,72	33,01	745,42	351,77	96,09	0,77	1,41	495,23	84,86	10,08	590,18
10	24,72	40,03	880,15	449,67	125,90	0,91	1,41	633,06	111,19	14,55	758,79
11	9,72	44,26	954,96	505,70	143,48	0,98	1,41	711,93	126,71	17,40	856,05
12	-5,28	44,83	964,76	513,12	145,83	0,99	1,41	722,37	128,79	17,79	868,96
13	-20,28	41,62	908,88	471,06	132,57	0,93	1,41	663,17	117,08	15,61	795,86
14	-35,28	35,32	791,12	384,50	105,92	0,81	1,41	541,31	93,54	11,50	646,35
15	-50,28	26,92	619,50	264,66	70,66	0,64	1,41	372,60	62,40	6,68	441,67
16	-65,28	17,25	405,71	130,99	34,00	0,42	1,41	184,41	30,02	2,55	216,99
17	-80,28	6,90	164,30	20,60	6,11	0,17	1,41	29,01	5,39	0,30	34,70
08 Apr	**ω**	**α**	**I**	**I_{bN}**	**I_{dh}**	**cosθ**	**R_b**	**I_{bc}**	**I_{dc}**	**I_{rc}**	**ASHRAE**
6	83,39	9,43	221,97	32,95	11,09	0,12	0,76	25,11	9,80	0,58	35,49
7	68,39	19,98	463,10	145,18	45,75	0,38	1,10	159,44	40,40	3,34	203,19
8	53,39	30,13	680,29	278,16	90,01	0,60	1,20	332,98	79,49	8,05	420,52
9	38,39	39,32	858,77	400,02	133,16	0,79	1,24	496,39	117,60	13,55	627,54
10	23,39	46,70	986,37	491,95	167,09	0,92	1,26	621,08	147,56	18,41	787,05
11	8,39	51,08	1054,42	542,27	186,11	0,99	1,27	689,70	164,36	21,31	875,37
12	-6,61	51,34	1058,27	545,15	187,20	0,99	1,27	693,63	165,32	21,48	880,43
13	-21,61	47,40	997,67	500,24	170,20	0,93	1,26	632,38	150,31	18,87	801,57
14	-36,61	40,31	876,74	412,75	137,80	0,80	1,24	513,60	121,69	14,19	649,48
15	-51,61	31,28	703,72	293,61	95,35	0,62	1,20	353,55	84,21	8,69	446,44
16	-66,61	21,21	490,37	160,65	50,72	0,40	1,12	179,20	44,79	3,82	227,81

17	-81,61	10,68	251,24	43,48	14,26	0,16	0,84	36,41	12,60	0,78	49,78
3 May	**ω**	**α**	**I**	**I_{bN}**	**I_{dh}**	**cosθ**	**R_b**	**I_{bc}**	**I_{dc}**	**I_{rc}**	**ASHRAE**
6	82,05	16,45	378,51	98,64	31,19	0,16	0,55	54,57	27,55	2,07	84,19
7	67,05	27,05	607,98	228,16	73,69	0,40	0,88	199,82	65,08	6,22	271,11
8	52,05	37,46	813,19	362,78	121,17	0,61	1,01	366,42	107,01	11,98	485,41
9	37,05	47,14	980,17	480,66	164,99	0,79	1,08	518,06	145,70	18,13	681,89
10	22,05	55,16	1097,55	566,85	198,14	0,91	1,11	630,96	174,98	23,25	829,19
11	7,05	59,93	1157,35	611,63	215,70	0,98	1,13	690,12	190,49	26,11	906,73
12	-7,95	59,78	1155,49	610,23	215,14	0,97	1,13	688,26	190,00	26,02	904,29
13	-22,95	54,75	1092,10	562,79	196,56	0,91	1,11	625,61	173,59	23,00	822,20
14	-37,95	46,60	971,49	474,38	162,61	0,78	1,07	509,90	143,60	17,78	671,28
15	-52,95	36,85	801,87	355,03	118,36	0,60	1,00	356,60	104,53	11,61	472,74
16	-67,95	26,41	594,80	220,01	70,91	0,38	0,86	190,09	62,63	5,92	258,63
17	-82,95	15,81	364,37	91,72	29,03	0,14	0,52	47,71	25,63	1,89	75,23
16 Jun	**ω**	**α**	**I**	**I_{bN}**	**I_{dh}**	**cosθ**	**R_b**	**I_{bc}**	**I_{dc}**	**I_{rc}**	**ASHRAE**
6	82,94	21,12	474,63	153,41	46,11	0,15	0,41	62,80	40,72	3,55	107,07
7	67,94	31,64	690,85	285,73	89,05	0,38	0,72	206,26	78,65	8,37	293,28
8	52,94	42,22	885,14	417,94	134,93	0,59	0,87	364,62	119,16	14,57	498,36
9	37,94	52,45	1044,27	532,62	176,66	0,76	0,95	508,12	156,02	20,99	685,13
10	22,94	61,48	1157,41	616,84	208,30	0,88	1,00	615,83	183,96	26,30	826,09
11	7,94	67,47	1216,85	661,84	225,52	0,94	1,02	674,01	199,17	29,33	902,51
12	-7,06	67,67	1218,56	663,14	226,02	0,94	1,02	675,69	199,61	29,42	904,72
13	-22,06	61,93	1162,41	620,60	209,73	0,88	1,00	620,69	185,22	26,55	832,46
14	-37,06	53,02	1052,22	538,47	178,84	0,76	0,96	515,55	157,94	21,34	694,84
15	-52,06	42,83	895,50	425,26	137,54	0,60	0,88	373,64	121,47	14,95	510,06
16	-67,06	32,26	702,92	293,64	91,72	0,39	0,73	215,42	81,00	8,71	305,13
17	-82,06	21,73	487,59	160,75	48,40	0,16	0,44	70,07	42,74	3,78	116,59
20 Jul	**ω**	**α**	**I**	**I_{bN}**	**I_{dh}**	**cosθ**	**R_b**	**I_{bc}**	**I_{dc}**	**I_{rc}**	**ASHRAE**
6	84,34	18,35	414,94	142,04	32,29	0,12	0,39	55,60	28,52	2,70	86,82
7	69,34	28,90	636,76	281,27	67,02	0,36	0,75	209,69	59,19	7,11	275,99
8	54,34	39,46	837,57	421,50	104,93	0,57	0,90	381,17	92,67	13,07	486,90
9	39,34	49,61	1003,70	544,15	140,02	0,75	0,99	537,42	123,66	19,43	680,51
10	24,34	58,51	1123,83	635,64	167,20	0,88	1,03	656,33	147,66	24,86	828,86
11	9,34	64,52	1189,80	686,71	182,71	0,95	1,05	723,36	161,36	28,13	912,85
12	-5,66	65,27	1197,10	692,40	184,45	0,96	1,06	730,85	162,90	28,51	922,25
13	-20,66	60,34	1145,24	652,16	172,19	0,90	1,04	677,96	152,07	25,90	855,93

14	-35,66	51,95	1037,76	569,87	147,58	0,79	1,00	570,69	130,34	20,90	721,92
15	-50,66	42,01	881,96	453,77	114,01	0,62	0,93	421,85	100,68	14,64	537,17
16	-65,66	31,50	688,46	316,35	76,26	0,42	0,80	251,58	67,35	8,47	327,39
17	-80,66	20,92	470,43	174,79	40,16	0,18	0,51	89,38	35,46	3,59	128,44
8 Aug	**ω**	**α**	**I**	**I_{bN}**	**I_{dh}**	**cosθ**	**R_b**	**I_{bc}**	**I_{dc}**	**I_{rc}**	**ASHRAE**
6	84,18	15,35	350,59	112,05	23,12	0,12	0,46	51,55	20,42	1,85	73,82
7	69,18	25,94	579,41	252,12	54,53	0,36	0,83	210,36	48,16	5,78	264,30
8	54,18	36,42	786,39	395,66	89,78	0,58	0,99	389,84	79,29	11,38	480,51
9	39,18	46,29	957,42	521,75	122,75	0,77	1,06	553,47	108,40	17,52	679,39
10	24,18	54,69	1080,88	615,84	148,38	0,90	1,10	677,68	131,04	22,81	831,54
11	9,18	60,10	1148,35	668,16	162,98	0,97	1,12	747,32	143,93	26,01	917,27
12	-5,82	60,70	1155,24	673,53	164,49	0,98	1,12	754,50	145,27	26,35	926,12
13	-20,82	56,23	1101,08	631,44	152,71	0,92	1,11	698,41	134,86	23,75	857,03
14	-35,82	48,34	989,56	546,02	129,28	0,80	1,07	585,36	114,17	18,83	718,37
15	-50,82	38,71	828,27	426,01	97,56	0,63	1,01	428,85	86,16	12,76	527,76
16	-65,82	28,31	628,19	284,84	62,33	0,42	0,88	250,34	55,04	6,92	312,31
17	-80,82	17,71	402,95	141,68	29,47	0,18	0,58	82,63	26,03	2,54	111,21
16 Sep	**ω**	**α**	**I**	**I_{bN}**	**I_{dh}**	**cosθ**	**R_b**	**I_{bc}**	**I_{dc}**	**I_{rc}**	**ASHRAE**
6	81,38	7,49	175,76	27,05	6,59	0,15	1,17	31,74	5,82	0,35	37,92
7	66,38	17,92	415,02	141,42	32,47	0,40	1,31	185,07	28,68	2,66	216,41
8	51,38	27,75	628,20	275,44	65,92	0,62	1,34	369,72	58,21	6,81	434,74
9	36,38	36,41	800,79	395,59	98,20	0,80	1,36	536,58	86,72	11,67	634,98
10	21,38	43,06	921,05	483,48	122,95	0,93	1,36	659,05	108,58	15,88	783,51
11	6,38	46,63	980,78	528,15	135,86	0,99	1,37	721,38	119,98	18,22	859,58
12	-8,62	46,33	975,92	524,49	134,79	0,99	1,37	716,27	119,04	18,02	853,34
13	-23,62	42,23	906,79	472,91	119,93	0,92	1,36	644,31	105,91	15,34	765,57
14	-38,62	35,23	778,12	379,36	93,73	0,78	1,35	514,01	82,77	10,95	607,74
15	-53,62	26,35	598,65	255,76	60,82	0,59	1,34	342,48	53,71	6,11	402,30
16	-68,62	16,39	380,60	121,93	27,88	0,37	1,30	158,48	24,62	2,18	185,28
17	-83,62	5,91	138,83	15,72	4,11	0,11	1,11	17,47	3,63	0,20	21,30
2 Oct	**ω**	**α**	**I**	**I_{bN}**	**I_{dh}**	**cosθ**	**R_b**	**I_{bc}**	**I_{dc}**	**I_{rc}**	**ASHRAE**
6	79,98	3,90	92,47	5,08	1,78	0,17	2,46	12,49	1,58	0,07	14,14
7	64,98	14,10	331,51	94,68	22,51	0,41	1,70	160,99	19,88	1,60	182,46
8	49,98	23,50	542,84	219,35	53,39	0,63	1,59	347,98	47,15	4,94	400,07
9	34,98	31,54	712,07	333,65	83,99	0,81	1,54	515,14	74,17	9,06	598,38
10	19,98	37,45	827,70	416,52	107,30	0,93	1,52	635,18	94,76	12,64	742,58

11	4,98	40,38	881,84	456,38	118,81	0,98	1,52	692,67	104,93	14,53	812,13
12	-10,02	39,77	870,80	448,21	116,44	0,97	1,52	680,90	102,83	14,13	797,86
13	-25,02	35,75	795,35	393,01	100,60	0,89	1,53	601,20	88,84	11,57	701,62
14	-40,02	29,03	660,61	297,90	74,21	0,75	1,55	463,11	65,54	7,67	536,31
15	-55,02	20,46	475,77	177,10	42,60	0,56	1,61	285,41	37,63	3,66	326,70
16	-70,02	10,73	253,39	56,81	13,72	0,33	1,79	101,72	12,12	0,85	114,68
07 Nov	**ω**	**α**	**I**	**I_{bN}**	**I_{dh}**	**cosθ**	**R_b**	**I_{bc}**	**I_{dc}**	**I_{rc}**	**ASHRAE**
7	63,81	5,30	128,04	21,60	3,57	0,40	4,29	92,63	3,15	0,20	95,98
8	48,81	13,84	331,88	125,55	19,06	0,60	2,52	316,24	16,84	1,72	334,80
9	33,81	20,85	493,60	231,86	36,64	0,77	2,15	499,63	32,35	4,18	536,16
10	18,81	25,73	602,18	309,38	50,37	0,88	2,02	625,00	44,49	6,47	675,96
11	3,81	27,95	650,23	344,82	56,88	0,93	1,97	680,99	50,23	7,66	738,88
12	-11,19	27,22	634,48	333,14	54,72	0,91	1,99	662,61	48,33	7,26	718,19
13	-26,19	23,63	556,00	275,95	44,36	0,83	2,07	571,49	39,18	5,43	616,10
14	-41,19	17,63	420,14	181,94	28,18	0,69	2,29	415,81	24,89	2,92	443,62
15	-56,19	9,80	236,15	70,67	10,67	0,51	2,97	209,83	9,43	0,80	220,05
16	-71,19	0,68	16,55	0,02	0,05	0,28	23,69	0,58	0,04	0,00	0,62
11 Dec	**ω**	**α**	**I**	**I_{bN}**	**I_{dh}**	**cosθ**	**R_b**	**I_{bc}**	**I_{dc}**	**I_{rc}**	**ASHRAE**
8	51,33	7,47	182,46	56,44	6,03	0,54	4,15	234,02	5,33	0,47	239,82
9	36,33	14,34	347,46	157,37	17,39	0,70	2,85	447,85	15,36	1,98	465,19
10	21,33	19,25	462,35	237,69	27,36	0,82	2,49	591,48	24,16	3,70	619,34
11	6,33	21,73	519,29	279,39	32,80	0,88	2,37	662,15	28,97	4,77	695,89
12	-8,67	21,52	514,42	275,78	32,33	0,87	2,38	656,11	28,55	4,68	689,33
13	-23,67	18,63	448,06	227,39	26,04	0,81	2,52	573,70	23,00	3,46	600,16
14	-38,67	13,39	324,72	142,25	15,60	0,68	2,95	419,12	13,78	1,70	434,60
15	-53,67	6,26	152,82	41,35	4,46	0,51	4,68	193,39	3,94	0,31	197,64

Table 54: ASHRAE model - Results

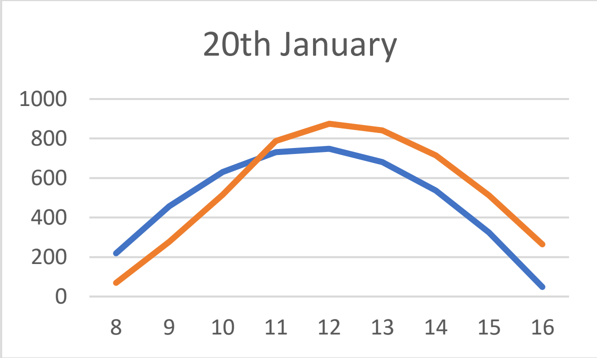
20th January
1000
800
600
400
200
0
8 9 10 11 12 13 14 15 16

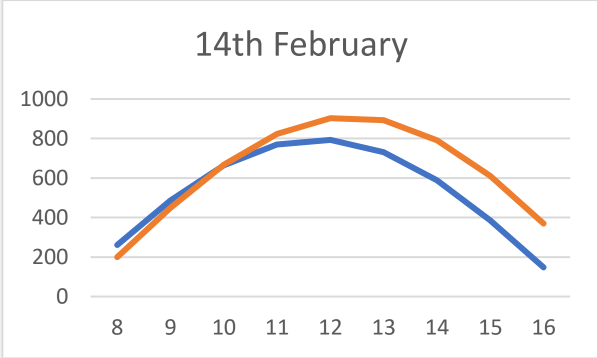
14th February
1000
800
600
400
200
0
8 9 10 11 12 13 14 15 16

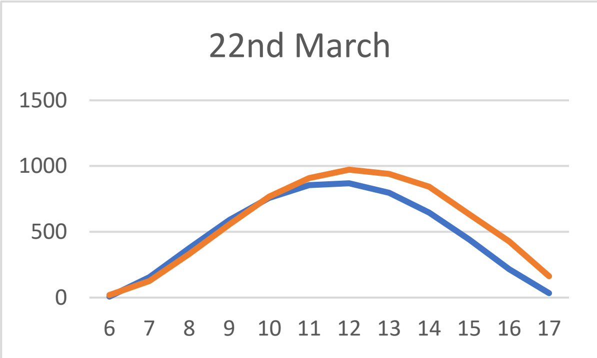
22nd March
1500
1000
500
0
6 7 8 9 10 11 12 13 14 15 16 17

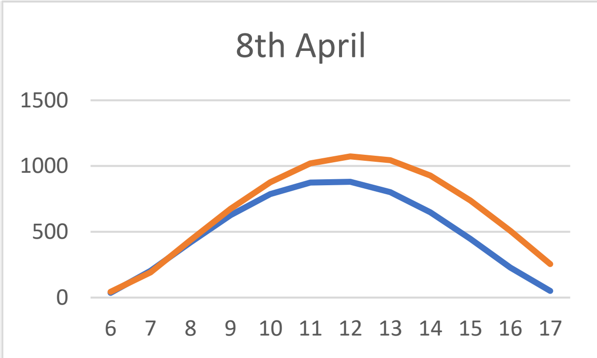
8th April
1500
1000
500
0
6 7 8 9 10 11 12 13 14 15 16 17

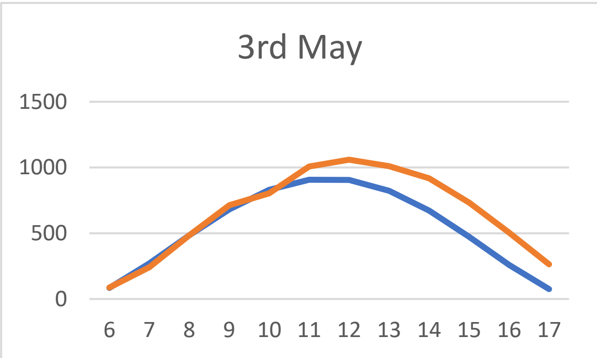
3rd May
1500
1000
500
0
6 7 8 9 10 11 12 13 14 15 16 17

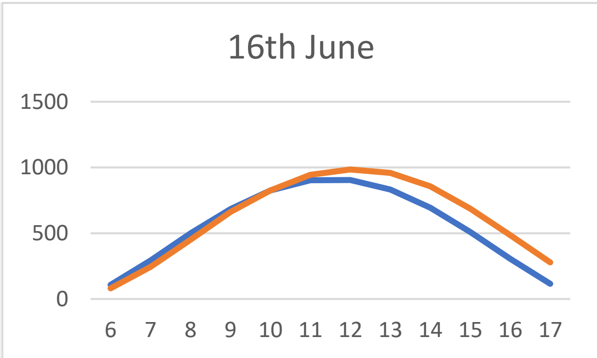
16th June
1500
1000
500
0
6 7 8 9 10 11 12 13 14 15 16 17

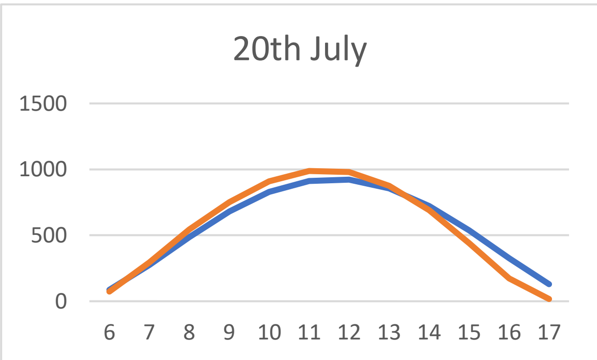
20th July
1500
1000
500
0
6 7 8 9 10 11 12 13 14 15 16 17

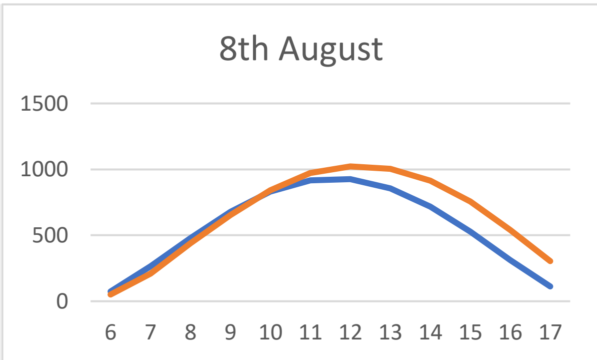
8th August
1500
1000
500
0
6 7 8 9 10 11 12 13 14 15 16 17

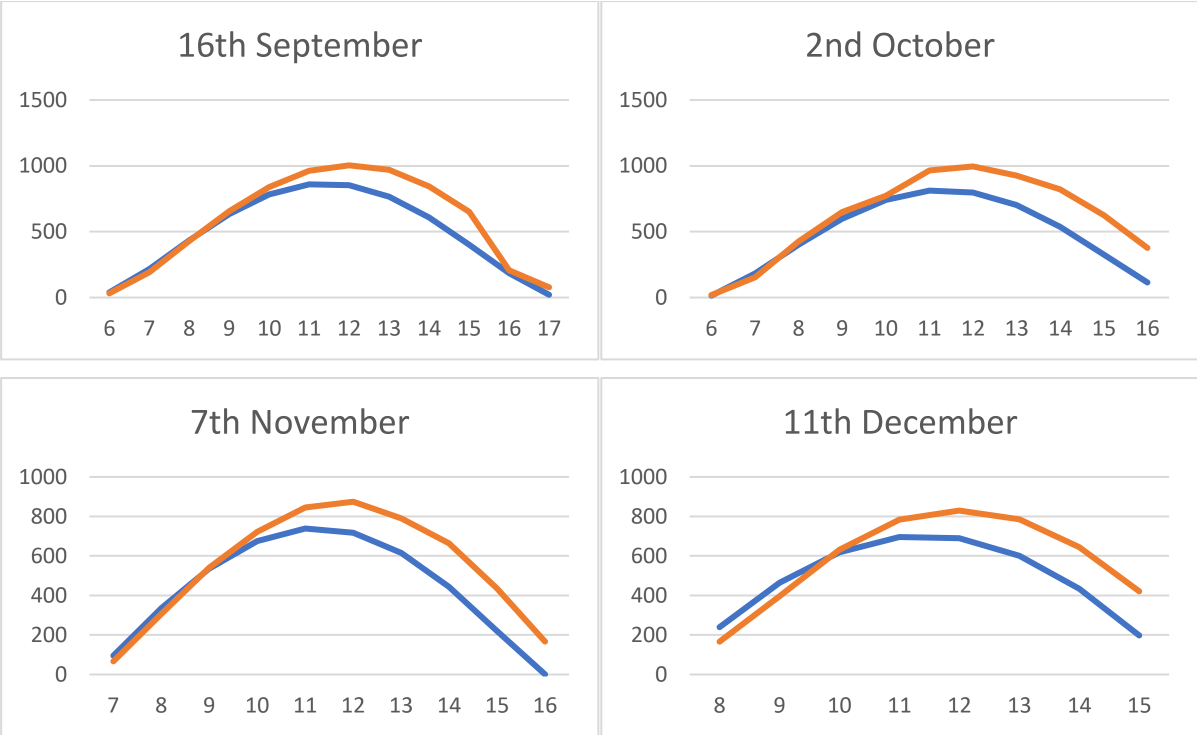

Figure 84: Comrpaison of the ASHRAE model results and the measured data

The graphs allow to notice the typical bell shape of the solar irradiance for a clear sky day. In the morning, until the sunshine, the irradiance is low, near zero. Then it increases up to a maximum, around 12 AM and 1 PM. The maximum value depends on the day of the year. Since the location considered in this study is in the northern emisphere at a latitude of about 45°, the highest values are between April and September, while the lowest are between October and March. During the afternoon the irradiance decreases until the sunset, where it reaches negligible values. A part the maximum values of irradiance, it can also be appreciate the different duration of the days along the year. The days that present the maximum irradiance are also the longest, while thoes with the lowest irradiance values are the shortest.

From the graphs above it can be seen that, apart for January, the values reported in the morning hours are the same for both the measured data and data from the model. Conversely, in the afternoon hours the measured data are higher with respect to the model. This means that the solar irradiance is higher than that predicted by the model. The results point out that the model seems to be quite correct and precise. The shape of the curves are similar, but some data are not. Different conclusions can be made. First of all, the instrument can present some errors in the measurement of the solar irradiance, but assuming its measures correct, the predicted data of the model are slightly lower than the measured. This means that the solar irradiance, for perfectly clear sky days, is higher than expected. Obviously the model is not the most precise one, it is quite simple, but permits to obtain a first approximation of the solar resource in a particular location. f

References

[1] IEA, Global air conditioner stock, 1990-2050, IEA, Paris https://www.iea.org/data-and-statistics/charts/global-air-conditioner-stock-1990-2050, IEA. Licence: CC BY 4.0

[2] Gunther M., Janotte N., Mezrhab A., Hennecke K., Schillings C., Wilbert S., Wolferstätter F., "Advanced CSP Teaching Materials Chapter 2 Solar Radiation", 2011

[3] https://solargis.com/maps-and-gis-data/download/world (last access 24 August 2023)

[4] https://en.wikipedia.org/wiki/Solarimeter (last access 18 July 2023)

[5] https://en.wikipedia.org/wiki/Pyrheliometer (last access 18 July 2023)

[6] Soteris A., "Solar thermal collectors and applications", 2004

[7] https://itssolar.co.za/water-heating/solar-water-heating/how-does-a-flat-plate-work/ (last access (12 July 2023)

[8] SHIP2FAIR, Deliverable 2.1, "Use Cases for the Integration of Solar Heat in Industrial Processes Identification and Characterization", 2019

[9] M. Abdur Razzaq, M. Hasanuzzaman, "Solar thermal power plant", 2022

[10] [Moss R.W., Henshall P., Arya F., Shire G.S.F., Hyde T., Eames P.C., "Performance and operational effectiveness of evacuated flat plate solar collectors compared with conventional thermal, PVT and PV panels", 2018

[11] T. Otanicar, R.A. Taylor, P.E. Phelan, "Prospects for solar cooling – An economic and environmental assessment", 2012

[12] http://worldenergy.co.kr/en/portfolio-item/hwar-l-2/ (las access 13 July 2023)

[13] Balaras C.A., Grossman G., Henning H., Infante Ferreira C.A., Podesser E., Wand L., Wiemken E., "Solar air conditioning in Europe – an overview", 2006

[14] Schematic of adsorption chiller lay-out | Download Scientific Diagram (researchgate.net) (last access 13 July 2023)

[15] https://www.coolingindia.in/economising-desiccant-powered-hvac-cooling-systems/ (last access 13 July 2023)

[16] Dincer I., Abu-Rayash A., "Community energy systems", 2020

[17] Gas turbine - Wikipedia

[18] 7F Heavy Duty Gas Turbine | 7F.04/7F.05 | GE Gas Power

[19] What is Brayton Cycle - Gas Turbine Engine - Definition (thermal-engineering.org)

[20] bing.com/newtabredir?url=https%3A%2F%2Fcogeneration.pro%2Fwhat-is-cogeneration-combined-heat-and-power%2F

[21] Combined cycle cogeneration gas turbine system. | Download Scientific Diagram (researchgate.net)

[22] https://www.araner.com/blog/vapor-compression-refrigeration-cycle (last access 19 July 2023)

[23] https://en.wikipedia.org/wiki/Vapor compression_refrigeration#/media/File:Refrigeration_PV_diagram.svg (last access 19 July 2023)

[24] Hwang Y., Al-Alili A., Radermacher R., "Review of solar thermal air conditioning technologies", 2014

[25] Srikhirin P., Aphornratana S., Chungpaibulpatana S., "A review of absorption refrigeration technologies", 2001

[26] Labus J. M., Bruno J. C., Coronas A., "Review on absorption technology with emphasis on small capacity absorption machines", 2013

[27] Kasperski J., Eichler J., "Ammonia-water absorption cycle on three-dimensional graphs - The Absorption 3D tool software", 2012

[28] https://arvengtraining.com/en/basics-of-shell-tube-heat-exchangers/ (last access 19 July 2023)

[29] Stutz B., Altamirano A., Le Pierrès N., "Review of small-capacity single-stage continuous absorption systems operating on binary working fluids for cooling: Compact exchanger technologies", 2020

[30] Mortazavi M., Nasr Isfahani R., Bigham S., Moghaddam S., "Absorption characteristics of falling film LiBr (lithium bromide) solution over a finned structure", 2015

[31] Ibarra-Bahena J., Romero R. J., "Performance of Different Experimental Absorber Designs in Absorption Heat Pump Cycle Technologies: A Review", 2014

[32] Chang Y., Wu L., Wu C., Jang L., ”Computer Simulation of an Ammonia-Water Absorption Cycle for Refrigeration: Using a Distillation Tower to Replace the Generator”, 2020

[33] Tao X., Thanganadar D., Patchigolla K., “Ammonia/Water Absorption Chiller of Different Cycle Configuration: Parametric Analysis Based on Heat Transfer Performance”, 2022

[34] Flores V., Román J., Montero Alpírez G., “Performance Analysis of different Working Fluids for an Absorption Refrigeration Cycle”, 2014

[35] https://www.britannica.com/science/solar-constant (last access 20 September 2023)

[36] Geographical latitude Definition & Meaning - Merriam-Webster (last access 20 September 2023)

[37] Solar Hour Angle & How to Calculate it – SolarSena (last access 20 September 2023)

[38] https://www.fao.org/3/x6541e/X6541E03.htm (last access on 20 September 2023)

List of figures

List of tables